Exploring the Frontiers of Female Fertility to Unlock the Full Potential of Assisted Reproduction

By

JULIANA IRENE CANDELARIA

DISSERTATION

Submitted in partial satisfaction of the requirements for the degree of

DOCTOR OF PHILOSOPHY

in

Animal Biology

in the

OFFICE OF GRADUATE STUDIES

of the

UNIVERSITY OF CALIFORNIA

DAVIS

Approved:

Anna C. Denicol, Chair

Fabio S. Lima

Pouya Dini

Committee in Charge

2024

DEDICATION

To my parents, who taught me that hard work, perseverance, and a kind heart will always help you get to higher places.

ACKNOWLEDGEMENTS

This dissertation would not have been possible without the guidance and support of advisors, colleagues, friends, and family. First, I am indebted to my Major Professor, Dr. Anna Denicol, for her steadfast commitment to each of my studies, my growth, and ultimate completion of my PhD degree. She taught me not only many skills at the lab bench, but also many skills in writing, critically thinking, and believing in myself even when I had doubts or frustrations. I cannot credit her enough for getting me where I am today. I would also like to thank my committee members, Dr. Fabio Lima and Dr. Pouya Dini, for their expertise and contributions to my dissertation research. I would like to show my gratitude to Dr. Ariella Shikanov for sharing her deep knowledge in bioengineering in reproductive sciences, which was pivotal to my PhD research and greatly aided with securing my independent funding.

I am grateful for the financial support provided to me by multiple sources. Thank you to the Animal Biology Graduate Group and the Animal Science Department for the awards that helped fund my PhD. I am also grateful for the NIH F31 Pre-doctoral Fellowship for selecting me as a recipient which also funded my PhD.

I am particularly appreciative of the many members of the Denicol Lab who have become great lifelong friends. I am thankful for Stephanie McDonnell and Amanda Morton who kept me in good company during many follicle collections. Further thanks to Dr. Ramon Botigelli and Rachel Braz Arcanjo for endless help with nearly all my experiments. I am extra grateful for Carly Guiltinan who was an excellent lab companion as we did many experiments together and became my dearest friend during our PhD journeys. I am thankful for Bethany Weldon who also remains a dear friend even after completion of her PhD. Outside of the lab, I could not imagine my time in graduate school without the multitude of friends made in Davis. They were always available for a laugh, a hike, or a shoulder to cry on, and for that I am thankful. Finally, I would like to thank my family, my friends back home, and my partner Sean for always supporting me no matter what obstacle came in the way. Their infinite encouragement was essential to me crossing the finish line.

TABLE OF CONTENTS

LIST OF FIGURES AND TABLES

ABSTRACT

In females, reproduction is a key facet of women's health, livestock production, and conservation of endangered species. The ovary is the gonad of the female and is a central component of female reproductive physiology as it houses the germ cells (i.e., oocytes) within follicles and produces hormones to coordinate folliculogenesis. The ovary is a target organ for developing novel assisted reproductive technologies (ART) such as safeguarding fertility via cryopreserving ovarian tissue containing follicles and developing strategies to grow early staged preantral follicles in vitro for oocyte production. Moreover, a better understanding of cellular and molecular events constituting early gonad development would be widely valuable to further advance ART that capitalizes on components of the ovary. In this work, we describe three aims using the bovine as a model and collectively expand our current knowledge in 1) ovarian tissue cryopreservation (OTC), 2) in vitro bovine preantral follicle development, and 3) in vitro differentiation of bovine embryonic stem cells (bESCs) into progenitors of bipotential gonad-like cells.

In Aim 1, we found that, overall, slow freezing outperformed vitrification when bovine ovarian fragments were thawed and cultured as indicated by higher rates of normal follicle morphology, lower rates of apoptosis in stromal cells, and proper expression of the gap junction protein connexin 37. In addition to the use of OTC and culturing ovarian tissue fragments to rescue folliculogenesis, in Aim 2 we explored the use of bioengineered and proteolytically degradable (poly)ethylene glycol (PEG) hydrogels for in vitro culture of isolated bovine preantral follicles. We also tested co-encapsulation of mesoderm-like cells (MeLCs) from bESCs or native bovine ovarian cells

(BOCs) with follicles to determine their propensity to become theca-like cells and improve folliculogenesis in vitro. After customizing a PEG hydrogel to complement bovine preantral follicle extracellular matrix (ECM) enzyme expression, we found that smaller follicles grew better in PEG hydrogels compared to two-dimensional control over ten days. However, MeLCs did not survive PEG hydrogel encapsulation process. Although BOCs could survive in PEG hydrogels throughout the culture period, BOCs did not better support follicle survival and development when co-encapsulated compared to PEG-only control. Moreover, the culture conditions did not maintain expression of selected genes essential for theca cell differentiation. Finally, in Aim 3, we tested the ability of bESCs to be driven towards the intermediate mesoderm (IM), early coelomic epithelium (eCE), and steroidogenic state during in vitro culture using several protocols. Our data indicated that inclusion of the steroidogenic factor-1 (SF1) agonist, RJW100, did not upregulate steroidogenic genes during the differentiation. Similarly, the cytokines basic fibroblast growth factor (bFGF) and bone morphogenic protein-4 (BMP4) were dispensable for inducing IM and eCE gene expression, and WNT activation was a predominant driver of eCE and IM gene expression, high concentrations of BMP4 led to upregulation of lateral plate mesoderm gene expression, and paraxial mesoderm gene expression remained unchanged across all regimens.

Collectively, this dissertation work sheds light on several facets of ovarian biology including a better understanding of the impacts of OTC, *in vitro* preantral folliculogenesis, and use of embryonic stem cells to recapitulate bipotential gonad somatic cell differentiation. Nevertheless, additional research is required to elucidate mechanisms that

are pivotal to both early folliculogenesis and early embryonic gonad formation in the bovine model.

CHAPTER 1

Review of the Literature

Introduction

The ovary is an essential reproductive organ in the female and is responsible for producing viable gametes (i.e., oocytes) and secretion of hormones such as estrogens and progesterone[1]. Histologically, the ovary comprises an outer portion called the cortex, and an inner portion called the medulla. In the postnatal ovary, individual oocytes are housed by somatic support cells within the ovarian cortex. The collective functional unit made of oocytes and somatic cells is called a "follicle." Within the follicle, the oocyte and surrounding granulosa cells engage in active bidirectional communication where the oocyte secretes growth factors that act on granulosa cells to stimulate metabolic processes to supply energy substrates that the oocyte is unable to produce[2]. These two cell types are encapsulated by a basement membrane. The ovarian reserve constitutes the collective population of the earliest staged follicles (i.e., primordial follicles) and determines the reproductive lifespan of a female as they selectively exit their quiescent state and commence growth after puberty. Immediately outside the basement membrane and as the development of the follicle continues, theca cells are recruited from the neighboring stromal cell environment to provide further endocrine and structural support. The entire process of follicle development (termed "folliculogenesis") is complex and highly coordinated such that ovulation yields a meiotically- and developmentally-competent oocyte that is ready to undergo fertilization[3]. Following ovulation, a corpus luteum forms in the ovary and becomes a transient yet indispensable organ that produces progesterone, thus preparing the female for embryo implantation and pregnancy.

Folliculogenesis begins with primordial follicles, which contain a single oocyte and a single layer of flattened granulosa cells[4]. Primordial follicles form in the early ovary either

during gestation (i.e., humans, non-human primates, cows, sheep, and pigs) or postnatally (i.e., rodents such as mice and hamsters) and remain dormant until triggered to activate[5]. The current central dogma in reproductive biology states that the ovarian reserve is finite, and de novo synthesis of new follicles does not occur in mammalian animals. As folliculogenesis progresses, a subset of primordial follicles activates and enter the growing pool by largely unknown mechanisms and become primary follicles with a single layer of cuboidal-shaped granulosa cells. This irreversible recruitment process is highly selective to avoid excessive utilization and early depletion of the ovarian reserve. Several mechanisms of primordial activation exist, including involvement of the PI3K-Akt-FOXO3[6], mTORC1-S6K1-rpS6 [7–9], and Hippo signaling pathway[10] in primordial follicle-granulosa cells and oocytes. Despite uncovering the general participation of these pathways in awakening the oocyte and promoting follicle activation, it has yet to be determined why and how the selection of certain primordial follicles occurs *in vivo*. Efforts in answering these questions will aid in better understanding early folliculogenesis, pinpoint origins of dysregulation resulting in primary ovarian insufficiency, and develop alternative fertility treatments that take advantage of the ovarian reserve in female patients and animals.

Further development of primary follicles leads to the secondary follicle stage. This transition is characterized by minute oocyte growth and, more notably, the proliferation of granulosa cells, thus forming additional layers within the follicle. Regulation of primary-to-secondary follicle growth has hardly been unraveled, but studies suggest that the major ovarian hormone, follicle-stimulating hormone (FSH), likely plays an important role in promoting development even during early follicle stages[11–15]. Paracrine and autocrine

factors also promote their development, although current knowledge in direct mechanisms for this phenomenon remain elusive. Initial expression of transforming growth factor beta (TGFβ) proteins GDF9 and BMP15 in the oocyte promote the hallmark granulosa cell proliferation[2,4,16,17]. Indeed, an additional aspect of secondary follicle growth is the recruitment of theca cells which is driven by GDF9 from the oocyte[16,18]. Secretion of GDF9 induces hedgehog signaling in granulosa cells. Indian hedgehog (IHH) and desert hedgehog (DHH) are produced by the granulosa cells and bind to the cell surface receptors PTCH1/2 on the surrounding pre-theca cells. Upon binding, PTCH1/2 releases its suppression of the receptor SMO, thus leading to activation of the transcription factors GLI1/2/3 and resulting in upregulation of theca-specific genes such as CYP17A1[19]. Theca cells are essential to produce the estrogen receptors androstenedione and testosterone. When androgens enter neighboring granulosa cells, they aromatize into estrogen, which then enters the systemic circulation and plays a vital role in the hypothalamus-pituitary-gonadal (HPG) axis[20]. Estrogen levels, in turn, regulate secretion of the gonadotrophs FSH and luteinizing hormone (LH) from the anterior pituitary in negative and positive feedback loops, further moderating follicle development in the ovary.

Follicles between the primordial and late secondary stages are termed “preantral” due to the absence of a fluid-filled antrum. The antral cavity forms by accumulating follicular fluid from blood sourced by the emerging vascular network within the theca cell layer. The antrum fluid buildup is thought to be primarily driven by changes in osmotic pressure from interior granulosa cells[21]. The antrum is crucial for holding follicular fluid that is rich with factors and nutrients for the oocyte. A cohort of small antral follicles selectively grow larger in diameter by responding to FSH stimulation. In mono-ovulatory species such as the

cow, a single antral follicle becomes dominant during one estrus cycle and is considered the pre-ovulatory follicle of the ovary. A surge of LH in response to increased circulating estradiol causes a cascade of cell signaling events leading to nuclear and cytoplasmic modifications within the oocyte that are collectively part of the maturation process that ultimately results in ovulation of the metaphase II oocyte[22,23]

Despite a large endowment of ovarian follicles found early in life, most follicles degenerate and fail to ovulate for reasons unbeknownst to researchers today. There is little understanding of ovarian follicle development's selection and growth process, especially in the preantral stage. Translation of research from rodent models has demonstrated species variation compared to large mammal species such as the bovine and human, likely due to the stark difference in folliculogenesis timeline, ovulation rate, and factors required for development. Moreover, safeguarding fertility by cryopreserving the primordial follicle population and associated stromal cells has gained wide attention but necessitates a thorough understanding of ovarian biology, especially if one aims to grow follicles post-thawing to supply oocytes for further use. A valuable approach to study the follicular microenvironment is to recapitulate the ovary in vitro. To do so, there is a pressing need to elucidate the embryonic origin of cells that constitute the ovary and their contribution to the process of folliculogenesis. This review aims to evaluate the current literature on 1) ovarian tissue cryopreservation, 2) progress in utilizing three-dimensional (3D) in vitro follicle culture methods, and 3) advancing understanding in early developmental biology and cellular differentiation of the bipotential gonad and ovary. Altogether, these three research areas underpin the overall scientific goal of preserving and restoring function of the ovary and follicle.

Ovarian tissue cryopreservation

Fertility preservation is a rising facet of women's health and is essential for animal production and species conservation. Typical methods of fertility preservation include cryopreserving oocytes or embryos. These options are available to adult women concerned about age-related fertility decline, female cancer patients facing gonadotoxic-related fertility decline from chemotherapy or radiation, and reproductive-age animals. However, as retrieval of mature oocytes is dependent on a female being pubertal and responding appropriately to hormonal stimulation, children patients who cannot delay cancer treatment or stimulation will exacerbate their malignancies or young or deceased animals are largely ineligible for this fertility preservation option. In addition, mature oocytes come from antral follicles, which are proportionately extremely low in quantity compared to preantral follicles, especially the primordial follicles that constitute the ovarian reserve. Hence, preantral follicles housing immature oocytes are a mostly unused pool of germplasm that could be harnessed for future assisted reproductive technologies and, therefore, ideal candidates for preservation. For these reasons, ovarian tissue cryopreservation (OTC) has been implemented as a resourceful safeguarding technique, especially in young girls, since it preserves the abundant ovarian reserve.

There are two approaches to ovarian tissue cryopreservation: slow freezing and vitrification. According to published literature and reports by the American Society for Reproductive Medicine, slow freezing is the most common and successful technique, as demonstrated by over 130 live births and restoration of ovarian activity in nearly 95% of cases after autotransplantation[24,25]. Indeed, the first report of any OTC procedure with transplantation was in 1953, using slow freezing of rat ovary tissue[26]. Slow freezing of

ovarian tissue begins by exposing cortical fragments to a low concentration of cryoprotectant agents (CPA) such as dimethyl sulfoxide (DMSO) or ethylene glycol. The CPA can penetrate the lipid bilayer of cells if it is a permeating agent (like DMSO), leading to dehydration and reduced intracellular capacity for ice formation, thus protecting the cells from cryoinjury. Nonpermeating cryoprotectants, such as sucrose, also drive water to exit cells as it creates a hypertonic environment extracellularly, similarly preventing intracellular ice formation. Slow freezing, as the name describes, decreases the temperature of the sample below the freezing point at a controlled slow rate, which aids in the coordinated dehydration, promotion of extracellular ice formation, and maintenance of tissue viability. For instance, stepped cooling curves to slow freeze for human ovarian cryopreservation can occur by the following: cooling at a rate of −2.0°C/min, followed by manual seeding to induce ice nucleation and cooling to −40.0°C at a rate of −0.3°C/min and −140°C at a rate of −10°C/min[27]. Despite a general basis for slow freezing, reported protocols such as differences in cryoprotectants and corresponding concentrations, timing intervals for cooling ramps, and temperature endpoints vary.

Vitrification occurs by rapidly chilling cells so that ice formation is prevented. It is often used in oocyte and embryo cryopreservation. By combining ultrafast cooling rates and high concentrations of CPAs, vitrification can convert supercooled liquid within tissue into a glass-like amorphous solid-state void of ice crystals. This method has been an attractive alternative to slow freezing for OTC since it is faster and does not require a special freezing machine. After equilibration in high concentrations of mixed CPAs, ovarian tissue fragments are placed on metal devices and directly plunged into liquid nitrogen to achieve vitrification[28]. Vitrification of human ovarian tissue fragments were first reported in 2003

by Isachenko et al. and the results showed that follicle and stroma morphology and hormone output during in vitro culture were most consistent with fresh tissue when ethylene glycol, egg yolk, and sucrose were present in the vitrification media[29]. Since this report, others have shown that vitrification can safeguard ovarian tissue both in fragmented pieces and whole organs[30–32]. However, successful vitrification, demonstrated by live births in humans after auto transplantation, has been extremely limited and only recently reported by two groups[10,33]. Execution of vitrification protocols is more skill-dependent and less established compared to slow freezing, thus leading to varying outcomes in tissue viability post-thawing.

Both vitrification and slow freezing can be appropriate methods for OTC, as demonstrated by dozens of studies. However, there has been also shown conflicting results[34,35]. In general, accomplishing effective cryopreservation of the ovary is difficult due to the inability to uniformly conduct heat and mass transfer across the tissue and cytotoxicity from CPAs. During slow freezing, ice crystal formation ideally occurs extracellularly and this phase transition from liquid to solid releases energy as latent heat[36]. Yet, during the process and during vitrification, cyclic thawing and re-freezing of cells can occur, spanning the entire tissue, leading to intratissue freezing injury[37]. For this reason, minimizing the sample volume while including a sufficient follicle, population is key to ensuring efficient heat and mass transfer for reduced cryodamage. Cytotoxicity is a common concern with cryopreservation as CPAs used can cause cell membrane disintegration[38]. As aforementioned, the heterogenous nature of tissue, which includes various cell types and extracellular matrix proteins, makes finding cryopreservation protocols compatible with all these tissue components very difficult. Most studies focus

on follicle and oocyte morphology as a key endpoint but do not shed light on the impacts of cryopreservation on the other cell populations and extracellular matrix proteins despite their crucial role in ovarian biology[39,40]. Moreover, developing the follicles post-thawing is the ultimate goal. Therefore, techniques to grow follicles that circumvent the need for surgical transplantation would be ideal.

In vitro folliculogenesis using 3D culture systems

Developing ovarian follicles using in vitro culture has the potential to resourcefully produce oocytes for downstream embryo production in women and other animals while circumventing the need for surgical transplantation of tissue. Attempts to grow follicles from the primordial stage through the preovulatory stage, yielding mature oocytes that can undergo fertilization and become viable offspring, has only been achieved in the mouse and at extremely low efficiency[41]. Typically, isolated follicles grown in vitro use 2-dimensional (2D) culture where follicles are placed in wells either individually or in groups. Despite evidence indicating mouse preantral follicles could be capable of growing in 2D culture, though inefficiently, there is a greater emphasis on maintaining the spherical 3-dimensional (3D) architecture of the ovarian follicle, which cannot be achieved in traditional 2D culture systems[42,43]. Indeed, loss of oocyte-granulosa contact, rupturing of the basement membrane, and structural flattening accompanied by granulosa cell migration have been reported when follicles are cultured in 2D systems for long time periods, and these aberrations greatly hamper follicle viability and growth[44]. For these reasons, technical advancements in 3D culture methods are being explored for use in

prolonged in vitro folliculogenesis, which is required to mimic the natural long-time span of follicle development needed in large mammalian species[45].

Naturally-derived biomaterials

Scaffolding biomaterials used to culture follicles in 3D can be naturally or synthetically derived. Collagen is a common natural extracellular matrix protein used for scaffolding in 3D preantral follicle culture due to its presence in vivo throughout the ovarian microenvironment[46–48]. The first report of using collagen for encapsulating preantral follicles in 3D culture was in 1989 by Torrance et al., who showed that isolated mouse follicles maintained their structure and showed cellular outgrowth within collagen hydrogels[49]. Since this report, many others have researched the use of collagen hydrogels, such as Abir et al. (2001), who showed that isolated small (30-50 μm) human preantral follicles survived a 24-hour culture only when encapsulated in 3D collagen hydrogel[50]. Joo et al. (2016) demonstrated that isolated mouse preantral follicles grew optimally, indicated by increased diameter and oocyte meiotic resumption when cultured 3D in 5 mg/ml collagen hydrogels[51]. In the bovine model, Schotanus et al. (1997) and Itoh et al. (2000) successfully grew small preantral follicles using collagen hydrogels but only in the presence of conditioned medium or medium containing luteinizing hormone, follicle-stimulating hormone, and insulin[52,53]. However, uncontrollable degradation is a major obstacle when using collagen, leading to loss of mechanical strength and structure, and thus diminished use as a biomaterial material for in vitro culture over the years. Similar to collagen, Matrigel is a concoction of extracellular matrix proteins extracted from mouse sarcoma cells and can be used to construct 3D hydrogels for *in vitro* folliculogenesis[54,55]. However, Matrigel presents a comparable issue to collagen of rapid degradation besides

being a generally undefined matrix substrate, making it a less-preferred scaffold for follicle culture.

Although not found in the ovary and instead derived from brown algae, alginate is a widely applied natural biomaterial for 3D culture due to its non-cytotoxic characteristics and allowance for diffusion of metabolites and fluids. By cross-linking its polysaccharide chains with divalent cation ions such as calcium, alginate can gelatinize and form stable hydrogels for cell encapsulation[56]. Many studies investigated the impact of alginate concentration, which in turn dictates the stiffness of alginate hydrogels, on growth and viability across various follicle stages and from various species. For example, West-Farrell et al. demonstrated that 1.5% alginate hampered follicle growth and antrum formation when compared to 0.5% alginate hydrogels in large mouse preantral follicles[57]. This is similar to Songasasen et al., (2011) who found that 1.5% alginate led to very similar outcomes where lower alginate concentrations equated to greater follicle growth in canine preantral follicles[58]. Yet, Park et al. (2012) determined that 0.25% alginate led to lower rates of mouse follicle survival and antrum formation compared to an even lower concentration of 0.125% alginate and 2D controls[59]. In contrast to these reports indicating a softer environment is optimal for larger preantral follicle development, primordial follicles of large mammalian species require a stiffer hydrogel setting. Primate primordial follicles had higher survival and optimal growth when encapsulated in 2% alginate compared to 0.5% alginate[45]. In humans, 1% alginate has been reported to sustain primordial and primary follicle viability and growth after 7 days of *in vitro* culture[60]. Although alginate maintains the 3D structure of follicles and shows encouraging results for growth and viability, its inertness creates a less favorable environment for the dynamic follicle volume

changes that occur during development. For these reasons, combining the structural integrity of alginate with biologically relevant ECM and adherence proteins can better mimic the natural ovarian architecture. Collagen, fibrin, and arginyl glycyl aspartic acid (RGD) peptides have been combined with alginate and successfully promote follicle development in vitro across many species[61–64]. Taking a step further, researchers have created more intricate alginate/collagen hydrogels with differing rigidities between inner and outer cores to mimic the ovarian medulla and cortex, respectively[65].

Scaffolding made by decellularized ovarian ECM (doECM) is an additional matrix that is naturally-derived and unlike the biomaterials mentioned above, can provide bioactive factors such as an array of peptide domains for cell adherence and communication to enclosed preantral follicles. In this case, ovarian tissue is subjected to decellularization protocols using enzymatic, chemical, or physical agents while preserving the mechanical and biochemical composition of the native ECM[66]. To provide structure, the doECM is solubilized into a hydrogel with a base such as alginate, thus reconstructing an ovarian microenvironment. Human preantral follicles remained viable during 7-day culture in a bovine and human doECM reconstituted using alginate as a hydrogel base[67]. Chiti et al. (2022) demonstrated that alginate hydrogels containing bovine doECM could maintain growth and viability in human preantral follicles similar to alginate-only controls, but this could not be achieved with in hydrogels only containing bovine doECM[68]. When human doECM with Matrigel was used to create hydrogels for murine and human preantral follicle encapsulation and xenotransplantation, 39% of follicles reached the antral stage[69]. Despite evidence indicating doECM can sustain follicle viability, it can present issues with immunoreactivity when transplanted and has inconsistency in biochemical profile.

This is similar to Songasasen et al., (2011) who found that 1.5% alginate led to very similar outcomes where lower alginate concentrations equated to greater follicle growth in canine preantral follicles[58]. Yet, Park et al. (2012) determined that 0.25% alginate led to lower rates of mouse follicle survival and antrum formation compared to an even lower concentration of 0.125% alginate and 2D controls[59]. In contrast to these reports indicating a softer environment is optimal for larger preantral follicle development, primordial follicles of large mammalian species require a stiffer hydrogel setting. Primate primordial follicles had higher survival and optimal growth when encapsulated in 2% alginate compared to 0.5% alginate[45]. In humans, 1% alginate has been reported to sustain primordial and primary follicle viability and growth after 7 days of *in vitro* culture[60]. Although alginate maintains the 3D structure of follicles and shows encouraging results for growth and viability, its inertness creates a less favorable environment for the dynamic follicle volume changes that occur during development. For these reasons, combining the structural integrity of alginate with biologically relevant ECM and adherence proteins can better mimic the natural ovarian architecture. Collagen, fibrin, and arginyl glycyl aspartic acid (RGD) peptides have been combined with alginate and successfully promote follicle development in vitro across many species[61–64]. Taking a step further, researchers have created more intricate alginate/collagen hydrogels with differing rigidities between inner and outer cores to mimic the ovarian medulla and cortex, respectively[65].

Scaffolding made by decellularized ovarian ECM (doECM) is an additional matrix that is naturally-derived and unlike the biomaterials mentioned above, can provide bioactive factors such as an array of peptide domains for cell adherence and communication to

enclosed preantral follicles. In this case, ovarian tissue is subjected to decellularization protocols using enzymatic, chemical, or physical agents while preserving the mechanical and biochemical composition of the native ECM[66] . To provide structure, the doECM is solubilized into a hydrogel with a base such as alginate, thus reconstructing an ovarian microenvironment. Human preantral follicles remained viable during 7-day culture in a bovine and human doECM reconstituted using alginate as a hydrogel base[67]. Chiti et al. (2022) demonstrated that alginate hydrogels containing bovine doECM could maintain growth and viability in human preantral follicles similar to alginate-only controls, but this could not be achieved with in hydrogels only containing bovine doECM[68]. When human doECM with Matrigel was used to create hydrogels for murine and human preantral follicle encapsulation and xenotransplantation, 39% of follicles reached the antral stage[69]. Despite evidence indicating doECM can sustain follicle viability, it can present issues with immunoreactivity when transplanted and has inconsistency in biochemical profile.

Synthetic biomaterials

Biomaterials made by synthetically derived substances have become an underscored alternative to natural biomaterials due to their defined composition and customizable chemical and physical properties. Polyethylene glycol (PEG) is a synthetic polymer that is widely used for tissue engineering and biomedical applications such as drug delivery[70,71]. In studies utilizing PEG hydrogels for 3D culture, researchers have fine-tuned various components of the system to optimize its use for specific cell types and purposes. For example, reactive functional groups on PEG arms can be crosslinked using protease-sensitive peptide sequences thus creating a dynamic 3D environment for cells in vitro. In the case of preantral follicles, PEG hydrogels with optimized swelling/gelation time and

crosslinker peptide sequences can be used to enhance mouse follicle culture [72]. Volumetric expansion of the growing follicle, which is particularly important for species such as cattle and humans, is permitted due to the precise degradation of the peptide sequences from follicle-secreted proteolytic enzymes. Upon stimulation with FSH and LH, mouse preantral follicles develop to the antral stage and yield MII oocytes capable of fertilization and early embryo development[72–74]. Furthermore, supplemental feeder cells and bioactive modification of PEG hydrogels can create a culture environment that better mimics in vivo conditions[75] . Preantral follicles co-cultured in PEG hydrogels with adipose-derived stem cells (ADSCs) or cultured in conditioned medium from ADSCs grown in PEG hydrogels have better survival and growth rates compared to follicles without ADSCs or cultured with conditioned medium from 2D ADSC culture, indicating that not only the follicle but also supporting cells benefit from the 3D culture environment[76].

Additionally, when hydrogels are modified with ECM-sequestering and basement membrane binder (BMB) peptides as an attempt to recapitulate the native ECM composition of the ovary, secondary follicles deposit ECM molecules and recreate a cell-matrix microenvironment, therefore promoting follicle development as demonstrated in mice[77]. Recently, the functionalization of PEG hydrogels with BMB peptides incorporated on Dextran fibers led to increased oocyte maturation from mouse primordial follicles compared to inert hydrogels lacking functionalization[78]. As a relatively novel and rising approach to growing preantral follicles in vitro, PEG hydrogels present a promising culturing system that could be tailored to follicles of different stages of development and adapted to the specific growth requirements of various species.

Development of the female gonad and attempts to recapitulate in vitro

The ovary is the gonad of the female and originates from the embryonic mesoderm. After gastrulation, the mesoderm continues lineage differentiation into the lateral plate mesoderm and the paraxial mesoderm at the lateral and medial aspects of the embryo, respectively. Additionally, the intermediate mesoderm arises anatomically between the lateral plate and paraxial mesoderm, ultimately giving rise to the urogenital system, including the gonads. In cattle, gastrulation occurs around embryonic day 14, where the primitive streak ingresses and delineates the nascent mesoderm[76]; however, further characterization of subsequent lineages has not been explored. Studies from rodents and other species show mesoderm specification and its subsequent lineages in response to signaling from several morphogens, including bone-morphogenic proteins (BMPs)[79] and fibroblast growth factors (FGFs)[80]. Concentration gradients of these morphogens govern proper body patterning of the embryo and play an active role in determining cell fate. For instance, the BMP signaling level along an embryo's medio-lateral axis specifies the different mesodermal lineages. Specifically, the absence, low, and high abundance of BMPs leads to the paraxial, intermediate, and lateral plate mesoderm, respectively[81]. The intermediate mesoderm gives rise to the mesonephros, and coelomic epithelium cells lining the ventromedial side of the mesonephros proliferate and ingress to create the genital ridge. Cells from the genital ridge are the precursor somatic support and stromal cells of the female and male gonads. As the genital ridge continues to develop but has not yet entered the sex-determination stage, it is considered the “bipotential gonad” and primordial germ cells begin arriving after migrating from the yolk sac of the embryo, which in cows occur approximately at 20-23 days of

development[82]. Based on the presence or absence of the *Sry* gene located on the Y chromosome, the bipotential gonad is fated to become a testis or ovary, respectively.

Proper gonadal development relies on precise spatiotemporal expression of several genes starting from embryonic gastrulation. The most detailed descriptions of these events come from mouse models. First, differentiation of the intermediate mesoderm requires expression of Odd-skipped related transcription factor (*Osr1*)[83,84] and LIM homeobox protein 1 (*Lhx1*)[85]. The coelomic epithelium, arising from the intermediate mesoderm, appears around embryonic day 9.5 in mice and expresses Wilms tumor suppressor (*Wt1*) and *Gata4*. Indeed, knock-out *Wt1* and *Gata4* mice fail to develop gonads due to a lack of coelomic epithelial cell proliferation, resulting in nonexistent genital ridges[86,87]. Moreover, the interaction of *Gata4* and *Wt1* has been suggested to play a role both before and after the sex-determination phase of gonad development, where GATA4 downregulates ovary-promoting genes in testes, and WT1 maintains gene signatures in a sex-specific manner[88]. Other genes required for initial bipotential gonad formation include nuclear receptor subfamily 5 group A member 1 [*Nr5a1* or steroidogenic factors-1 (*Sf1*)] [89] and LIM homeobox 9 (*Lhx9*)[90,] which both show transcript expression in the urogenital ridge of mice also at embryonic day 9.5. At around embryonic day 11.5-12.0, the bipotential gonad will initiate sexual differentiation to become testes or ovaries based on the presence and expression of the *Sry* gene[91].

Much of today's knowledge of somatic-cell gonad development is based on studies using mouse models. To further understand gonad formation across species and replicate developmental events, researchers have employed pluripotent stem cells (PSCs) to mimic the signature events of gonad differentiation in vitro. The generation of

intermediate mesoderm-like cells has been described by several groups where exposure of human PSCs to the glycogen synthase kinase-3b inhibitor CHIR99021 and sequential exposure to FGF2 and/or retinoic acid yielded cells positive for PAX2 (intermediate mesoderm marker) and LHX1[92,93]. Treatment of PSCs with CHIR99021 activates WNT signaling in a similar manner to in vivo gastrulating cells that are specified to become the mesoderm layer expressing Brachyury[94,95]. Likewise, FGF and retinoic acid treatments mimic the morphogenic stimulus that causes the anterior-posterior body patterning after gastrulation[96,97]. Taken further, human PSCs that are induced to mesoderm-like cells can be subsequently exposed to BMPs to initiate cellular programming to become bipotential gonad-like cells. In conjunction with WNT signaling, modulation of BMP expression is key to driving cells to the bipotential gonad-like phenotype[98]. Specifically, the inhibition and successive activation of BMP signaling is more efficient in upregulating *EMX2*, *GATA4*, *WT1*, and *LHX9* compared to no inhibition but subsequent activation of BMP signaling. Without BMP inhibition, human PSCs instead upregulated lateral plate mesoderm genes[98].

Human fibroblasts can be reprogrammed to iPSCs and used to generate gonadal-like cells after stepwise induction and formation of organoids to drive differentiation. Gutierrez et al. (2018) utilized human iPSCs to create Sertoli-like cells from embryoid bodies co-cultured with human testis tumor NT2D1 feeder cells[99]. To further mimic the development of bipotential gonads and form organoids with distinguishable 3D male-gonad features without feeder cells, Knarston et al. (2020) utilized human iPSCs and drove differentiation first to the intermediate mesoderm fate, then into bipotential gonad-like and Sertoli-cell-like cells[100]. Cells were first cultured as a monolayer in the presence

of CHIR, FGF9, heparin, and BMP4 for 7 days. Then, cells were pelleted to form organoids and guide self-aggregation. After an additional 14 days of culture, cells exhibited a testis-like phenotype. Shin et al. directly differentiated human embryonic stem cells into Leydig-like cells of the testis that expressed key steroidogenic genes and secreted testosterone[101]. In 2023, Gonen et al. reported successful differentiation of human iPSCs to generate Sertoli-like cells that produced AMH, migrated similarly to in vivo epithelial-mesenchymal transition that occurs at the coelomic epithelium and formed tubular structures[102]. To further validate their protocol, they showed that 46 XY human iPSCs containing a phenotypically-abberant NR5A1 variant could not faithfully recapitulate key stages of Sertoli cell differentiation. However, CRISPR/Cas9 correction of the variant rescued the ability of differentiated cells to self-aggregate and form tubular structures following the protocol.

Despite many efforts and reported achievements in generating bipotential gonad or testis-like cells from pluripotent stem cells, there are scarce reports of progress in developing protocols for female gonad-like cells. Due to this lack of a cell culture system and accessibility of *in vivo* samples, investigating molecular mechanisms constituting early differentiation of the female gonad remains difficult to accomplish. In a similar approach to male studies utilizing embryoid bodies, female hESCs can be aggregated and driven to a granulosa cell-like state upon exposure to factors such as BMPs, WNTs, activin A, and FGFs[103]. Other studies have applied transgenic overexpression methods to direct the differentiation of iPSCs into granulosa-like cells and further demonstrated the capacity of these cells to aggregate with human primordial germ cell-like cells and form follicles containing germ-like cells[104]. Specifically, the overexpression of *NR5A1* and

RUNX1 or *RUNX2* was sufficient to generate granulosa-like cells. Yet, others have reported that NR5A1 drives steroidogenic properties in cells but are not explicitly gonad-like in female iPSCs[105]. Hence, further research to understand the developmental processes comprising gonad development would be beneficial when considering the origin of diseases and disorders in sexual development.

Conclusion and Future Directions

Advancements in female reproductive biology research, from OTC to restoring fertility using follicles and *in vitro* systems, have grown exponentially in the last decade. Progress in 1) safeguarding fertility, 2) creating follicle culture systems that are dynamic and biomimetic, and 3) developing early gonad model systems will continue as researchers unravel fundamental biological mechanisms. Importantly, the interplay of each of these facets will facilitate overall progress in bettering female reproductive health in women and other animal species. For example, dissecting the developmental biology of gonadogenesis will provide information for creating an appropriate culture environment to support folliculogenesis *in vitro,* beginning at early follicle stages. This is especially desirable in large mammalian species as most studies have been conducted in mice and translation of applications has been mostly unsuccessful. The overarching endpoint of these studies would be to gain knowledge in ovary biology such that therapeutic interventions could be implemented. The interventions may include creating oocytes for embryo production, reinstating the endocrine function of the ovary, providing methods to do toxicology and contraception testing, and modeling disorders of sex development. As accurate biological information becomes available from future studies examining the early

stages of gonadal- and folliculogenesis, researchers and clinicians can harness the preservation and restoration of female gonadal tissue and gametes.

REFERENCES

1. Oktem, O. & Oktay, K. The Ovary. *Ann N Y Acad Sci* **1127**, 1–9 (2008).

2. Kidder, G. M. & Vanderhyden, B. C. Bidirectional communication between oocytes and follicle cells: ensuring oocyte developmental competence. *Can J Physiol Pharmacol* **88**, 399–413 (2010).

3. Gougeon, A. Regulation of Ovarian Follicular Development in Primates: Facts and Hypotheses. *Endocr Rev* **17**, 121–155 (1996).

4. Choi, Y. & Rajkovic, A. Genetics of early mammalian folliculogenesis. *Cellular and Molecular Life Sciences* **63**, 579 (2006).

5. Hsueh, A. J. W., Kawamura, K., Cheng, Y. & Fauser, B. C. J. M. Intraovarian control of early folliculogenesis. *Endocr Rev* **36**, 1–24 (2015).

6. Li, J. *et al.* Activation of dormant ovarian follicles to generate mature eggs. *Proc Natl Acad Sci U S A* **107**, 10280–10284 (2010).

7. Sato, Y. & Kawamura, K. Rapamycin treatment maintains developmental potential of oocytes in mice and follicle reserve in human cortical fragments grafted into immune-deficient mice. *Mol Cell Endocrinol* **504**, 110694 (2020).

8. Dou, X. *et al.* Short-term rapamycin treatment increases ovarian lifespan in young and middle-aged female mice. *Aging Cell* **16**, 825–836 (2017).

9. Adhikari, D. *et al.* Tsc/mTORC1 signaling in oocytes governs the quiescence and activation of primordial follicles. *Hum Mol Genet* **19**, 397–410 (2010).

10. Kawamura, K. *et al.* Hippo signaling disruption and Akt stimulation of ovarian follicles for infertility treatment. *Proceedings of the National Academy of Sciences* **110**, 17474–17479 (2013).

11. Hardy, K. *et al.* Onset and heterogeneity of responsiveness to FSH in mouse preantral follicles in culture. *Endocrinology* **158**, 134–147 (2017).

12. Candelaria, J. I., Rabaglino, M. B. & Denicol, A. C. Ovarian preantral follicles are responsive to FSH as early as the primary stage of development. *Journal of Endocrinology* **247**, 153–168 (2020).

13. Adriaens, I., Cortvrindt, R. & Smitz, J. Differential FSH exposure in preantral follicle culture has marked effects on folliculogenesis and oocyte developmental competence. *Hum Reprod* **19**, 398–408 (2004).

14. Aguiar, F. L. N. *et al.* FSH supplementation to culture medium is beneficial for activation and survival of preantral follicles enclosed in equine ovarian tissue. *Theriogenology* **85**, 1106–1112 (2016).

15. McLaughlin, M. & Telfer, E. E. Oocyte development in bovine primordial follicles is promoted by activin and FSH within a two-step serum-free culture system. *Reproduction* **139**, 971–978 (2010).

16. Dong, J. *et al.* Growth differentiation factor-9 is required during early ovarian folliculogenesis. *Nature* **383**, 531–535 (1996).

17. Galloway, S. M. *et al.* Mutations in an oocyte-derived growth factor gene (BMP15) cause increased ovulation rate and infertility in a dosage-sensitive manner. *Nat Genet* **25**, 279–283 (2000).

18. Liu, C., Peng, J., Matzuk, M. M. & Yao, H. H.-C. Lineage specification of ovarian theca cells requires multicellular interactions via oocyte and granulosa cells. *Nat Commun* **6**, 1–11 (2015).

19. Cowan, R. G. & Quirk, S. M. Cells responding to hedgehog signaling contribute to the theca of ovarian follicles. *Reproduction* **161**, 437–448 (2021).

20. Adashi, E. Y. Endocrinology of the ovary. *Human Reproduction* **9**, 815–827 (1994).

21. Rodgers, R. J. & Irving-Rodgers, H. F. Formation of the Ovarian Follicular Antrum and Follicular Fluid1. *Biol Reprod* **82**, 1021–1029 (2010).

22. Richards, J. S., Russell, D. L., Ochsner, S. & Espey, L. L. Ovulation: new dimensions and new regulators of the inflammatory-like response. *Annu Rev Physiol* **64**, 69–92 (2002).

23. Mehlmann, L. M. Stops and starts in mammalian oocytes: recent advances in understanding the regulation of meiotic arrest and oocyte maturation. *Reproduction* **130**, 791–799 (2005).

24. Donnez, J. & Dolmans, M.-M. Ovarian cortex transplantation: 60 reported live births brings the success and worldwide expansion of the technique towards routine clinical practice. *J Assist Reprod Genet* **32**, 1167–1170 (2015).

25. Dolmans, M. M. *et al.* Transplantation of cryopreserved ovarian tissue in a series of 285 women: a review of five leading European centers. *Fertil Steril* **115**, 1102–1115 (2021).

26. Parkes, A. S. & Smith, A. U. Regeneration of rat ovarian tissue grafted after exposure to low temperatures. *Proceedings of the Royal Society of London. Series B-Biological Sciences* **140**, 455–470 (1953).

27. Lee, S. *et al.* Comparison between slow freezing and vitrification for human ovarian tissue cryopreservation and xenotransplantation. *Int J Mol Sci* **20**, (2019).

28. Herraiz, S. *et al.* Improving ovarian tissue cryopreservation for oncologic patients: Slow freezing versus vitrification, effect of different procedures and devices. *Fertil Steril* **101**, (2014).

29. Isachenko, E., Isachenko, V., Rahimi, G. & Nawroth, F. Cryopreservation of human ovarian tissue by direct plunging into liquid nitrogen. *European Journal of Obstetrics & Gynecology and Reproductive Biology* **108**, 186–193 (2003).

30. Gandolfi, F. *et al.* Efficiency of equilibrium cooling and vitrification procedures for the cryopreservation of ovarian tissue: comparative analysis between human and animal models. *Fertil Steril* **85**, 1150–1156 (2006).

31. Bordes, A. *et al.* Normal gestations and live births after orthotopic autograft of vitrified–warmed hemi-ovaries into ewes. *Human Reproduction* **20**, 2745–2748 (2005).

32. Kagawa, N., Silber, S. & Kuwayama, M. Successful vitrification of bovine and human ovarian tissue. *Reprod Biomed Online* **18**, 568–577 (2009).

33. Suzuki, N. *et al.* Successful fertility preservation following ovarian tissue vitrification in patients with primary ovarian insufficiency. *Human Reproduction* **30**, 608–615 (2015).

34. Wang, T. *et al.* Human single follicle growth in vitro from cryopreserved ovarian tissue after slow freezing or vitrification. *Human Reproduction* **31**, 763–773 (2016).

35. Shi, Q., Xie, Y., Wang, Y. & Li, S. Vitrification versus slow freezing for human ovarian tissue cryopreservation: A systematic review and meta-anlaysis. *Sci Rep* **7**, 1–9 (2017).

36. Pegg, D. E. The relevance of ice crystal formation for the cryopreservation of tissues and organs. *Cryobiology* **60**, S36–S44 (2010).

37. Bank, H. Freezing injury in tissue cultured cells as visualized by freeze-etching. *Exp Cell Res* **85**, 367–376 (1974).

38. Gurtovenko, A. A. & Anwar, J. Modulating the structure and properties of cell membranes: the molecular mechanism of action of dimethyl sulfoxide. *J Phys Chem B* **111**, 10453–10460 (2007).

39. Ouni, E. *et al.* A blueprint of the topology and mechanics of the human ovary for next-generation bioengineering and diagnosis. *Nat Commun* **12**, (2021).

40. Hummitzsch, K. *et al.* Transcriptome analyses of ovarian stroma: tunica albuginea, interstitium and theca interna. *Reproduction* **157**, 545–565 (2019).

41. Eppig, J. J. & O'Brien, M. J. Development in vitro of mouse oocytes from primordial follicles. *Biol Reprod* **54**, 197–207 (1996).

42. Xu, M. *et al.* Encapsulated Three-Dimensional Culture Supports Development of Nonhuman Primate Secondary Follicles1. *Biol Reprod* **81**, 587–594 (2009).

43. Xu, M., Banc, A., Woodruff, T. K. & Shea, L. D. Secondary follicle growth and oocyte maturation by culture in alginate hydrogel following cryopreservation of the ovary or individual follicles. *Biotechnol Bioeng* **103**, 378–386 (2009).

44. West, E. R., Shea, L. D. & Woodruff, T. K. Engineering the follicle microenvironment. *Semin Reprod Med* **25**, 287–299 (2007).

45. Hornick, J. E., Duncan, F. E., Shea, L. D. & Woodruff, T. K. Isolated primate primordial follicles require a rigid physical environment to survive and grow in vitro. *Hum Reprod* **27**, 1801–1810 (2012).

46. Parkes, W. S. *et al.* Hyaluronan and Collagen Are Prominent Extracellular Matrix Components in Bovine and Porcine Ovaries. *Genes* vol. 12 Preprint at https://doi.org/10.3390/genes12081186 (2021).

47. Berkholtz, C. B., Shea, L. D. & Woodruff, T. K. Extracellular matrix functions in follicle maturation. *Semin Reprod Med* **24**, 262–269 (2006).

48. Hartanti, M. D. *et al.* Morphometric and gene expression analyses of stromal expansion during development of the bovine fetal ovary. *Reprod Fertil Dev* **31**, 482–495 (2019).

49. Torrance, C., Telfer, E. & Gosden, R. G. Quantitative study of the development of isolated mouse pre-antral follicles in collagen gel culture. *J Reprod Fertil* **87**, 367–374 (1989).

50. Abir, R. *et al.* Morphological study of fully and partially isolated early human follicles. *Fertil Steril* **75**, 141–146 (2001).

51. Joo, S. *et al.* The effect of collagen hydrogel on 3D culture of ovarian follicles. *Biomedical Materials* **11**, 65009 (2016).

52. Schotanus, K., Hage, W. J., Vanderstichele, H. & van den Hurk, R. Effects of conditioned media from murine granulosa cell lines on the growth of isolated bovine preantral follicles. *Theriogenology* **48**, 471–483 (1997).

53. Itoh, T. & Hoshi, H. Efficient isolation and long-term viability of bovine small preantral follicles in vitro. *In Vitro Cell Dev Biol Anim* **36**, 235–240 (2000).

54. Higuchi, C. M., Maeda, Y., Horiuchi, T. & Yamazaki, Y. A Simplified Method for Three-Dimensional (3-D) Ovarian Tissue Culture Yielding Oocytes Competent to Produce Full-Term Offspring in Mice. *PLoS One* **10**, e0143114 (2015).

55. Oktem, O. & Oktay, K. The role of extracellular matrix and activin-A in in vitro growth and survival of murine preantral follicles. *Reproductive Sciences* **14**, 358–366 (2007).

56. Vanacker, J. & Amorim, C. A. Alginate: A Versatile Biomaterial to Encapsulate Isolated Ovarian Follicles. *Ann Biomed Eng* **45**, 1633–1649 (2017).

57. West-Farrell, E. R. *et al.* The mouse follicle microenvironment regulates antrum formation and steroid production: Alterations in gene expression profiles. *Biol Reprod* **80**, 432–439 (2009).

58. Songsasen, N., Woodruff, T. K. & Wildt, D. E. In vitro growth and steroidogenesis of dog follicles as influenced by the physical and hormonal microenvironment. *Reproduction* **142**, 113 (2011).

59. Park, K. E. *et al.* Effects of alginate hydrogels on in vitro maturation outcome of mouse preantral follicles. *Tissue Eng Regen Med* **9**, 170–174 (2012).

60. Amorim, C. A., Van Langendonckt, A., David, A., Dolmans, M.-M. & Donnez, J. Survival of human pre-antral follicles after cryopreservation of ovarian tissue, follicular isolation and in vitro culture in a calcium alginate matrix. *Human Reproduction* **24**, 92–99 (2009).

61. Kreeger, P. K., Deck, J. W., Woodruff, T. K. & Shea, L. D. The in vitro regulation of ovarian follicle development using alginate-extracellular matrix gels. *Biomaterials* **27**, 714–723 (2006).

62. Shikanov, A., Xu, M., Woodruff, T. K. & Shea, L. D. Interpenetrating fibrin–alginate matrices for in vitro ovarian follicle development. *Biomaterials* **30**, 5476–5485 (2009).

63. Xu, J. *et al.* Fibrin promotes development and function of macaque primary follicles during encapsulated three-dimensional culture. *Hum Reprod* **28**, 2187–2200 (2013).

64. Brito, I. R. *et al.* Fibrin–alginate hydrogel supports steroidogenesis, in vitro maturation of oocytes and parthenotes production from caprine preantral follicles cultured in group. *Reproduction in Domestic Animals* **51**, 997–1009 (2016).

65. Choi, J. K., Agarwal, P., Huang, H., Zhao, S. & He, X. The crucial role of mechanical heterogeneity in regulating follicle development and ovulation with engineered ovarian microtissue. *Biomaterials* **35**, 5122–5128 (2014).

66. Parmaksiz, M., Dogan, A., Odabas, S., Elçin, A. E. & Elçin, Y. M. Clinical applications of decellularized extracellular matrices for tissue engineering and regenerative medicine. *Biomedical Materials* **11**, 22003 (2016).

67. Nikniaz, H. *et al.* Comparing various protocols of human and bovine ovarian tissue decellularization to prepare extracellular matrix-alginate scaffold for better follicle development in vitro. *BMC Biotechnol* **21**, 8 (2021).

68. Chiti, M.-C. *et al.* Ovarian extracellular matrix-based hydrogel for human ovarian follicle survival in vivo: A pilot work. *J Biomed Mater Res B Appl Biomater* **110**, 1012–1022 (2022).

69. Pors, S. E. *et al.* Initial steps in reconstruction of the human ovary: survival of pre-antral stage follicles in a decellularized human ovarian scaffold. *Human Reproduction* **34**, 1523–1535 (2019).

70. Peppas, N. A., Keys, K. B., Torres-Lugo, M. & Lowman, A. M. Poly(ethylene glycol)-containing hydrogels in drug delivery. *Journal of Controlled Release* **62**, 81–87 (1999).

71. Bhattarai, S. R. *et al.* Novel biodegradable electrospun membrane: scaffold for tissue engineering. *Biomaterials* **25**, 2595–2602 (2004).

72. Shikanov, A., Smith, R. M., Xu, M., Woodruff, T. K. & Shea, L. D. Hydrogel network design using multifunctional macromers to coordinate tissue maturation in ovarian follicle culture. *Biomaterials* **32**, 2524–2531 (2011).

73. Ihm, J. E., Lee, S. T., Han, D. K., Lim, J. M. & Hubbell, J. A. Murine ovarian follicle culture in PEG-hydrogel: Effects of mechanical properties and the hormones FSH and LH on development. *Macromol Res* **23**, 377–386 (2015).

74. Ahn, J. Il *et al.* Culture of preantral follicles in poly(ethylene) glycol-based, three-dimensional hydrogel: a relationship between swelling ratio and follicular developments. *J Tissue Eng Regen Med* **9**, 319–323 (2015).

75. Kim, J. *et al.* Characterization of the crosslinking kinetics of multi-arm poly(ethylene glycol) hydrogels formed via Michael-type addition. *Soft Matter* **12**, 2076–2085 (2016).

76. Tomaszewski, C. E. *et al.* Adipose-derived stem cell-secreted factors promote early stage follicle development in a biomimetic matrix. *Biomater Sci* **7**, 571–580 (2019).

77. Tomaszewski, C. E., DiLillo, K. M., Baker, B. M., Arnold, K. B. & Shikanov, A. Sequestered cell-secreted extracellular matrix proteins improve murine folliculogenesis and oocyte maturation for fertility preservation. *Acta Biomater* **132**, 313–324 (2021).

78. Nason-Tomaszewski, C. E., Thomas, E. E., Matera, D. L., Baker, B. M. & Shikanov, A. Extracellular matrix-templating fibrous hydrogels promote ovarian tissue remodeling and oocyte growth. *Bioact Mater* **32**, 292–303 (2024).

79. Winnier, G., Blessing, M., Labosky, P. A. & Hogan, B. L. M. Bone morphogenetic protein-4 is required for mesoderm formation and patterning in the mouse. *Genes Dev* **9**, 2105–2116 (1995).

80. Schulte-Merker, S. & Smith, J. C. Mesoderm formation in response to Brachyury requires FGF signalling. *Current Biology* **5**, 62–67 (1995).

81. James, R. G. & Schultheiss, T. M. Bmp signaling promotes intermediate mesoderm gene expression in a dose-dependent, cell-autonomous and translation-dependent manner. *Dev Biol* **288**, 113–125 (2005).

82. Wrobel, K.-H. & Süß, F. Identification and temporospatial distribution of bovine primordial germ cells prior to gonadal sexual differentiation. *Anat Embryol (Berl)* **197**, 451–467 (1998).

83. So, P. L. & Danielian, P. S. Cloning and expression analysis of a mouse gene related to Drosophila odd-skipped. *Mech Dev* **84**, 157–160 (1999).

84. Wang, Q., Lan, Y., Cho, E. S., Maltby, K. M. & Jiang, R. Odd-skipped related 1 (Odd 1) is an essential regulator of heart and urogenital development. *Dev Biol* **288**, 582–594 (2005).

85. Shawlot, W. & Behringer, R. R. Requirement for LIml in head-organizer function. *Nature* **374**, 425–430 (1995).

86. Wilhelm, D. & Englert, C. The Wilms tumor suppressor WT1 regulates early gonad development by activation of Sf1. *Genes Dev* **16**, 1839–1851 (2002).

87. Hu, Y.-C., Okumura, L. M. & Page, D. C. Gata4 Is Required for Formation of the Genital Ridge in Mice. *PLoS Genet* **9**, e1003629 (2013).

88. Rudigier, L. J., Dame, C., Scholz, H. & Kirschner, K. M. Ex vivo cultures combined with vivo-morpholino induced gene knockdown provide a system to assess the role of WT1 and GATA4 during gonad differentiation. *PLoS One* **12**, e0176296 (2017).

89. Luo, X., Ikeda, Y. & Parker, K. L. A cell-specific nuclear receptor is essential for adrenal and gonadal development and sexual differentiation. *Cell* **77**, 481–490 (1994).

90. Birk, O. S. *et al.* The LIM homeobox gene Lhx9 is essential for mouse gonad formation . *Nature* **403**, 909–913 (2000).

91. Hacker, A., Capel, B., Goodfellow, P. & Lovell-Badge, R. Expression of Sry, the mouse sex determining gene. *Development* **121**, 1603–1614 (1995).

92. Lam, A. Q. *et al.* Rapid and efficient differentiation of human pluripotent stem cells into intermediate mesoderm that forms tubules expressing kidney proximal tubular markers. *Journal of the American Society of Nephrology* **25**, 1211–1225 (2014).

93. Kumar, N. *et al.* Generation of an expandable intermediate mesoderm restricted progenitor cell line from human pluripotent stem cells. *Elife* **4**, 1–24 (2015).

94. Lindsley, R. C., Gill, J. G., Kyba, M., Murphy, T. L. & Murphy, K. M. Canonical Wnt signaling is required for development of embryonic stem cell-derived mesoderm. *Development* **133**, 3787–3796 (2006).

95. Zhao, M., Tang, Y., Zhou, Y. & Zhang, J. Deciphering Role of Wnt Signalling in Cardiac Mesoderm and Cardiomyocyte Differentiation from Human iPSCs: Four-dimensional control of Wnt pathway for hiPSC-CMs differentiation. *Sci Rep* **9**, 19389 (2019).

96. Deimling, S. J. & Drysdale, T. A. Fgf is required to regulate anterior–posterior patterning in the Xenopus lateral plate mesoderm. *Mech Dev* **128**, 327–341 (2011).

97. Kudoh, T., Wilson, S. W. & Dawid, I. B. Distinct roles for Fgf, Wnt and retinoic acid in posteriorizing the neural ectoderm. *Development* **129**, 4335–4346 (2002).

98. Sepponen, K. *et al.* The role of sequential BMP signaling in directing human embryonic stem cells to bipotential gonadal cells. *Journal of Clinical Endocrinology and Metabolism* **102**, 4303–4314 (2017).

99. Rodríguez Gutiérrez, D., Eid, W. & Biason-Lauber, A. A Human Gonadal Cell Model From Induced Pluripotent Stem Cells. *Front Genet* **9**, (2018).

100. Knarston, I. M. *et al.* An In Vitro Differentiation Protocol for Human Embryonic Bipotential Gonad and Testis Cell Development. *Stem Cell Reports* **15**, 1377–1391 (2020).

101. Shin, E.-Y., Park, S., Choi, W. Y. & Lee, D. R. Rapid Differentiation of Human Embryonic Stem Cells into Testosterone-Producing Leydig Cell-Like Cells In vitro. *Tissue Eng Regen Med* **18**, 651–662 (2021).

102. Gonen, N. *et al.* In vitro cellular reprogramming to model gonad development and its disorders. *Sci Adv* **9**, (2023).

103. Lan, C.-W., Chen, M.-J., Jan, P.-S., Chen, H.-F. & Ho, H.-N. Differentiation of Human Embryonic Stem Cells Into Functional Ovarian Granulosa-like Cells. *J Clin Endocrinol Metab* **98**, 3713–3723 (2013).

104. Smela, M. D. P. *et al.* Directed differentiation of human iPSCs to functional ovarian granulosa-like cells via transcription factor overexpression. *Elife* **12**, (2023).

105. Danti, L. *et al.* CRISPR/Cas9-mediated activation of NR5A1 steers female human embryonic stem cell-derived bipotential gonadal-like cells towards a steroidogenic cell fate. *J Ovarian Res* **16**, 194 (2023).

CHAPTER 2

Assessment of Ovarian Tissue and Follicular Integrity After Cryopreservation Via Slow Freezing or Vitrification Followed By *In vitro* Culture

Published in Fertility and Sterility Science

Candelaria, Juliana I. et al. F&S Science, Volume 5, Issue 2, 154 - 162

Abstract

Ovarian tissue cryopreservation (OTC) is a promising fertility safeguarding method as it preserves the abundant preantral follicle population. Slow freezing and vitrification are two methods of OTC and have shown conflicting results in terms of success across species. Furthermore, culturing ovarian tissue after it has been thawed could circumvent the requirement to surgically transplant tissue for further promoting folliculogenesis. In this study, the objective was to evaluate ovarian tissue and follicle integrity before and after slow freezing or vitrification and post-thawing in-vitro culture. Bovine ovarian cortical tissue was subjected to either slow freezing or vitrification and subsequent in-vitro culture. Tissue and follicle integrity were assessed before and after cryopreservation and culture. Hematoxylin and eosin staining was used to assess follicle stages and morphology and stromal cell density. TUNEL staining was used to examine apoptosis and Masson's trichrome staining was used to evaluate collagen content in stromal environment. Immunofluorescent staining was used to localize and quantify connexin 37 and Ki67 expression. We found that regardless of previous cryopreservation, ovarian tissue culture resulted in a decreased percentage of primordial and increased percentage of primary follicles compared to fresh tissue, indicating that follicle activation was not negatively affected by cryopreservation. However, both culture and cryopreservation followed by culture decreased the percentage of normal preantral follicles when compared to fresh tissue that had not been cultured. Culture and/or cryopreservation did not impact stromal cell number, but there was increased cell apoptosis in tissue that was cultured following vitrification compared to tissue that was not cultured. Tissue culture regardless of cryopreservation resulted in decreased collagen deposition. There were less follicles

expressing connexin 37 in vitrified and thawed tissue compared to all other treatments. Cryopreservation and/or culture of ovarian tissue did not change the percentage of follicles that contained Ki67-positive granulosa cells or the percentage of Ki67-positive granulosa cells within those follicles. Based on these data, we conclude that tissue cryopreservation followed by culture does not affect follicle activation and growth, but it decreases the proportion of viable follicles within the tissue. Slow freezing was superior to vitrification as indicated by a greater proportion of follicles with normal morphology, lower stromal cell apoptosis, and maintenance of connexin 37 expression post-thawing and after culture.

Introduction

A common adverse effect of cancer therapies is decreased fertility that often leads to premature ovarian insufficiency. With a rise in both incidence and survival rates of cancer in females[1-3], there is greater emphasis on post-treatment quality-of-life care which includes fertility preservation options. Often, cancer treatment cannot be delayed until ovarian stimulation and oocyte retrieval are performed for oocyte or embryo cryopreservation. Furthermore, exposure to ovary-stimulating hormones to retrieve oocytes is often contraindicated particularly in prepubertal girls. Therefore, ovarian tissue cryopreservation (OTC) becomes an emerging option to preserve the ovarian follicular reserve. Indeed, the American Society for Reproductive Medicine no longer considers OTC to be experimental and thus this technique can be used when ovarian stimulation is not possible[4].

Ovarian tissue cryopreservation is performed via slow freezing or vitrification. Slow freezing has been the standard approach due to its success in restoring endocrine function and notable pregnancy and birth rates post-transplantation[5]. During slow freezing, cortical tissue fragments are exposed to low concentrations of cryoprotectant agents such as dimethyl sulfoxide (DMSO) or ethylene glycol (EG), and then exposed to slowly, controlled decreasing temperatures. As a result, the tissue is gradually dehydrated and less likely to endure ice crystal formation. In comparison, vitrification is an ultra-fast cryopreservation technique that uses a mixture of different cryoprotectants at high concentrations and ultra-rapid cooling of tissue by direct immersion in liquid nitrogen. However, the complex structure of ovarian tissue creates a barrier for proper heat and mass transfer that is essential to successful vitrification[6]. Various studies have compared

the efficacy of slow freezing and vitrification but show conflicting results likely because of variation in protocols, species studied, and endpoints examined[7-12].

Autotransplantation of thawed ovarian tissue permits in vivo follicle development, however this approach risks reintroducing malignant cells to the patient. As an alternative, in vitro follicle development from frozen-thawed tissue has gained widespread research interest. Yet, large knowledge gaps exist regarding the cellular and molecular consequences of cryopreservation by either technique after thawing and in vitro culture. In fact, there are no reports of successful production of competent oocytes, let alone healthy birth, from post-thawing in vitro cultured human ovarian tissue likely due to limited understanding of how OTC impacts the ovarian microenvironment. For instance, changes to the extracellular matrix (ECM) caused by OTC are often overlooked, despite its dynamic role in folliculogenesis. The collagen-rich ECM interacts with various cells to promote differentiation, migration, and provide mechanical support[13]. Additionally, the communication between the oocyte and surrounding granulosa cells through gap junctions is imperative to follicle development by facilitating the movement of signaling molecules and metabolites[14,15]. Connexin 37 (CX37) is a major gap junction protein present between the oocyte and granulosa cells[16] that has been shown to be impacted by the process of cryopreservation in mice[17]. The human ovary ECM composition and follicular dynamics more closely resembles large mammals such as the bovine, compared to the mouse[18-20] underscoring the importance of utilizing the cow as the model for this research. The impact of tissue and follicle culture, with or without cryopreservation, on the quality and developmental potential of the resulting oocyte is still not completely understood, partially due to the lack of culture conditions that promote follicle growth in

humans and large animal species. In order for ovarian tissue and follicle culture to be an efficient assisted reproductive technology, clinical outcomes must be associated with detailed cellular and molecular evaluation of the gametes and their surrounding tissue.

Therefore, this study aimed to compare the integrity of slow-frozen and vitrified ovarian tissue post-thawing and culturing for 5 days. We used published cryopreservation protocols that reported success based on high follicle viability or a live birth from bovine or human tissue. Here we demonstrate the consequences of cryopreservation to cellular and molecular aspects of the oocyte, granulosa cells, stromal cells, and the ECM of ovarian tissue.

Material and methods

Materials were purchased from Fisher Scientific unless otherwise noted. Bovine ovaries were sourced from healthy cows at reproductive age at a local USDA-inspected abattoir; therefore, no live animals were used and no animal care and use protocol was required.

Ovarian tissue processing

Ovaries were transported in saline solution at room temperature (RT). Ovaries with visible small antral follicles were washed with phosphate-buffered saline (PBS) with 100 IU penicillin, 100 µg/mL streptomycin (pen/strep). Ovarian cortex, void of corpora lutea or large antral follicles was fragmented into pieces of 3 x 5 x 1 mm. Four ovaries from independent collections were used. Each ovary yielded 12 pieces of tissue, totaling 48 fragments. Fragments were held in cortex wash medium (TCM199 containing 3 mg/mL

BSA, 25 mM HEPES, 1 mM sodium pyruvate, 100 nM non-essential amino acids, pen/strep) during fragmentation. Eight fragments were randomly assigned to different treatments: fresh-no-culture (FN), fresh-culture (FC), slow-frozen thaw-only (ST), vitrified thaw-only (VT), slow-frozen-culture (SC), or vitrified-culture (VC). Fresh-no-culture tissue fragments were immediately fixed in 10% neutral buffered formalin (NBF). Cultured tissue was maintained in vitro for 5 days as detailed below.

Slow freeze protocol

Tissue was slow frozen following a published protocol[21] with small modifications. Briefly, cortical fragments were placed in cryovials and equilibrated in slow freezing medium [α-MEM base with 1.5M dimethyl sulfoxide (DMSO) and 10% (v/v) fetal bovine serum (FBS)] for 20 minutes at 20°C. Then, the tissue underwent controlled slow freezing using a programmable slow freezer (Cryologic CL-5500, Victoria, Australia) beginning at 20 °C and decreasing at 2°C/min to −7°C, seeded and held at −7°C for 10 minutes, and then cooled at 0.3°C/min to −38°C. Finally, cryovials were plunged in liquid nitrogen and stored for one month.

Vitrification protocol

Tissue fragments were vitrified following published protocols[22,23] with small modifications. First, fragments were equilibrated in cryoprotectant solution [α-MEM base with 7.5% (v/v) DMSO, 7.5% (v/v) ethylene glycol, and 20% (v/v) FBS] for 5 minutes. Then, fragments were transferred into vitrification medium [α-MEM base with 15% (v/v) DMSO, 15% (v/v) ethylene glycol, and 20% (v/v) FBS] for 1-2 minutes before being loaded onto a Cryosupport device and plunged into liquid nitrogen. The Cryosupport device was

adapted by Suzuki et al. Once vitrified, the tissue on the Cryosupport device was inserted into a cryovial and stored in liquid nitrogen for 1 month.

Thawing protocol

Slow-frozen vials were taken out of liquid nitrogen and exposed to RT for 1 minute. Then, the vials were placed in a water bath at 37°C until medium was melted. The tissue was placed in 3 washes of slow frozen thawing medium (α-MEM with 10% FBS) to remove the cryoprotectant. Tissue on the Cryosupport device was submerged in 38.5°C warming solution (α-MEM with 20% FBS) for 30 seconds, then transferred to 3 washes of RT warming solution. For both cryopreservation techniques, the tissue was washed with PBS prior to being cultured or fixed overnight in 10% NBF.

Ovarian cortex tissue culture

Tissue was cultured for 5 days on well insert membranes (2 pieces per well) inside six-well plates containing culture medium (α-MEM with Glutamax containing 3 mg/mL BSA, 10 mg/L insulin, 5.5 mg/L transferrin, 6.7 µg/L selenious acid, pen/strep, 100 nM non-essential amino acids, 50 µg/mL ascorbic acid) supplemented with 100 ng/mL of human recombinant FSH (RayBiotech, Peachtree Corners, GA, USA) at 38.5°C and 5% CO_2 in air. Medium was changed every day. Tissue was washed with PBS after culture and fixed in 10% NBF overnight.

Histological evaluation of follicle and stromal population

Tissue samples embedded in paraffin and sliced into 6-µm thick sections. A total of 540 µm of tissue was analyzed per sample. Sections were stained with H&E and only follicles where the oocyte nucleus was visible were counted. Follicles classified as

morphologically normal had an intact basement membrane, no pyknotic nuclei, spherical oocyte, and no vacuoles present. Follicles were classified as abnormal if any of the previous criteria were not met. Follicles were categorized by developmental stage using published classifications[24]. Proportions of normal and abnormal follicles and follicles at each stage of development were calculated. Stromal cell density was measured by averaging the number of cell nuclei in six random 10,000 μm^2 fields void of follicles after images were captured using a brightfield microscope (Revolve, Echo Labs, San Diego, CA, USA).

Terminal deoxynucleotidyl transferase dUTP nick end labeling (TUNEL) assay

Apoptotic stromal cells were assessed using the TUNEL-based assay ApopTag® Peroxidase In-Situ Apoptosis Detection Kit (EMD Millipore Corporation, Temecula, CA, USA) following manufacturer's instructions. DNAse-treated tissue was used as a positive control and samples without TdT as a negative control. Apoptotic cells were counted in ten random 10,000 μm^2 fields void of follicles. Proportion of apoptotic cells were calculated by dividing positive cells by total nuclei in each field and averaged.

Masson's Trichrome stain

Sections were subjected to Masson's Trichrome stain using Trichrome Stain Kit (Abcam, Boston, MA, USA) following manufacturer's instructions. Images were captured using an inverted brightfield microscope (Revolve). Employing a previously published protocol[25] collagen intensity was quantified by averaging the intensity in six random 51,000 μm^2 fields that included the epithelium and tunica albuginea using ImageJ software (National Institutes of Health).

Immunofluorescent detection of Ki67 and Connexin 37

Fragments were frozen in OCT, sectioned into 12-µm slices, and placed on slides. Immunofluorescent detection was carried out as previously described[26] using 0.5 µg/mL rabbit anti-human CX37 (ab181701, Abcam) or 1 µg/mL rabbit anti-human Ki67 (ab15580, Abcam) antibody overnight at 4°C. Rabbit isotype IgG or no primary antibody were used as negative controls. CX37 expression intensity in the oocyte was measured using ImageJ. Follicles with Ki67-positive granulosa cells were considered "Ki67-positive" and quantified. The proportion of granulosa cells that were Ki67-positive was calculated in follicles that contained at least one Ki67-positive cell.

Statistical analysis

Statistical analysis was performed using RStudio software. Data normality was tested using Shapiro-Wilk test. When appropriate, proportion data was logit-transformed before analysis and then converted to percentages. Normally distributed data was analyzed using ANOVA including the effect of treatment and replicate. Tukey was used as a post-hoc test as needed. Data that were not normally distributed were log-transformed or subjected to a Kruskal-Wallis nonparametric test with pairwise comparisons using Dunn's test. Results are displayed as mean ± SEM. Comparisons associated with a P value <0.05 were considered significant.

Results

A total of 698 follicles were analyzed across treatments and replicates (primordial = 291, primary = 293, early secondary = 114).

Follicle stages and morphology

All preantral follicle stages found in the ovarian cortical fragments (primordial, primary, and early secondary) were represented across all treatments. As expected, there was a greater percentage ($P < 0.05$) of primordial follicles in ovary fragments that were not cultured compared to cultured (Figure 1.1A). There was no difference in the percentage of primordial follicles between FN tissue and after thawing ST (P=0.43) or VT tissue (P = 0.71). In contrast, cultured tissue had a greater percentage ($P < 0.05$) of primary follicles compared to non-cultured tissue. Similarly, there was no difference in the percentage of primary follicles between FC and SC (P = 0.94), or VC tissue (P = 0.96), indicating that primordial follicle activation in culture occurred similarly in cryopreserved and fresh cultured tissue. There was no difference in the percentage of early secondary follicles across all treatment groups (P = 0.08). When analyzing normal follicles exclusively (all stages combined; Figure 1.1B), we first found that FC had decreased ($P < 0.05$) percentage of normal follicles compared to FN. When comparing cultured tissue, FC and SC tissue had similar percentages of normal (P = 0.26), indicating the slow freezing process did not further decrease follicle viability compared with tissue that was not frozen. However, VC tissue had a lower percentage of normal follicles compared to FC ($P < 0.05$). After thawing, ST and VT had similar percentages of normal follicles (P=0.61), but both were lower than FN ($P < 0.05$). Culturing tissue after thawing (SC and VC) did not change the percentage of normal follicles compared to freeze-thaw only (ST vs SC, P = 0.80; VT vs VC, P = 0.37).

Next, we aimed to understand how cryopreservation and culture impacted the morphology of follicles of different stages. We conducted this analysis such that

uncultured (FN, ST, and VT) tissue was compared together and cultured (FC, SC, and VC) were compared together due to the effect of culture on follicle stage (Figure 1.1C and D). We found that, compared to FN, both ST and VT had decreased percentages of normal primordial ($P < 0.05$) and early secondary follicles ($P < 0.05$). However, primary follicles maintained normal morphology post-thawing in both cryopreservation techniques ($P < 0.05$). When examining normality of follicles after culture, we found that VC had a lower percentage ($P < 0.05$) of normal primordial follicles compared to FC and VC. Between culture treatments, there was no difference in percentage of normal primary follicles ($P = 0.174$) or early secondary follicles ($P = 0.10$). Representative images of normal and abnormal follicles are shown in Figure 1.1E.

Stromal cell and TUNEL-positive cell count

There was no difference in the number of stromal cells between treatments ($P = 0.22$; Figure 1.2A). The percentage of apoptotic stromal cells was higher in VC tissue compared to FN ($P < 0.05$; Figure 1.2B and C). All other treatments had similar proportion of apoptotic cells as found in FN tissue.

Masson's trichrome staining

Overall, we found that culturing tissue decreased collagen content, regardless of previous cryopreservation by either technique (Figure 1.3A and B**)**. Fresh-no-culture tissue had greater collagen content compared to FC ($P < 0.05$). Similarly, ST and VT had greater collagen intensity compared to SC and VC, respectively ($P < 0.05$). There was no difference in collagen intensity between FN and ST or VT ($P = 0.90$), confirming that culture was the main driver of collagen loss. Likewise, there was no difference in the

collagen intensity between FC and SC or VC (FC vs SC; $P = 0.99$, FC vs VC; $P = 0.83$).

Connexin 37 expression

We found expression of CX37 mainly in the ooplasm (Figure 1.4A). Interestingly, we noted that 25% of the follicles in VT tissue lacked expression of CX37 compared to 10% or less for all other treatments (Figure 1.4B). There was no difference in expression level between FN and FC tissue ($P = 1.0$) and ST and SC ($P = 1.0$; Figure 1.4C). Vitrified culture tissue had greater CX37 staining intensity compared to (VT) ($P < 0.001$).

Ki67 expression

We found Ki67-positive GCs in all culture treatments (Figure 1.4D). We found the highest percentage of follicles that had Ki67-positive cells in FC tissue (Figure 1.4E). Despite having a numerically lower percentage of Ki67-positive follicles, no difference was found in SC and VC compared to FC (P=0.17). In follicles that showed Ki67-positive GCs, there was also no difference in the percentage of Ki67-positive GCs within that follicle (Figure 1.4E). Overall, previous cryopreservation by either slow freezing or vitrification did not affect the ability of preantral follicle GCs to proliferate during in vitro culture.

Discussion

Ovarian tissue cryopreservation is an efficient method of safeguarding fertility in young female cancer patients by maximizing use of the ovarian reserve[27]. In a clinical setting, ovarian tissue can be biopsied or isolated after an ovariectomy and subjected to

cryopreservation. Moreover, culturing tissue in vitro after cryopreservation to promote follicle development circumvents the need of surgically transplanting tissue back into a patient. Given the enormous potential but still inconsistent success with the use of ovarian tissue cryopreservation as an assisted reproduction technology, it is critical that closer animal models, as well as more detailed cellular and molecular evaluations be used to advance this field. The bovine ovary closely resembles the human ovary regarding tissue composition, follicle and oocyte size, and length of folliculogenesis, making the cow a suitable model given the more direct application to humans. Here we examined molecular aspects of the oocyte, granulosa cells and stromal cells, as well as the ECM composition. Importantly, this study tested published protocols that successfully led to live births but did not evaluate the aforementioned molecular alterations that could be present. When analyzing the follicular populations, we found that both cultured slow-frozen and vitrified tissue had increased percentages of primary follicles compared to non-cultured counterparts, indicating that cryopreservation-maintained viability and promoted activation of primordial follicles. Indeed, the percentage of primary follicles in cryopreserved, cultured tissue was similar to freshly cultured tissue. However, we found a decrease in the percentage of normal primordial follicles in the tissue that was only cryopreserved and thawed (no culture), as previously reported[28]. Following culture, SC had a similar proportion of normal primordial follicles compared to FC, whereas VC had fewer normal primordial follicles signifying that deleterious effects of vitrification were still apparent after culture. In this regard, slow freezing may be superior to vitrification. Our findings are somewhat in contrast with a study in primates where secondary follicles had greater rates of normal morphology and antrum formation after isolation and culture when

tissue was vitrified compared to slow freezing[29]. Although our study did not evaluate late secondary/early antral follicles, this difference may be due to a combination of the size of early secondary follicles thus making the early secondary follicles more susceptible to the damaging effects of OTC. Moreover, the distribution of follicle stages is often variable by tissue piece[30,31] and there are much fewer early secondary follicles for evaluation. However, it is worth noting that simply culturing tissue negatively affected follicle morphology, corroborating other studies[32] and demonstrating that less-than-optimal culture conditions remain an issue. In the current experiments, Ki67 labeling was used to evaluate whether cryopreservation and culture affected proliferation of GCs. Interestingly, we found no difference in the percentage of follicles that had Ki67-positive cells or in the percentage of Ki67-positive cells within these follicles between treatments, indicating that slow freezing and vitrification did not affect the proliferative ability of GCs.

Although ovarian stromal cells remain largely uncharacterized, immune cells, endothelial cells, and structural support cells such as fibroblasts have been identified and could be impacted by OTC[33,34]. Stromal cell viability is imperative to follicle development after OTC since pre-theca cells originate from the stromal environment. We found no difference in the density of stromal cells between treatments, in contrast to studies where ovine vitrified ovary tissue and cultured human ovary cortex exhibited a decrease in stromal cell density[35,36]. However, we observed an increase in apoptotic stromal cells following vitrification and culture. Our data are in contrast with comparable studies which demonstrated that vitrification was superior to slow freezing at maintaining stromal cell morphology after 24-hour culture[37] and viability after thawing[38].

The ovarian extracellular matrix, predominantly made of collagen, provides

scaffolding for stromal cells and follicles, impacts cell behavior via physical adhesion and mechanical tension, and sequesters important paracrine factors involved in cell-to-cell communication[13,39]. Our results show culture was the main driver of collagen loss. Regardless of cryopreservation, culturing decreased the amount of collagen in the outer and mid-cortex regions. These findings corroborate a study which found that culture decreased collagen content in human ovary cortex[36]. Moreover, loosening of the surrounding ovary microenvironment promotes activation of primordial follicles, a process which could occur due to less collagen present[40]. We focused on examining the more superficial region of ovary cortex due to the higher prevalence of collagen and localization of follicles[41]. Thus, modifications of the ECM in this region could be stark and more likely impact folliculogenesis. The patterning, orientation, and geometry of ECM fibers in the ovary can play an important role in organ function, especially between puberty and menopause[42]. We consider the possibility that culturing tissue can reshape the collagen fiber network of the ovary and/or change the representation of cell phenotypes which could alter production of collagen.

Finally, we assessed expression of CX37 due to the specific role of this protein forming channels and facilitating communication between granulosa cells and oocyte during the preantral phase of development. First, we corroborated previous findings by showing that CX37 is expressed predominantly throughout the ooplasm of bovine preantral follicles[43]. Disruption of connexin protein expression by factors such as cryopreservation could impede future follicle development. In bovine GV-stage oocytes, vitrification caused hemichannel opening as a stress response[44] and, during this process, propagation of ice nucleation between cells can be facilitated by connexin channels and

is dependent on decreasing temperature[45,46]. We found that a greater proportion of follicles lacked CX37 signal in vitrified-thawed tissue. However, CX37 fluorescence intensity became higher when vitrified tissue was cultured, potentially in a compensatory manner. These findings were interesting since others reported downregulation of mRNA for *Gja4* (the transcript for CX37) after culturing previously cryopreserved preantral follicles in mice[47]. In a separate study, CX37 expression was mostly absent in the oocyte of follicles found in vitrified-culture goat ovarian tissue[48]. Due to the importance of connexins in oocyte development, modulation in its expression or function could lead to aberrations in oocyte quality thus affecting embryo production in clinical IVF settings. Overall, our findings and the findings from others indicate that cryopreservation, and perhaps more so vitrification, could be detrimental to the expression of CX37.

Conclusion: Ovarian tissue culture, regardless of cryopreservation, results in primordial follicle activation, partial loss of follicle viability, and loss in collagen content. Tissue vitrification was more detrimental to ovarian and follicular cells as it resulted in greater proportion of apoptotic stromal cells after culture and lower percentages of normal follicles after thawing and culture. Moreover, vitrification seemed to disrupt CX37 expression within preantral follicles. Future research should include isolation of follicles in post-thawed and cultured tissue to assess downstream OTC impacts and optimizing of in vitro culture methods for follicle activation and growth to yield competent oocytes for assisted reproduction.

REFERENCES

1. Siegel, R. L., Miller, K. D. & Jemal, A. Cancer statistics, 2020. *CA Cancer J Clin* **70**, 7–30 (2020).

2. Ugai, T. *et al.* Is early-onset cancer an emerging global epidemic? Current evidence and future implications. *Nat Rev Clin Oncol* **19**, 656–673 (2022).

3. di Martino, E. *et al.* Incidence trends for twelve cancers in younger adults—a rapid review. *Br J Cancer* **126**, 1374–1386 (2022).

4. Committee, P. & Society, A. Fertility preservation in patients undergoing gonadotoxic therapy or gonadectomy: a committee opinion. *Fertil Steril* **112**, 1022–1033 (2019).

5. Shi, Q., Xie, Y., Wang, Y. & Li, S. Vitrification versus slow freezing for human ovarian tissue cryopreservation: A systematic review and meta-anlaysis. *Sci Rep* **7**, 1–9 (2017).

6. Arav, A. & Natan, Y. Directional freezing: A solution to the methodological challenges to preserve large organs. *Semin Reprod Med* **27**, 438–442 (2009).

7. Lee, S. *et al.* Comparison between slow freezing and vitrification for human ovarian tissue cryopreservation and xenotransplantation. *Int J Mol Sci* **20**, (2019).

8. Herraiz, S. *et al.* Improving ovarian tissue cryopreservation for oncologic patients: Slow freezing versus vitrification, effect of different procedures and devices. *Fertil Steril* **101**, (2014).

9. Isachenko, V. *et al.* Human ovarian tissue vitrification versus conventional freezing: Morphological, endocrinological, and molecular biological evaluation. *Reproduction* **138**, 319–327 (2009).

10. Kawahara, T. *et al.* Vitrification versus slow freezing of human ovarian tissue: a comparison of follicle survival and DNA damage. *Fertil Steril* **108**, e56–e57 (2017).

11. Labrune, E. *et al.* Cellular and Molecular Impact of Vitrification Versus Slow Freezing on Ovarian Tissue. *Tissue Eng Part C Methods* **26**, 276–285 (2020).

12. Terren, C., Fransolet, M., Ancion, M., Nisolle, M. & Munaut, C. Slow Freezing Versus Vitrification of Mouse Ovaries: from Ex Vivo Analyses to Successful Pregnancies after Auto-Transplantation. *Sci Rep* **9**, 19668 (2019).

13. Woodruff, T. K. & Shea, L. D. The Role of the Extracellular Matrix in Ovarian Follicle Development. *Reproductive Sciences* **14**, 6–10 (2007).

14. Kidder, G. M. & Mhawi, A. A. Gap junctions and ovarian folliculogenesis. *Reproduction* **123**, 613–620 (2002).

15. Veitch, G. I., Gittens, J. E. I., Shao, Q., Laird, D. W. & Kidder, G. M. Selective assembly of connexin37 into heterocellular gap junctions at the oocyte/granulosa cell interface. *J Cell Sci* **117**, 2699–2707 (2004).

16. Carabatsos, M. J., Sellitto, C., Goodenough, D. A. & Albertini, D. F. Oocyte-granulosa cell heterologous gap junctions are required for the coordination of nuclear and cytoplasmic meiotic competence. *Dev Biol* **226**, 167–179 (2000).

17. Lee, R. K.-K. *et al.* Abnormally low expression of connexin 37 and connexin 43 in subcutaneously transplanted cryopreserved mouse ovarian tissue. *J Assist Reprod Genet* **25**, 489–497 (2008).

18. Lind, A.-K. *et al.* Collagens in the human ovary and their changes in the perifollicular stroma during ovulation. *Acta Obstet Gynecol Scand* **85**, 1476–1484 (2006).

19. Luck, M. R., Zhao, Y. & Silvester, L. M. Identification and localization of collagen types I and IV in the ruminant follicle and corpus luteum. *Journal of Reproduction and Fertility-Supplements only* 517–522 (1995).

20. Parkes, W. S. *et al.* Hyaluronan and Collagen Are Prominent Extracellular Matrix Components in Bovine and Porcine Ovaries. *Genes* vol. 12 Preprint at https://doi.org/10.3390/genes12081186 (2021).

21. Celestino, J. J. de H. *et al.* Preservation of bovine preantral follicle viability and ultra-structure after cooling and freezing of ovarian tissue. *Anim Reprod Sci* **108**, 309–318 (2008).

22. Bao, R. M. *et al.* Development of vitrified bovine secondary and primordial follicles in xenografts. *Theriogenology* **74**, 817–827 (2010).

23. Suzuki, N. *et al.* Successful fertility preservation following ovarian tissue vitrification in patients with primary ovarian insufficiency. *Human Reproduction* **30**, 608–615 (2015).

24. Candelaria, J. I. & Denicol, A. C. Characterization of isolated bovine preantral follicles based on morphology, diameter and cell number. *Zygote* **28**, 154–159 (2020).

25. Chen, Y., Yu, Q. & Xu, C. A convenient method for quantifying collagen fibers in atherosclerotic lesions by ImageJ software. in (2017).

26. Candelaria, J. I., Rabaglino, M. B. & Denicol, A. C. Ovarian preantral follicles are responsive to FSH as early as the primary stage of development. *Journal of Endocrinology* **247**, 153–168 (2020).

27. Nahata, L. *et al.* Ovarian tissue cryopreservation as standard of care: what does this mean for pediatric populations? *J Assist Reprod Genet* **37**, 1323–1326 (2020).

28. Choi, J. *et al.* Cryopreservation of the mouse ovary inhibits the onset of primordial follicle development. *Cryobiology* **54**, 55–62 (2007).

29. Ting, A. Y., Yeoman, R. R., Lawson, M. S. & Zelinski, M. B. In vitro development of secondary follicles from cryopreserved rhesus macaque ovarian tissue after slow-rate freeze or vitrification. *Human Reproduction* **26**, 2461–2472 (2011).

30. Schmidt, K. L. T., Byskov, A. G., Nyboe Andersen, A., Muller, J. & Yding Andersen, C. Density and distribution of primordial follicles in single pieces of cortex from 21 patients and in individual pieces of cortex from three entire human ovaries. *Human Reproduction* **18**, 1158–1164 (2003).

31. Alves, K. A. *et al.* Preantral follicle density in ovarian biopsy fragments and effects of mare age. *Reprod Fertil Dev* **29**, 867–875 (2017).

32. Bjarkadottir, B. D., Walker, C. A., Fatum, M., Lane, S. & Williams, S. A. Analysing culture methods of frozen human ovarian tissue to improve follicle survival. *Reproduction and Fertility* **2**, 59–68 (2021).

33. Kinnear, H. M. *et al.* The ovarian stroma as a new frontier. *Reproduction* **160**, R25–R39 (2020).

34. Guiltinan, C., Weldon, B., Soto, D. A., Ross, P. J. & Denicol, A. C. 60 Single-cell transcriptome analysis of fetal and adult bovine ovaries reveals developmental progression in cell population composition and function. *Reprod Fertil Dev* **35**, 156 (2023).

35. Silva, L. M. *et al.* Effect of Catalase or Alpha Lipoic Acid Supplementation in the Vitrification Solution of Ovine Ovarian Tissue. *Biopreserv Biobank* **16**, 258–269 (2018).

36. Grosbois, J., Bailie, E. C., Kelsey, T. W., Anderson, R. A. & Telfer, E. E. Spatio-temporal remodelling of the composition and architecture of the human ovarian cortical extracellular matrix during in vitro culture. *Hum Reprod* **38**, 444–458 (2023).

37. Keros, V. *et al.* Vitrification versus controlled-rate freezing in cryopreservation of human ovarian tissue. *Human Reproduction* **24**, 1670–1683 (2009).

38. Chang, H. J. *et al.* Optimal condition of vitrification method for cryopreservation of human ovarian cortical tissues. *Journal of Obstetrics and Gynaecology Research* **37**, 1092–1101 (2011).

39. Irving-Rodgers, H. F. & Rodgers, R. J. Extracellular matrix of the developing ovarian follicle. *Semin Reprod Med* **24**, 195–203 (2006).

40. Nagamatsu, G., Shimamoto, S., Hamazaki, N., Nishimura, Y. & Hayashi, K. Mechanical stress accompanied with nuclear rotation is involved in the dormant state of mouse oocytes. *Sci Adv* **5**, 1–13 (2019).

41. Henning, N. F. C. & Laronda, M. M. The matrisome contributes to the increased rigidity of the bovine ovarian cortex and provides a source of new bioengineering tools to investigate ovarian biology. *bioRxiv* 2021.10.06.463107 (2021) doi:10.1101/2021.10.06.463107.

42. Ouni, E. *et al.* A blueprint of the topology and mechanics of the human ovary for next-generation bioengineering and diagnosis. *Nat Commun* **12**, (2021).

43. Nuttinck, F. *et al.* Comparative immunohistochemical distribution of Connexin 37 and Connexin 43 throughout folliculogenesis in the bovine ovary. *Mol Reprod Dev* **57**, 60–66 (2000).

44. Szymańska, K. J., Ortiz-Escribano, N., Van den Abbeel, E., Van Soom, A. & Leybaert, L. Connexin hemichannels and cell death as measures of bovine COC vitrification success. *Reproduction* **157**, 87–99 (2019).

45. Acker, J. P., Elliott, J. A. W. & McGann, L. E. Intercellular ice propagation: Experimental evidence for ice growth through membrane pores. *Biophys J* **81**, 1389–1397 (2001).

46. Higgins, A. Z. & Karlsson, J. O. M. Effects of intercellular junction protein expression on intracellular ice formation in mouse insulinoma cells. *Biophys J* **105**, 2006–2015 (2013).

47. Xu, M., Banc, A., Woodruff, T. K. & Shea, L. D. Secondary follicle growth and oocyte maturation by culture in alginate hydrogel following cryopreservation of the ovary or individual follicles. *Biotechnol Bioeng* **103**, 378–386 (2009).

48. Donfack, N. J. *et al.* Stroma cell-derived factor 1 and connexins (37 and 43) are preserved after vitrification and in vitro culture of goat ovarian cortex. *Theriogenology* **116**, 83–88 (2018).

Figures

Figure 1.1

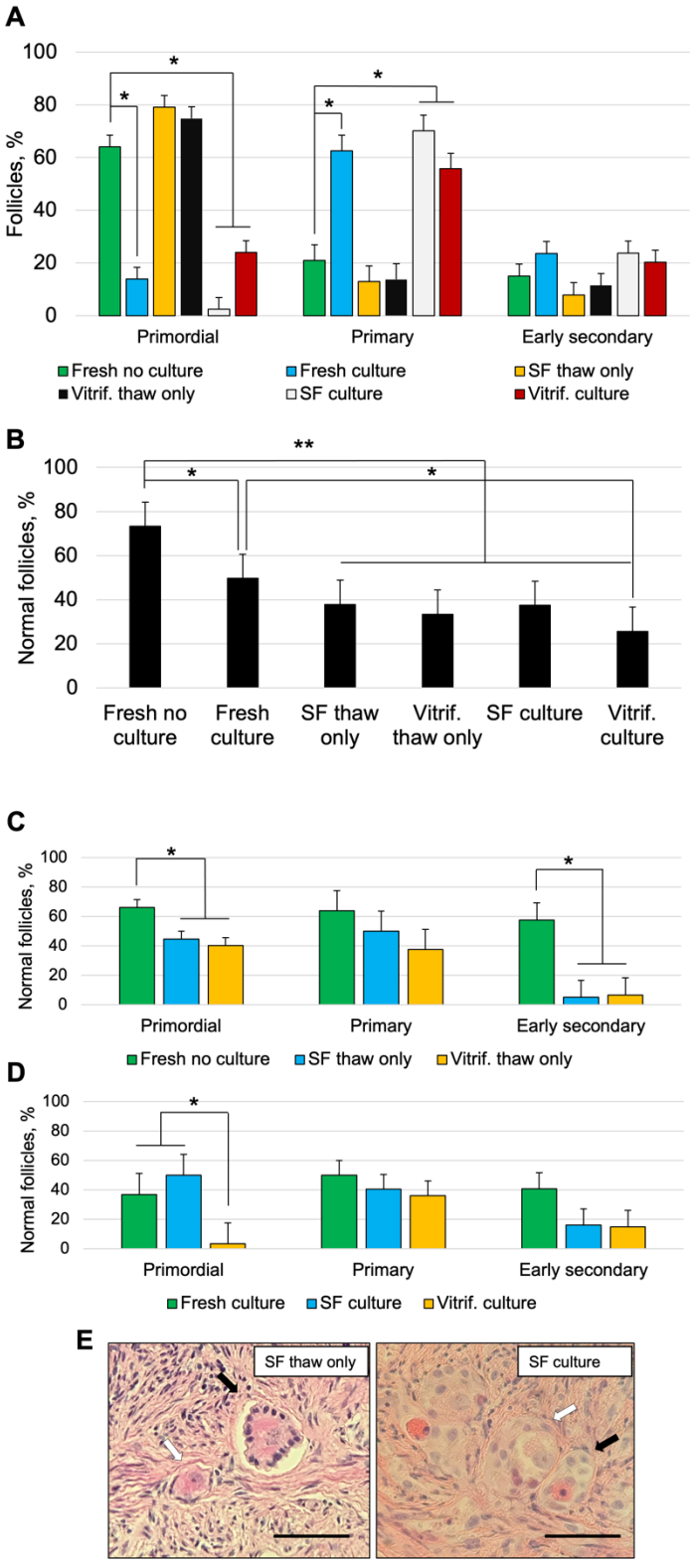

Figure 1.1. Morphology and viability assessment of bovine preantral follicles in situ before and after cryopreservation and culture. (**A**) The proportion of follicles in each stage of development found in fresh ovarian tissue fragments (fresh no culture), fragments that were cultured (fresh culture), slow-frozen and thawed (SF thaw only), vitrified and thawed (Vitrif. thaw only), slow-frozen and cultured (SF culture), and vitrified and cultured (Vitrifi. culture). (**B**) The proportion of follicles was classified as normal in each group. (**C**) The proportion of normal follicles of each stage found in tissue that was not cultured or cryopreserved, compared with cryopreserved and thawed tissue. (**D**) The proportion of normal follicles of each stage found in tissue that was cultured without or after cryopreservation. (**E**) Representative images of hematoxylin and eosin-stained tissue containing normal (white arrows) and abnormal (black arrows) preantral follicles in slow-frozen thaw-only and slow-frozen cultures. Significant differences between groups are indicated by $*P < 0.05$, $**P < 0.01$. Scale bar = 50 μm. Data are presented as mean ± SEM.

Figure 1.2

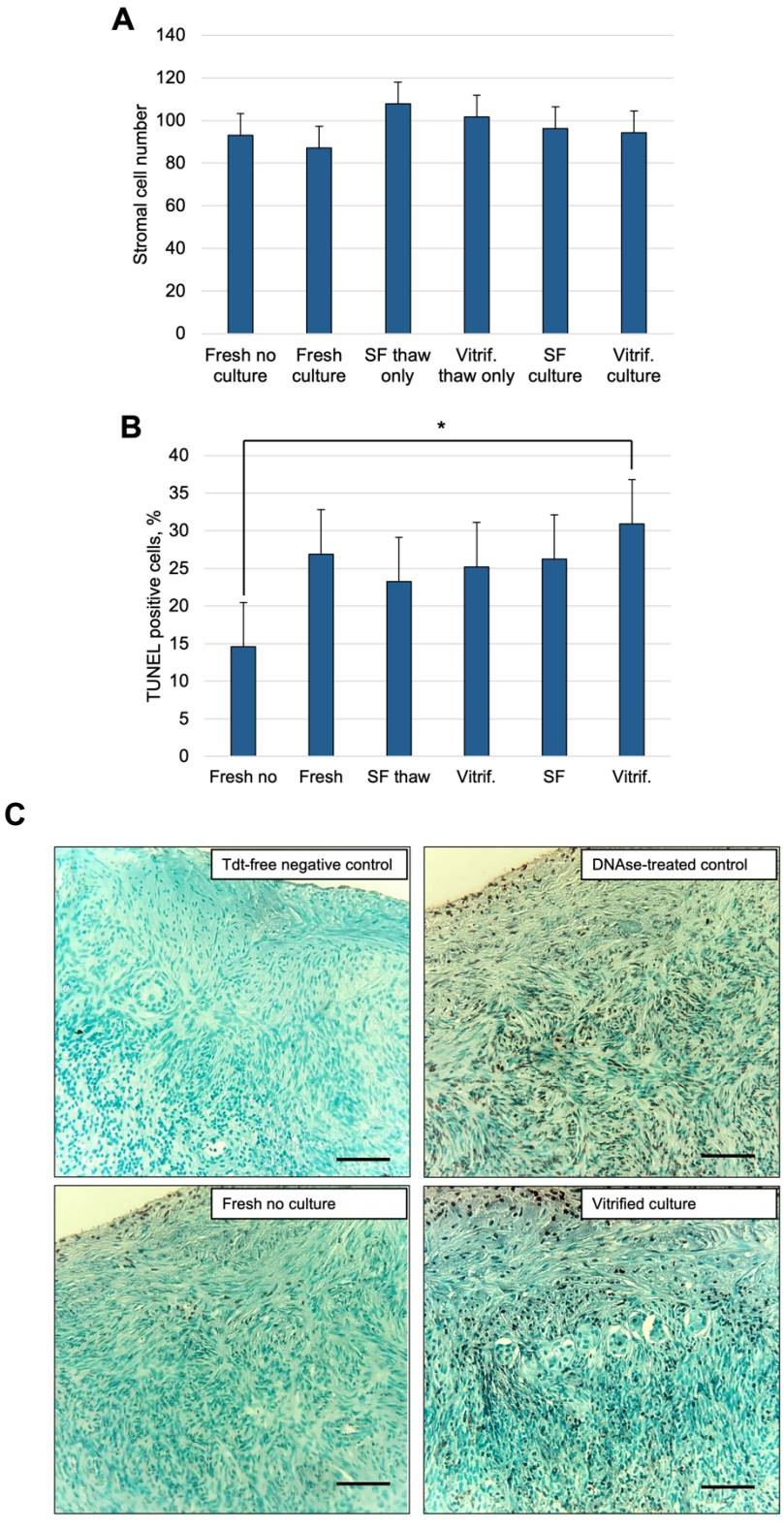
A
Stromal cell number
140
120
100
80
60
40
20
0
Fresh no culture
Fresh culture
SF thaw only
Vitrif. thaw only
SF culture
Vitrif. culture
B
*
TUNEL positive cells, %
40
35
30
25
20
15
10
5
0
Fresh no
Fresh
SF thaw
Vitrif.
SF
Vitrif.
C
Tdt-free negative control
DNAse-treated control
Fresh no culture
Vitrified culture

Figure 1.2. Cell density and apoptosis of stromal cells within ovarian cortical tissue before and after cryopreservation and culture. (**A**) Average number of stromal cells in 100 mm x 100 mm fields. (**B**) Proportion of TUNEL-positive (apoptotic) stromal cells in 100 mm x 100 mm fields. (**C**) Representative images of TUNEL-stained ovarian cortex fragments in terminal deoxynucleotidyl transferase-free negative control samples, DNAse-treated positive control samples, and fresh no culture and vitrified-culture samples. SF = slow frozen; Tdt = terminal deoxynucleotidyl transferase; TUNEL = terminal deoxynucleotidyl transferase dUTP nick end labeling; Vitrif. = vitrified. Scale bar = 100 μm. Data are presented as mean ± SEM. Significant differences between groups are indicated by $*P < 0.05$.

Figure 1.3

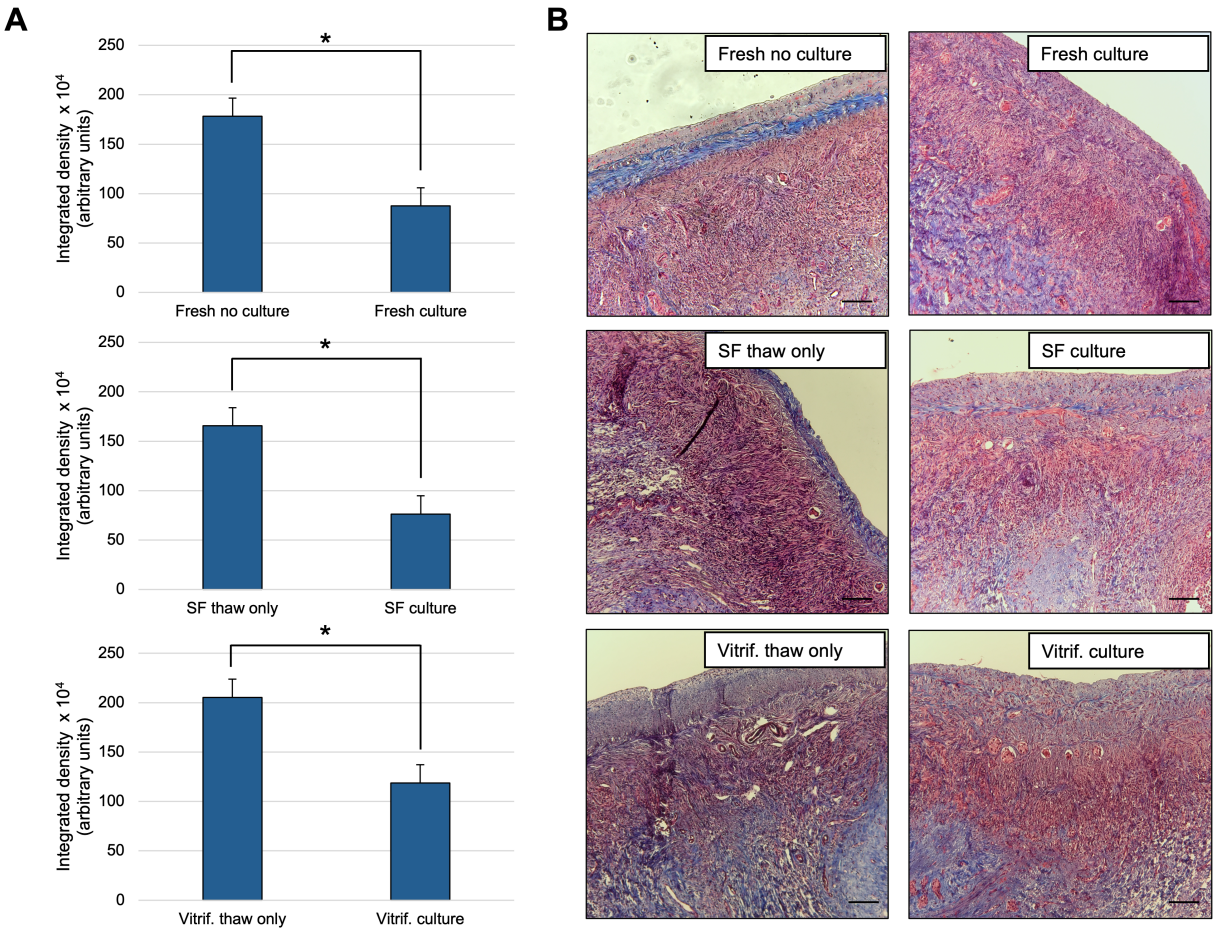

Figure 1.3. Masson's trichrome stain (collagen content) of ovary cortical tissue before and after cryopreservation and culture. (**A**) Quantification of collagen content between groups. (**B**) Representative images of Masson's trichrome-stained tissue. SF = slow frozen; vitrif. = vitrified. Scale bar = 100 μm. Data are presented as mean ± SEM. Significant differences between groups are indicated by *$P < 0.05$.

Figure 1.4

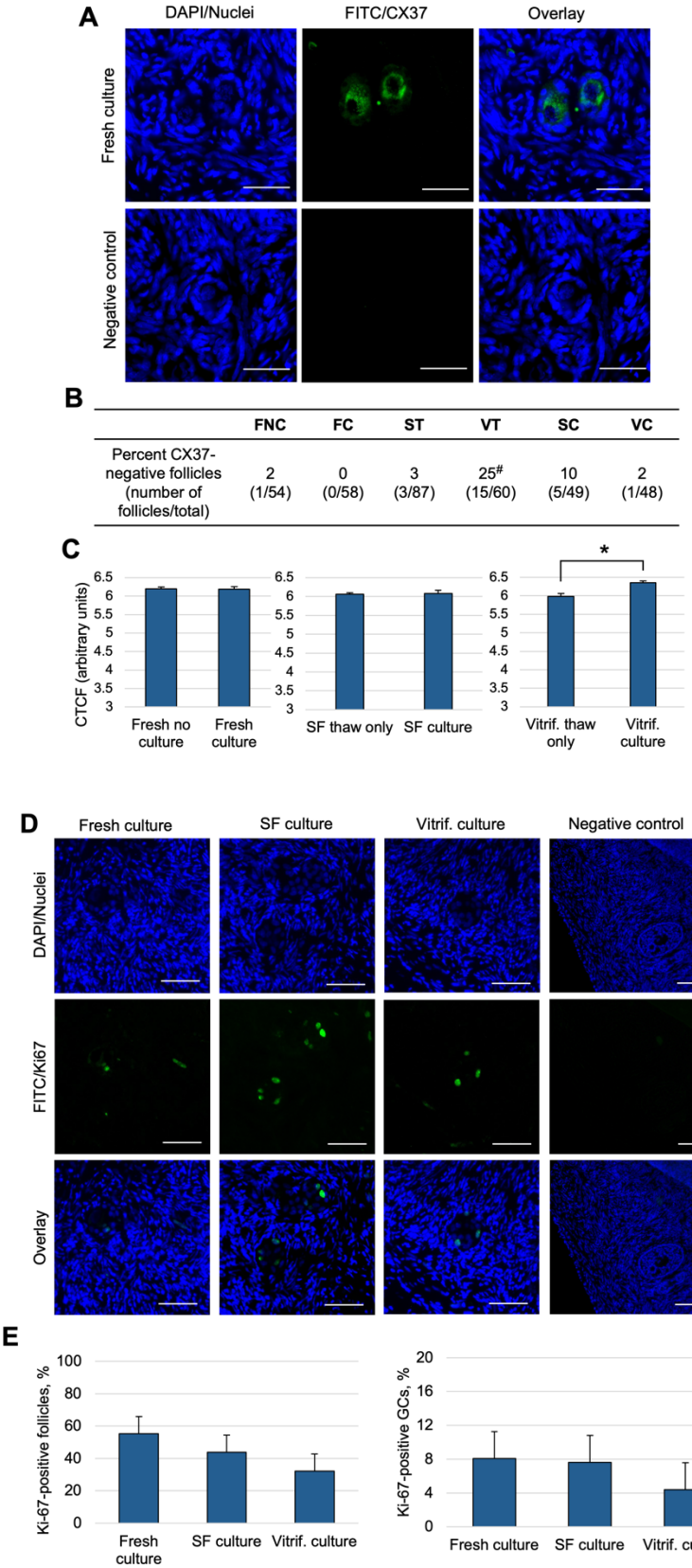
A
DAPI/Nuclei
FITC/CX37
Overlay
Fresh culture
Negative control
B
FNC FC ST VT SC VC
Percent CX37-negative follicles (number of follicles/total)
2 (1/54) 0 (0/58) 3 (3/87) 25# (15/60) 10 (5/49) 2 (1/48)
C
CTCF (arbitrary units)
6.5 6 5.5 5 4.5 4 3.5 3
*
Fresh no culture
Fresh culture
SF thaw only
SF culture
Vitrif. thaw only
Vitrif. culture
D
Fresh culture
SF culture
Vitrif. culture
Negative control
DAPI/Nuclei
FITC/Ki67
Overlay
E
Ki-67-positive follicles, %
100 80 60 40 20 0
Fresh culture
SF culture
Vitrif. culture
Ki-67-positive GCs, %
20 16 12 8 4 0
Fresh culture
SF culture
Vitrif. culture

Figure 1.4. Immunofluorescent staining of gap junction protein (CX37) and proliferation marker (Ki67) in preantral follicle granulosa cells within ovarian cortical fragments. (**A**) Representative images of connexin 37 (CX37) expression in oocytes. Scale bar = 50 μm. (**B**) Proportion of CX37-negative follicles between treatments. (**C**) Quantification of CX37 abundance. (**D**) Representative images of Ki67 expression in granulosa cells within follicles. Scale bar = 50 μm. (**E**) Proportions of Ki67-positive follicles and Ki67-positive granulosa cells (GCs) in cultured tissue samples. Significant differences between groups are indicated by *P <0.05 and compared with fresh no culture (in B) are indicated by #P < 0.05. Data are presented as mean ± SEM. Negative control = 100 μm. CTCF = corrected total cell fluorescence; FC = fresh culture; FN = fresh no culture; SC = slow frozen cultured; ST = slow frozen-thawed culture; VC = vitrified cultured; VT = vitrified thawed.

CHAPTER 3

Evaluating the Use of Bioengineered (Poly)ethylene Hydrogels Containing Ovarian Cells to Promote Bovine in vitro Preantral Folliculogenesis

Abstract

In vitro small preantral follicle culture capitalizes on a resourceful pool of immature oocytes that can be used for assisted reproductive technologies. However, there has been very limited success growing small (i.e. primary and early secondary) preantral follicles in a large mammal species, such as the bovine, due to the prolonged culture time required and extensive remodeling and volumetric expansion of the follicles. In this study, we tested the use of customized three-dimensional (poly)ethylene glycol (PEG) hydrogels for *in vitro* bovine preantral follicle culture. PEG hydrogels were custom designed with peptide crosslinkers that are sensitive to proteases produced by bovine preantral follicles. Overall, we did not observe a difference in the percentage of follicles that grew or a percent change from the initial size between two-dimensional (2D) control and PEG hydrogels. However, when follicles were size matched at day 0, we found that smaller preantral follicles showed more growth over 10 days in PEG hydrogels compared to 2D control. Moreover, larger follicles maintained their size in PEG hydrogels, whereas follicles cultured in 2D control decreased in size. When bovine ovarian cells (BOCs) or mesoderm-like cells (MeLCs) were added to the PEG system and cultured for 10 days, only BOCs maintained viability. However, when follicles were supplemented with BOCs or encapsulated alone in PEG hydrogels, follicles did not grow and seemed to be nonviable. We found that BOCs did not maintain expression of markers characteristic of theca cells, although they decreased expression of apoptosis-related genes compared to the day of isolation. Overall, our data show that the PEG hydrogel holds promise as a future *in vitro* culture system for bovine preantral follicles, particularly at the primary stage of development; however, improvements to the system are needed.

Introduction

Folliculogenesis is a complex and selective process that produces a limited quantity of meiotically- and developmentally-competent oocytes over a female's lifespan. The molecular processes that coordinate the activation, growth, and maturation of ovarian follicles have yet to be fully elucidated, especially during the early preantral stages of development. Progress in understanding preantral folliculogenesis has been hindered by the lack of appropriate *in vitro* culture systems to permit further research. This is particularly true in large mammals (i.e., cows and humans). Preantral folliculogenesis has prolonged developmental timelines and sizeable volumetric changes between the primordial and pre-ovulatory follicle stages. A significant advantage of performing *in vitro* folliculogenesis beginning at the preantral stage includes establishing an alternative fertility preservation and restoration method by utilizing the vast preantral follicle pool for oocyte production[1]. More specifically, this approach would be beneficial for prepubertal girls suffering from blood-borne malignancies or genetically elite animals for food production or wildlife conservation as isolated preantral follicles could be matured in vitro without the risk of reintroducing malignant cells or surgical intervention, as could be the case with the culture of ovarian tissue fragments.

Several groups have attempted recapitulation of bovine preantral folliculogenesis, but there has been little success in efficiently growing follicles to the preovulatory stage and yielding metaphase II oocytes. Although 2-dimensional culture systems have shown some promise in supporting bovine preantral follicle growth[2-4], mounting evidence suggests 3-dimensional (3D) culture systems better promote development due to their ability to maintain a follicle's spherical configuration and preserve cell contact both within

the follicular unit (i.e., granulosa cell and oocyte interface) and outside the basement membrane where theca cells are located[5-8]. Collagen and alginate are common biomaterials used to create hydrogels for in vitro follicle culture. However, pitfalls include uncontrollable degradation and biological inertness, respectively. Therefore, a highlighted alternative is the use of bioengineered 3D hydrogel culture systems that permit orderly degradation by the follicle while retaining the mechanical support necessary to keep its spherical structure[9-10]. Polyethylene glycol (PEG) hydrogels constructed with proteolytically-degradable peptide crosslinkers have been used for the mouse in vitro folliculogenesis and demonstrated success in growing preantral follicles to the antral stage producing metaphase II oocytes[11]. Likewise, adding adipose-derived stem cells (ADSCs) or conditioned media from ADSCs to PEG hydrogels containing mouse preantral follicles further aided development and survival[12]. As an additional advancement to the system, PEG hydrogels can be customized with basement membrane-binding fibers, which create a template for extracellular-matrix (ECM) deposition and retention by encapsulated cells, thus better mimicking the ovarian microenvironment and driving preantral follicle growth[13,14]. Despite the promise demonstrated in mice, the use of PEG hydrogels for large mammal in vitro preantral follicle culture has not been reported.

Moreover, investigating native or stem-cell-derived ovarian cell supplementation in the hydrogel system to determine their propensity to become theca cells and its advantageous effect on follicle growth has not been directly assessed. Indeed, early preantral follicles do not contain theca cells and must recruit precursor cells from the stromal environment to build the essential theca layer. Hence, adding cells to the system

could be beneficial when starting with primordial- or primary-stage follicles. The hedgehog signaling pathway drives theca cell differentiation and recruitment[15-17.] Therefore, cells added to the culture system should also harbor the cellular machinery to respond to hedgehog ligands expressed by the follicular granulosa cells.

In this study, we describe using a PEG hydrogel culture system for the in vitro development of bovine preantral follicles. We hypothesized culture in PEG hydrogels would improve the growth and viability of bovine preantral follicles. By examining the gene expression of ECM-degrading enzymes of primary- and early secondary-stage follicles, we tailored the hydrogel design to complement bovine follicle enzyme secretion. Based on the evidence that cell supplementation improves mouse follicle development, we also examined the effect of a renewable cell source, mesoderm-like cells (MeLCs) derived from bovine embryonic stem cells and dissociated bovine ovarian cells on bovine preantral follicle growth in vitro using PEG hydrogels. Finally, we addressed whether co-encapsulated cells of either origin would exhibit a phenotype typical of pre-theca cells when cultured in PEG hydrogels.

Material and methods

All materials were purchased from Thermo Fisher Scientific unless otherwise specified.

Follicle Isolation and bovine ovary single-cell dissociation

Fresh bovine preantral follicles were isolated as previously described[18]. Follicles were maintained in warmed follicle wash media until subsequent experiments. For bovine ovary single-cell dissociation (n = 3 replicates), cortical tissue (250-300 mg) was

fragmented into 500 μm^2 pieces incubated with Hank's balanced salt solution (Ca^{2+}/Mg^{2+}) containing 1 mg/mL collagenase IV, 1 U/mL DNase I, and 50 µg/mL Liberase (5401119001, Sigma Aldrich). The solution with tissue was shaken at 38.5 °C for 20 min, pipetted 15 times using a serological pipette, and shaken again for 20 min to aid in the dissociation of cells mechanically. Enzymatic activity was stopped by adding 20% v/v fetal bovine serum to the solution. The tissue-dissociated solution was filtered through a 100 µm then through a 35 µm cell strainer. Cells collected after final filtration were centrifuged (300 x*g* for 5 min), and the resulting pellet was resuspended in 1 mL Hank's balanced salt solution without Ca^{2+}/Mg^{+} until encapsulation.

Bovine embryonic stem cell and mesoderm-like cell culture

Bovine embryonic stem cells were routinely cultured feeder-free as previously described[19]. For mesoderm induction, bESCs were passaged onto 4-well vitronectin-coated plates in mesoderm-induction media (GMEM medium, 15% knockout serum replacement, 0.1 mM NEAA, 2mM GlutaMAX, 1mM Na Pyruvate, 0.1mM β-mercaptoethanol (M6250, Sigma Aldrich), 100 U/mL Penicillin, and 100 µg/mL streptomycin and supplemented with 3 µm CHIR99021 (Tocris Bioscience, 44-231-0) and 70 ng/mL Activin A (338-AC, R&D Systems). Cells were cultured in the mesoderm-induction medium for 48 hours with daily medium change, and after that, the cells were considered "mesoderm-like cells" (MeLCs) and used for subsequent experiments.

Conventional and quantitative reverse transcription PCR (qRT-PCR)

Freshly isolated follicles were pooled by stage and snap-frozen in minimal PBS. To examine the expression of transcripts for extracellular-matrix degrading enzymes, primary follicles (n = 3 pools of 46-56 follicles per pool) and early secondary follicles (n = 3 pools of 34-40 follicles per pool) were subjected to RNA isolation using a protocol with a combination of Trizol, Purelink DNase treatment, and Qiagen RNeasy Micro Kit. The final total RNA was eluted into 14 µl of RNase-free water. Bovine ovarian cells (BOCs) and mesoderm-like cells (MeLCs) were pelleted, snap-frozen, and subjected to RNA isolation following manual instructions using the Qiagen RNeasy Micro Kit. Maximum available RNA mass was used for cDNA synthesis of primary and early secondary follicles, and 1 µg of total RNA was used for cDNA synthesis of BOCs and MeLCs (RevertAid cDNA Reverse Transcription Kit). For RT-qPCR, 1 µl of cDNA, 1x SsoAdvanced Universal SYBR Green Supermix (1725271, Bio-Rad), and 250 nM of forward and reverse primers (primer sequences listed in Table 1) were mixed for 10 µl total volume and pipetted into 96-well plates. The reaction was carried out in the CFX96 Touch Deep Well Real-Time PCR Detection System (Bio-Rad). Cycling conditions were an initial denaturation step at 95 ºC for 30 sec followed by 40 cycles of denaturation at 95 ºC for 10 sec, annealing at 60 ºC for 30 sec, and extension at 60 ºC for 5 sec. Each assay included a melt curve analysis and non-template control to confirm the specificity of PCR products for each gene. For conventional PCR, PCR products from quantitative PCR reactions were ran on a 2% agarose gel to visualize the PCR products.

For RT-qPCR experiments using *BAX* and *BCL2* primers, a standard curve of fresh bovine ovarian cells was used to estimate quantity of mRNA present in unknown samples

of BOCs. The ratio of *BAX*/*BCL2* was calculated from mRNA quantity of respective genes and used to determine if cells were in a pro- or anti-apoptotic state.

PEG hydrogel materials, preparation, and follicle encapsulation

PEG hydrogel experiments were conducted using 8-arm PEG vinyl sulfone (PEG-VS) (40 kDa, >99% purity, JenKem Technology) and crosslinked with MMP- and Plasmin-sensitive peptide sequences (Ac-GCRD**VPMS**MRGGDRCG**YKNS**CG, i.e. YKNS/VPMS) (2391.8 g/mol, >90%, Celtek Peptides). PEG and crosslinker peptide were dissolved in isotonic 50 mM HEPES buffer and mixed to a final composition containing 5% PEG-VS with a 1:1 stoichiometric ratio of VS to thiol (side chain present on cysteines in peptide sequence). 16 µl hydrogels containing preantral follicles were formed between parafilm-lined glass slides and gelatinized for up to 10 min. Then, hydrogels were transferred to warmed follicle maintenance media to swell and placed in a humidified incubator (37°C). Freshly isolated follicles were maintained in warmed follicle wash media until encapsulation. In experiment 1, follicles (n = 1-4) were first washed in 10% PEG-VS and either encapsulated in PEG hydrogels or placed into 2D culture. Hydrogel-encapsulated and 2D culture follicles were placed into individual wells of a 96-well plate containing follicle culture media (1:1 ratio of α-MEM and F12 with glutamine supplemented with 3 mg/mL bovine serum albumin, 100 ng/mL penicillin/streptomycin, 1 mM sodium pyruvate, 1 % (v/v) non-essential amino acids, 10 mg/l insulin, 5.5 mg/l transferrin and 6.7 µg/L selenium (ITS), 100 ng/mL human recombinant follicle stimulating hormone (228-12609-2, RayBiotech), and 50 µg/mL ascorbic acid. Half of the spent media was changed every 2 days and follicles were cultured for 10 days. To assess follicle growth over the

culture period, the average of 2 perpendicular diameter measurements were taken on day 0, day 5, and day 10 using an inverted microscope (Revolve, Echo Labs). The percentage of growing and non-growing follicles (growth defined as having at least a 5% increase in diameter by day ten compared to day 0) and percent increase in size in growing-only follicles was calculated. In total, 15 replicates were conducted with a total of 216 follicles (n = 153 in PEG and n = 63 in 2D control)

Cell viability staining and quantification

Bovine ovarian cells and MeLCs were resuspended in PEG-VS + crosslinker peptide VPMS/YKNS at a concentration of 1, 2, 10, and 20 x 10^6 cells/mL to test cell viability immediately after encapsulation, 5 and 10 days after in vitro culture. Hydrogels were cultured individually in 96-well plates with 150 µl of follicle culture media with half media changes every two days. After culture, hydrogels were incubated for 10 min with pre-equilibrated alpha-MEM containing two µM propidium iodide (PI) and 1:1000 Hoechst (1 µg/mL final concentration). Negative control hydrogels were void of propidium iodide and used to set exposure limits during imaging. Hydrogels were imaged using an epifluorescent microscope (Revolve). The total number of cells and viable cells were quantified using ImageJ after converting to binary images where PI/Hoechst-positive cells were white, and the background was black. The total number of cells positive for PI was divided by the total cells quantified by Hoechst staining to determine the percentage of unviable cells. The percentage of viable cells was determined by subtracting the percentage of unviable cells from 100. The experiment was repeated four times using three hydrogels per cell density for each replicate.

Bovine ovarian cells with follicle encapsulation and culture in PEG

To test the impact of BOC and co-encapsulation on follicle viability and growth and theca cell differentiation during in vitro culture, hydrogels were either 1) encapsulated with only follicles, 2) encapsulated with 5 x 10^6 BOCs/mL only or 3) co-encapsulated with follicles and 5 x 10^6 BOCs/mL BOCs. Hydrogels contained 1-5 follicles per gel. Hydrogel formation and follicle encapsulation were performed as previously described with the addition of staining follicles with cell membrane marker PKH26 prior to encapsulation to better visualize follicles. Hydrogels were cultured as described above for 10 days, and half of the spent medium was changed every other day. Follicles were considered viable if the basement membrane was attached, the follicles were void of vacuoles, and granulosa cells were not darkened or mishappened. To recover cells for RT-qPCR, the hydrogels were incubated in phenol red-free alpha-MEM with Liberase (1.3 wünsch units/mL) and incubated at 37 °C and 5% CO_2 for 30 min with repeated pipetting to degrade the hydrogel and extract the cells. After centrifugation, the cell pellet was used for RNA extraction, cDNA synthesis and RT-qPCR as described above.

Statistical analysis

All data was first assessed for normality using a Shapiro-Wilk test. The PEG growth data was subjected to a one-way ANOVA using RStudio with the effect of replicating included in the model. Cell viability and RT-qPCR data were subjected to a one-way ANOVA or Kruskal-Wallis test if data was not normally distributed using Graph Prism. Post-hoc tests (Tukey's and Dunn's for ANOVA and Kruskal-Wallis, respectively) were

conducted when appropriate. Comparisons were considered significantly different when associated with $P < 0.05$.

Results

We first examined the expression of ECM-degrading enzyme genes in three pools of bovine primary and early secondary follicles that express the critical follicle marker gene *FSHR*. Matrix metalloproteinases (MMPs) and plasminogen activators are ECM-degrading enzymes pivotal in tissue remodeling. We found that the bovine primary and early secondary follicles express MMP2, although we only found MMP2 in one pool in early secondaries. However, neither follicle stage expressed *MMP9* (Figure 2.1A). Plasminogen-activator urokinase (*PLAU*) was expressed in primary and early secondary follicles from one pool, but not in the second or third pool. Similarly, Plasminogen-activator tissue (*PLAT*) was expressed in primary follicles of one pool and in early secondary follicles from two other pools (Figure 2.1A). Since we collectively found mRNA expression of *MMP2* and plasminogen enzymes, we proceeded with designing and using an 8-arm PEG hydrogel that is functionalized with VPMS (MMP-sensitive) and YKNS (plasminogen-sensitive) peptide sequences (Figure 2.1B).

Next, we tested the hypothesis that bovine preantral follicles are more likely to grow and demonstrate greater growth rate when encapsulated in PEG hydrogels compared to 2D traditional methods after 10 days of culture. We found no difference in the percentage of growing follicles between PEG (35.8% ± 6.58%) and 2D control (30.3% ± 6.58%) ($P = 0.56$) (Figure 2.2A). We found that replicate affected the percentage of

growing/non-growing follicles ($P < 0.05$) where some replicates (i.e. individual ovary) had more follicles grow in either condition compared to other replicates. Of the replicates where at least one follicle demonstrated growth in either condition, we found no difference ($P = 0.50$) in the growth rate (PEG: 18.8% ± 4%, control: 22.7% ± 4%) (Figure 2.2B). Additionally, there was no effect of replicate ($P = 0.78$).

We further examined the diameter changes between day 0, 5, and 10 in follicles within a narrow range of starting diameters, corresponding to their stage of development within the primary to early secondary. As shown in Figure 2.3A, follicles that were 40-50 µm at day 0 showed an increase in diameter at day 10 only when cultured in PEG hydrogels (53.3 ± 3.76 µm) compared to 2D control (49.3 ± 3.03 µm) ($P < 0.05$). Follicles that were 51-60 µm at day 0 and cultured in PEG hydrogels or 2D control showed no change in diameter size over 10 days (PEG: $P = 0.08$; control: $P = 0.83$) (Figure 2.3B). Follicles starting at 61-70 µm showed a significant decrease in diameter by day 10 of culture in control conditions ($P < 0.05$). However, follicles cultured in PEG showed no difference over time ($P = 0.68$) thus maintained their size (Figure 2.3C). Taken further, day 5 and day 10 follicles were significantly smaller ($P < 0.05$) in control follicles compared to similar PEG follicles timepoints. When we combined the starting diameters (40-60 µm), PEG hydrogels outperformed the control conditions as day 5 follicles were larger in PEG compared to 2D control ($P < 0.05$) (Figure 2.3D). Moreover, by day 10, PEG hydrogel follicles had a significant increase in diameter compared to day 0 ($P < 0.05$), whereas control follicles showed no difference ($P = 0.72$).

Based on the finding that PEG hydrogels promoted growth in smaller, but not larger, preantral follicles and growth became stagnant between day 5 and day 10, we

tested the hypothesis that supplementing the PEG hydrogel with support cells would aid in further growth. Indeed, primary and early secondary preantral follicles lack theca cells and therefore need the exogenous addition of theca-precursor cells required for continued development. We first explored the gene expression profile of mesoderm-like cells (MeLCs; a renewable cell source from bovine embryonic stem cells) and dissociated native bovine ovarian cells (BOCs) to determine if they expressed genes important for theca cell differentiation and recruitment into the follicular unit. Hedgehog signaling-responsive genes (*SMO*, *PTCH1*, *GLI1*) and the pericyte marker *CSPG4* are particularly important pre-theca cell markers[16,20]. We confirmed that primary and early secondary follicles expressed the hedgehog ligand *IHH* while only early secondary follicles express *DHH* (Figure 2.4A). As expected, the bovine ovary cortex and medulla also expressed *IHH* and *DHH.* MeLCs expressed *DHH*, *SMO*, *PTCH1*, *GLI1,* and *CSPG4*. Besides *GLI1* which was only detected in the medulla, hedgehog-responsive gene expression was similarly seen in the ovary cortex and medulla (Figure 2.4B). With confirmation of hedgehog signaling gene expression in both MeLCs and BOCs, we proceeded to evaluate cell viability of both cell types when encapsulated in PEG hydrogels and cultured for 10 days (Figure 2.5A and B). Mesoderm-like cells failed to maintain viability even shortly after encapsulation at day 0 (2 x 10^6 cells/mL) as indicated by widespread PI staining (Figure 2.5B). When encapsulated at 1 or 2 x 10^6 cells/mL, BOCs showed low cell viability (data not shown), whereas concentrations of 10 or 20 x 10^6 cells/mL showed high viability (70-90%) (Figure 2.5C). Therefore, we continued testing only BOC supplementation in PEG hydrogels with follicles. We found that neither control (no BOCs encapsulated) nor hydrogels with BOCs supported follicle viability over the culture period

(100% unviable follicles after 10 days (n = 65 follicles); 5 replicates) (Figure 2.6A). Moreover, gene expression analysis of pre-theca cell markers after 10 days of culture revealed a decrease in expression of *PTCH1* ($P < 0.01$) and *GLI1* ($P < 0.05$) when compared to day 0 fresh cells in both BOCs cultured alone and co-encapsulated with follicles (Figure 2.6B). There was a decrease in expression of *SMO* when cells were co-encapsulated with follicles compared to day 0 ($P < 0.05$). We found a decrease in both *BAX* and *BCL2* in BOCs that were cultured with follicles and a decrease in *BCL2* in BOCs cultured in PEG hydrogels alone ($P < 0.05$) (Figure 2.6C). However, there was no difference in the *BAX*/*BCL2* ratio, thus indicating no difference in the pro- versus anti-apoptotic balance between cultured BOCs and fresh BOCs.

Discussion

To our knowledge, this study is the first to utilize a novel bioengineered PEG hydrogel system for the *in vitro* culture of bovine preantral follicles. Since maintaining the structural integrity of the follicle has become a main concern with 2D culture, hydrogels represent a viable option since they provide a framework to maintain the 3D configuration of follicles while permitting growth. Indeed, the theory to build a culture system complete with extracellular matrix components like the ovary has been suggested when early studies first explored bovine preantral in vitro development[21]. The use of PEG hydrogels for mouse preantral follicle in vitro culture has highlighted its strong capability of promoting growth[11]. Further adaptations to include sophisticated ECM components in the hydrogel design have permitted mouse follicle growth *in vitro,* starting as early as the primordial stage[13]. We first examined the gene expression of ECM-degrading enzymes in primary

and early secondary follicles to design a proteolytically-degradable PEG hydrogel that would most likely be compatible with bovine preantral follicles. Collectively, we found mRNA transcripts for *MMP2*, *PLAU*, and *PLAT* in both follicle stages. However, across 3 separate pools of primary and early secondary follicles, there was variability in the expression of each ECM-degrading enzyme. To this extent, we conclude that there is heterogeneity between follicles, which may lead to the discrepancy in growth and survival when cultured in PEG hydrogels. Although we consistently did not find *MMP9* in either primary of early secondary follicles, others have reported secretion of MMP2 and MMP9 in the media of cultured bovine preantral follicles[22]. Similarly, goat preantral and early antral follicles express *MMP9* when cultured with FSH[23]. Degradation of the ECM is imperative to remodeling the ovary to accommodate follicle growth and, ultimately, ovulation. These data provide evidence that bovine preantral follicles are likely capable of modifying their surrounding ECM. Proteases also have corresponding inhibitors, which were not examined in this study. However, their presence could modulate each protease's bioactivity and follicle growth dynamics in the hydrogel.

In this study, we found that PEG hydrogels outperformed 2D control by showing greater growth over the 10-day period in primary follicles (starting diameter of 40-60 μm), but not primary-to-early-secondary transitionary follicles (61-70 μm). However, primary-to-early-secondary transitionary follicles maintained their size when cultured in PEG hydrogels, whereas they decreased in size when cultured in 2D control conditions. Although the follicles were not stained for viability post-culture, the decrease in size could indicate granulosa cell apoptosis or cellular dehydration, leading to reduced cell volume. Interestingly, there was a notable difference in the percentage of follicles that grew

between replicates (each represented by one ovary), further underlining the biological variability between samples, which is reflected in the results. Of note, primary follicles showed a decreased rate of growth in both PEG and control between day 5 and 10 of culture. This stagnation of growth suggested that either 1) the long-term culture conditions remain substandard for bovine small preantral follicles or 2) follicles canonically slow their growth at this stage of development, which is a phenomenon seen in mice[24].

We tested the hypothesis of enhancing the bovine follicle culture system with cellular supplementation as others have shown that the addition of stromal cells, fibroblasts, and adipose-derived stem cells promotes survival and growth of preantral follicles in numerous species[12,25-28]. Mesoderm-like cells (MeLCs) are a renewable cell source that could differentiate into a cell type resembling ovarian cells; hence these cells might be primed to become theca-like and complement the early preantral follicle unit. As a control comparison, we utilized dissociated bovine ovarian cells (BOCs) to include in the PEG hydrogel system. We compared the survivability of MeLCs and BOCs in PEG hydrogels without co-encapsulating follicles to determine an appropriate cell concentration. First, MeLCs did not survive in PEG hydrogels even shortly after encapsulation. We consider that the MeLCs, which have undergone an acute and recent induction process, are a sensitive cell type that cannot withstand the stressors of trypsinization, encapsulation, and alternative culture media exposure. We proceeded with testing varying concentrations of BOCs and found that 5, 10, and 20 x 10^6 cells/mL provided sufficient survivability. Intriguingly, BOCs formed cell aggregates that look strikingly similar to follicles after 10 days of culture. Further immunostaining with oocyte markers DDX4 and CX37 showed that aggregates were, in fact, not follicles as they

lacked signal for either protein in the interior of the aggregate. It is likely that, due to the absence of basement membrane binding proteins in the PEG composition, cells could not adhere to the matrix, resulting in self-aggregation. Indeed, cell-extracellular matrix interactions are important for mediating complex cellular responses such as migration, proliferation, and differentiation[29]. Thus, BOCs were likely incapable of integrating well throughout the hydrogel. Nevertheless, our data suggests that it can persist in the hydrogel, thus leading us to use BOCs as a cell supplementation source to complement the follicle culture system.

When we tested the hypothesis that follicles co-encapsulated with BOCs would have better survivability and growth, we found similarly high rates (100%) of atresia between follicles co-encapsulated and follicles in PEG-only hydrogels. This finding was perplexing since the first experiment comparing 2D culture to PEG culture showed moderate rates of growth between both conditions. We pose the possibility that the prolonged protocol required to dissociate ovarian tissue, isolate and label follicles, and process for encapsulation causes detrimental effects to follicle viability. Optimization for a streamlined protocol may be required to achieve improved results. Furthermore, when we analyzed expression of genes known to be important for pre-theca cell phenotype (*SMO*, *PTCH1*, *GLI1,* and *CSPG4*), we found lower expression of all genes after the cells were cultured with or without follicles present compared to day 0 freshly dissociated cells. We also detected a general decrease in *BAX* and *BCL2,* which could indicate mRNA downregulation as cells are in a suboptimal state. These data suggest that the PEG culture condition does not maintain the native profile of ovarian cells, and further system optimization is required. One method to shorten the protocol could be to in vitro culture

dissociated cells prior to encapsulation[30]. However, it is likely that this approach also changes the cell phenotype. As aforementioned, including basement membrane binding in the PEG hydrogel would better recapitulate the ovarian microenvironment and help maintain proper cell identity as well a migration towards the follicle to become theca-like cells. Finally, due to follicle death, hedgehog ligands were probably not being secreted, and therefore, there was no effect on upregulating or maintaining the hedgehog signaling pathway in the neighboring BOCs.

Overall, the PEG hydrogel system exhibits modest promise as a 3D culture system for in vitro bovine preantral follicle development. Further enhancement of the system is required to improve culture conditions for *in vitro* growth of bovine preantral follicles.

REFERENCES

1. Bus, A., Langbeen, A., Martin, B., Leroy, J. L. M. R. & Bols, P. E. J. Is the pre-antral ovarian follicle the 'holy grail'for female fertility preservation? *Anim Reprod Sci* **207**, 119–130 (2019).

2. Gutierrez, C. G., Ralph, J. H., Telfer, E. E., Wilmut, I. & Webb, R. Growth and Antrum Formation of Bovine Preantral Follicles in Long-Term Culture In Vitro1. *Biol Reprod* **62**, 1322–1328 (2000).

3. Araújo, V. R., Gastal, M. O., Wischral, A., Figueiredo, J. R. & Gastal, E. L. Long-term in vitro culture of bovine preantral follicles: Effect of base medium and medium replacement methods. *Anim Reprod Sci* **161**, 23–31 (2015).

4. Rossetto, R. *et al.* Impact of insulin concentration and mode of FSH addition on the in vitro survival and development of isolated bovine preantral follicles. *Theriogenology* **86**, 1137–1145 (2016).

5. Gomes, J. E., Correia, S. C., Gouveia-Oliveira, A., Cidadão, A. J. & Plancha, C. E. Three-dimensional environments preserve extracellular matrix compartments of ovarian follicles and increase FSH-dependent growth. *Mol Reprod Dev* **54**, 163–172 (1999).

6. Belli, M. *et al.* Towards a 3D culture of mouse ovarian follicles. *International Journal of Developmental Biology* **56**, 931–937 (2013).

7. Xu, M. *et al.* Encapsulated Three-Dimensional Culture Supports Development of Nonhuman Primate Secondary Follicles1. *Biol Reprod* **81**, 587–594 (2009).

8. Xu, J. *et al.* Fibrin promotes development and function of macaque primary follicles during encapsulated three-dimensional culture. *Hum Reprod* **28**, 2187–2200 (2013).

9. Ihm, J. E., Lee, S. T., Han, D. K., Lim, J. M. & Hubbell, J. A. Murine ovarian follicle culture in PEG-hydrogel: Effects of mechanical properties and the hormones FSH and LH on development. *Macromol Res* **23**, 377–386 (2015).

10. Mendez, U., Zhou, H. & Shikanov, A. Synthetic PEG Hydrogel for Engineering the Environment of Ovarian Follicles. in *Methods in Molecular Biology* (ed. Chawla, K.) 115–128 (Springer New York, New York, NY, 2018). doi:10.1007/978-1-4939-7741-3_9.

11. Shikanov, A., Smith, R. M., Xu, M., Woodruff, T. K. & Shea, L. D. Hydrogel network design using multifunctional macromers to coordinate tissue maturation in ovarian follicle culture. *Biomaterials* **32**, 2524–2531 (2011).

12. Tomaszewski, C. E. *et al.* Adipose-derived stem cell-secreted factors promote early stage follicle development in a biomimetic matrix. *Biomater Sci* **7**, 571–580 (2019).

13. Nason-Tomaszewski, C. E., Thomas, E. E., Matera, D. L., Baker, B. M. & Shikanov, A. Extracellular matrix-templating fibrous hydrogels promote ovarian tissue remodeling and oocyte growth. *Bioact Mater* **32**, 292–303 (2024).

14. Tomaszewski, C. E., DiLillo, K. M., Baker, B. M., Arnold, K. B. & Shikanov, A. Sequestered cell-secreted extracellular matrix proteins improve murine folliculogenesis and oocyte maturation for fertility preservation. *Acta Biomater* **132**, 313–324 (2021).

15. Wijgerde, M., Ooms, M., Hoogerbrugge, J. W. & Grootegoed, J. A. Hedgehog signaling in mouse ovary: Indian hedgehog and desert hedgehog from granulosa cells induce target gene expression in developing theca cells. *Endocrinology* **146**, 3558–3566 (2005).

16. Cowan, R. G. & Quirk, S. M. Cells responding to hedgehog signaling contribute to the theca of ovarian follicles. *Reproduction* **161**, 437–448 (2021).

17. Russell, M. C., Cowan, R. G., Harman, R. M., Walker, A. L. & Quirk, S. M. The hedgehog signaling pathway in the mouse ovary. *Biol Reprod* **77**, 226–236 (2007).

18. McDonnell, S. P., Candelaria, J. I., Morton, A. J. & Denicol, A. C. Isolation of Small Preantral Follicles from the Bovine Ovary Using a Combination of Fragmentation, Homogenization, and Serial Filtration. *JoVE* (2022) doi:doi:10.3791/64423.

19. Soto, D. A. *et al.* Simplification of culture conditions and feeder-free expansion of bovine embryonic stem cells. *Sci Rep* **11**, 1–15 (2021).

20. Spicer, L. J. *et al.* The hedgehog-patched signaling pathway and function in the mammalian ovary: A novel role for hedgehog proteins in stimulating proliferation and steroidogenesis of theca cells. *Reproduction* **138**, 329–339 (2009).

21. Figueiredo, J. R. de *et al.* Extracellular matrix proteins and basement membrane: Their identification in bovine ovaries and significance for the attachment of cultured preantral follicles. *Theriogenology* **43**, 845–858 (1995).

22. McCaffery, F. H., Leask, R., Riley, S. C. & Telfer, E. E. Culture of bovine preantral follicles in a serum-free system: Markers for assessment of growth and development. *Biol Reprod* **63**, 267–273 (2000).

23. Ferreira, A. C. A. *et al.* Pituitary porcine FSH, and recombinant bovine and human FSH differentially affect growth and relative abundances of mRNA transcripts of preantral and early developing antral follicles in goats. *Anim Reprod Sci* **219**, 106461 (2020).

24. Richard, S., Anderson, N. J., Zhou, Y. & Pankhurst, M. W. Mouse primary follicles experience slow growth rates after activation and progressive increases that influence the duration of the primary follicle phase. *Biol Reprod* **109**, 684–692 (2023).

25. Tagler, D. *et al.* Embryonic Fibroblasts Enable the Culture of Primary Ovarian Follicles Within Alginate Hydrogels. *Tissue Eng Part A* **18**, 1229–1238 (2012).

26. Grubliauskaitė, M. *et al.* Influence of ovarian stromal cells on human ovarian follicle growth in a 3D environment. *Hum Reprod Open* **2023**, (2023).

27. Tingen, C. M. *et al.* A macrophage and theca cell-enriched stromal cell population influences growth and survival of immature murine follicles in vitro. *Reproduction* **141**, 809–820 (2011).

28. Green, L. J., Zhou, H., Padmanabhan, V. & Shikanov, A. Adipose-derived stem cells promote survival, growth, and maturation of early-stage murine follicles. *Stem Cell Res Ther* **10**, 1–13 (2019).

29. Hynes, R. O. Stretching the boundaries of extracellular matrix research. *Nat Rev Mol Cell Biol* **15**, 761–763 (2014).

30. Jafari, H. *et al.* Ovarian Cell Encapsulation in an Enzymatically Crosslinked Silk-Based Hydrogel with Tunable Mechanical Properties. *Gels* **7**, 138 (2021).

Figures and tables

Figure 2.1

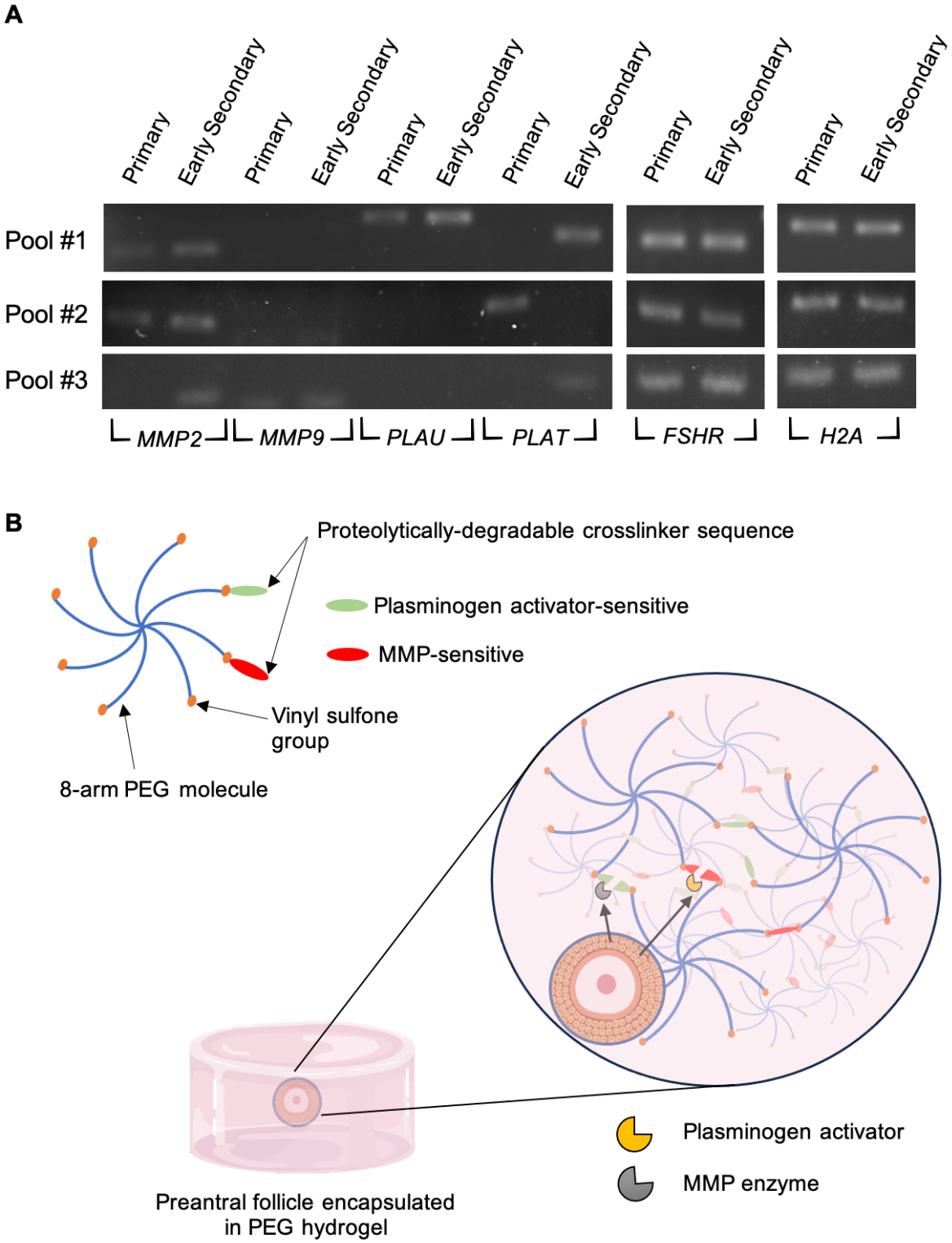

Figure 2.1. (**A**) PCR agarose gel of primary and early secondary follicles expressing mRNA for *MMP2, MMP9, PLAU, PLAT, FSHR,* and *H2A.* (**B**) Schematic of PEG hydrogel for in vitro folliculogenesis. MMP = matrix metalloproteinase.

Figure 2.2

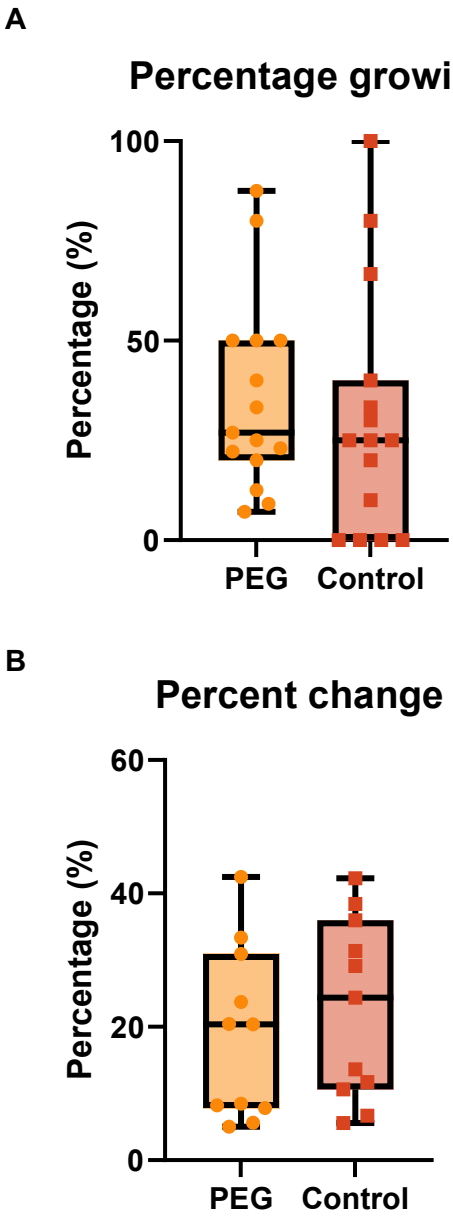

Figure 2.2. Bovine preantral follicle in vitro growth using PEG or 2D control culture systems. Percentage of preantral follicles that grew (**A**) and percent change in growth from follicles that grew (**B**).

Figure 2.3

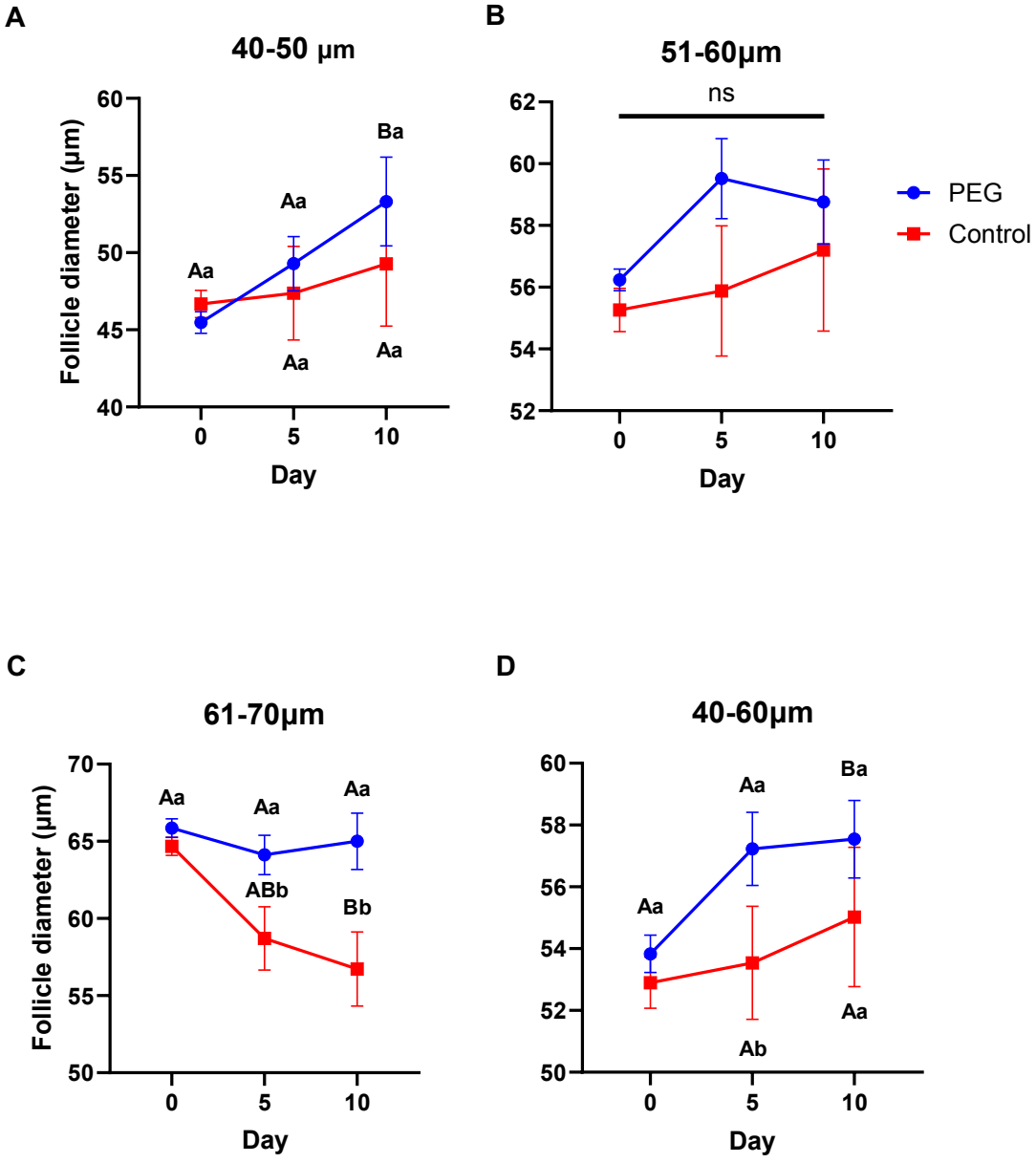

Figure 2.3. Bovine preantral follicle diameter growth during in vitro culture in PEG hydrogels or 2D control. Starting diameters at day 0 for 40-50 µm (**A**), 51-60 µm (**B**), 61-70 µm (**C**) and combined data for 40-60µm (**D**). Lowercases letters that differ = significant difference ($P < 0.05$) between treatment groups in the same day. Uppercase letters that differ = significant difference ($P < 0.05$) within the same treatment group but compared to day 0. Data shown as mean ± SEM.

Figure 2.4

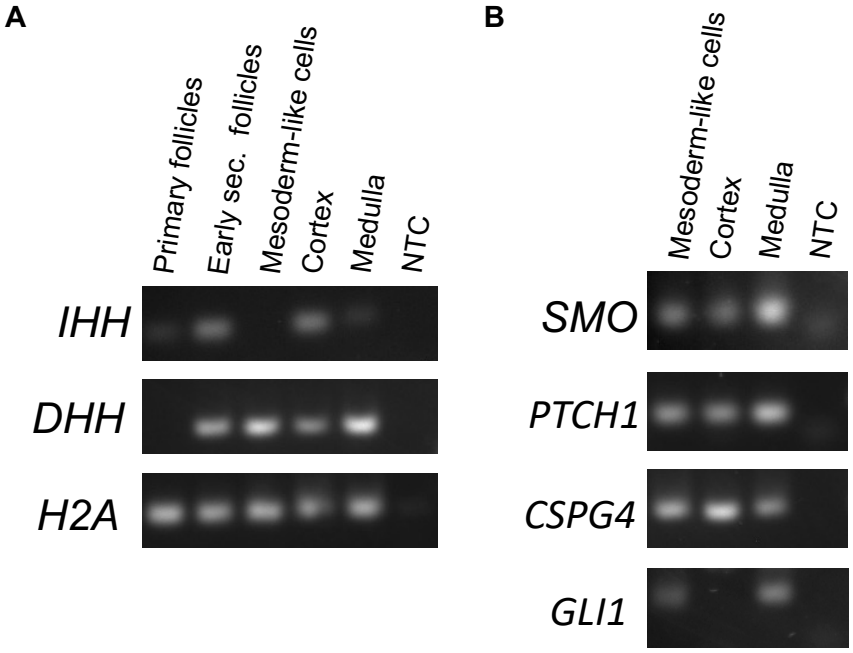

Figure 2.4. PCR of HH signaling mRNA (**A)** Ligands *DHH* and *IHH* gene expression in bovine primary and early secondary follicles, mesoderm-like cells (MeLCs), and freshly dissociated bovine cortex and medulla cells. *H2A* as a reference gene. (**B**) HH responsive genes mRNA (pre-theca cell markers) expressed in MeLCs, cortex, and medulla cells.

Figure 2.5

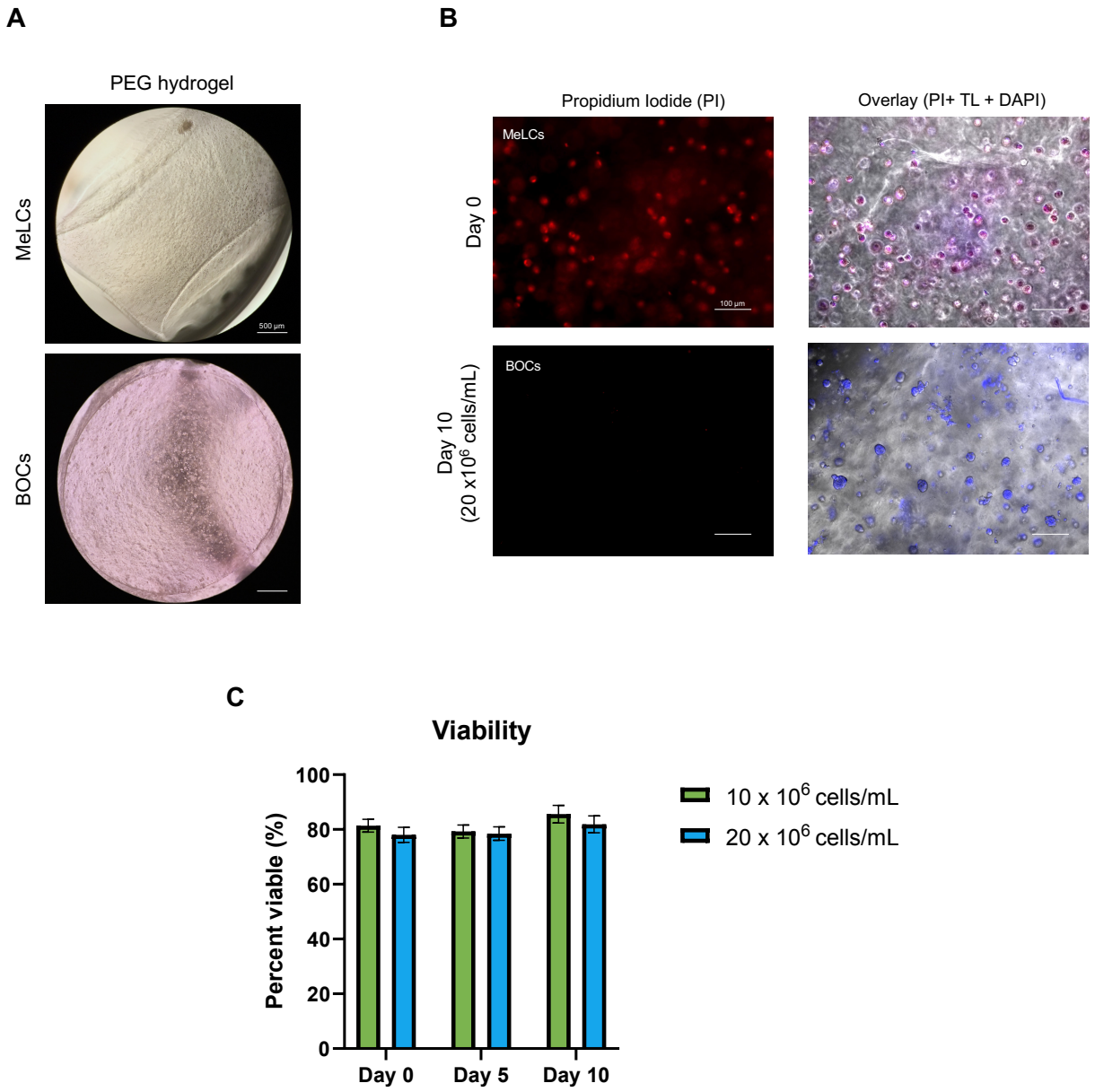

Figure 2.5. Mesoderm-like cells (MeLCs) and bovine ovarian cells (BOCs) in PEG hydrogels for in vitro culture. (**A**) encapsulated cells. (**B**) propidium iodide (PI) viability stain at day 0 and day 10 of culture in MeLCs and BOCs, respectively. TL = trans luminescent. (**C**) percentage of viable cells from PI staining in BOCs at 10 x 10^6 and 20 x 10^6 cells/mL during different culture periods

Figure 2.6

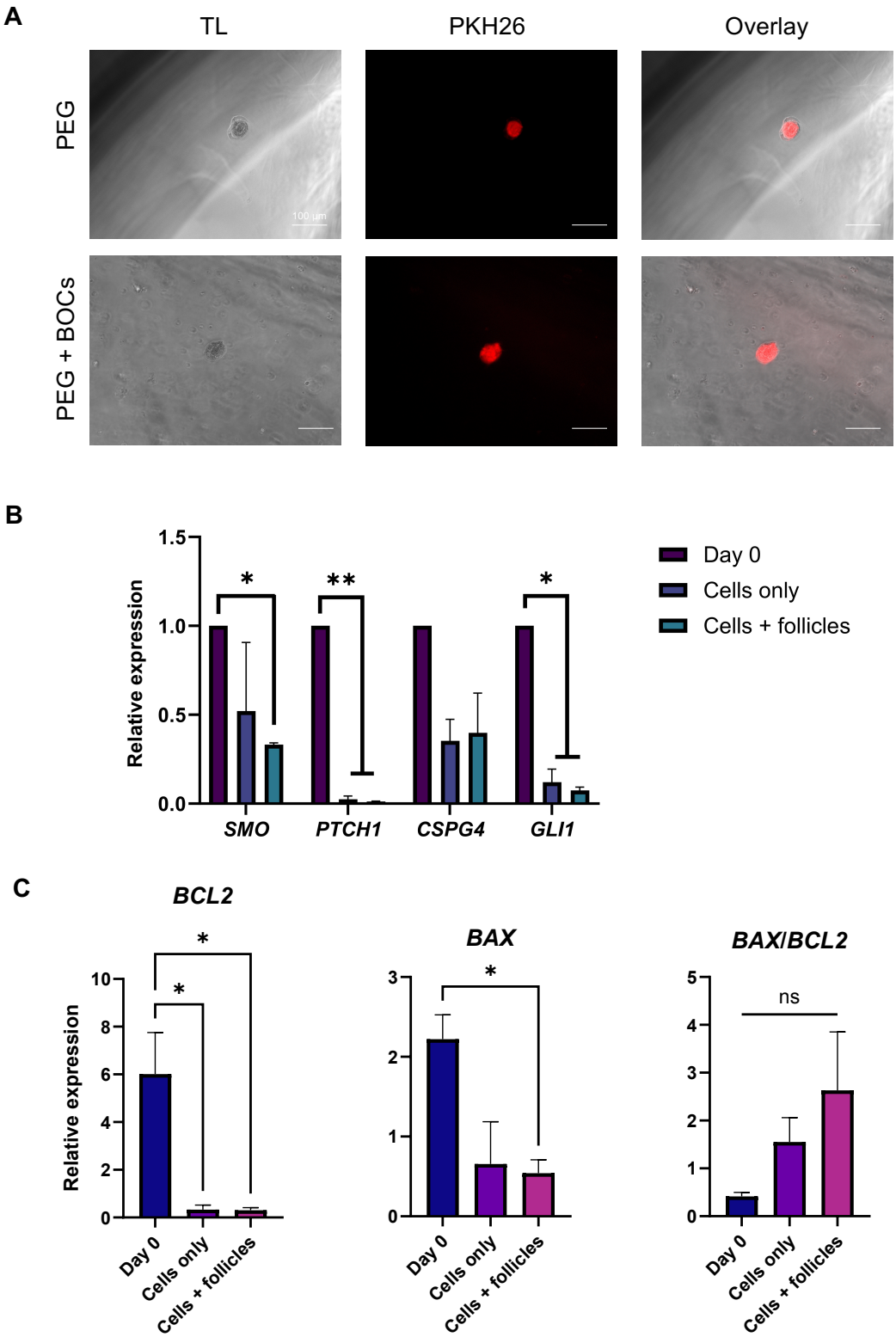
A
TL
PKH26
Overlay
PEG
PEG + BOCs
100 µm
B
Relative expression
1.5
1.0
0.5
0.0
*
**
*
SMO
PTCH1
CSPG4
GLI1
Day 0
Cells only
Cells + follicles
C
BCL2
BAX
BAX/BCL2
Relative expression
10
8
6
4
2
0
3
2
1
5
4
3
2
1
*
*
*
ns
Day 0
Cells only
Cells + follicles

Figure 2.6. Bovine preantral follicles encapsulated in PEG hydrogels with or bovine ovarian cells (BOCs). (**A**) PKH26 staining to mark follicles within hydrogels. (**B**) mRNA expression of pre-theca marker genes in BOCs after culture with or without follicles co-encapsulated. (**C**) mRNA expression of anti-apoptotic (*BCL2*) and pro-apoptotic (*BAX*) and ratio of *BAX*/*BCL2* of BOCs at day 0 and after culturing with or without follicles in PEG hydrogels. Data are presented as mean ± SEM. * = $P < 0.05$, ** = $P < 0.01$.

Table 1. Primer List

Primer Name	Forward Sequence (5'-3')	Reverse Sequence (5'-3')	Product size (base pairs)
BAX	CAT GAG GTC AAC CCT CGG GA	TAG GGA AGC CCA TGC TGA GT	117
BCL2	GAG TTC GGA GGG GTC ATG TG	GGG CCA TAC AGC TCC ACA AA	158
CSPG4	CTG GAG GAA CAA AGG TCT CTG G	ACT GCG TGA TCT GGA AAA GCA	140
DHH	GCA TGC ATT GCA GGT CGT C	ACG TGG GCA GAA TGC TAG TC	145
GLI1	CCT TCA AAG CCC AGT ACA TGC	GTG CGT CTT CAG ATT TTC CAG	122
IHH	CGG CTT CGA CTG GGT GTA TT	GGC TGA GTG CTC GGA CTT G	70
MMP2	ATC GTC TTC GAC GGC ATC TC	TTC GCC AGA TGA ATC GGT CC	70
MMP9	CTT CAC CTT TGA GGG TCG CT	TGG GTG TAG AGT CTC TCG CT	138
PLAT	TCG GCA GGC CCT CTA TTC TT	ACG TGG CGG TAG CAT CTA TTT	89
PLAU	TGG GTC AGT CAC GGC TTA AC	ACG GAT CTT CAG CAA GGC AAT	131
H2A.2	GAG GAG CTG AAC AAG CTG TTG	TTG TGG TGG CTC TCA GTC TTC	104
ACTB	CTC TTC CAG CCT TCC TTC CT	GGG CAG TGA TCT CTT TCT GC	178

CHAPTER 4

In Vitro Differentiation of Bovine Embryonic Stem Cells Toward Progenitors of Bipotential Gonad-like Somatic Cells

Abstract

Somatic cells of the mammalian gonad originate from the mesoderm, which differentiates into the intermediate mesoderm (IM), coelomic epithelium (CE), and then bipotential gonad (BG) via cell signaling by specific morphogens. Stem cell-based models have recapitulated stepwise gonadal cell differentiation in vitro. However, reports of successful cell induction into BG-like cells still need to be available. We hypothesized that bESCs would differentiate into IM, early CE (eCE), and steroidogenic-like state after exposure to an SF1 agonist, RJW100, or sustained WNT activation with short duration of activin A (Nodal) and bFGF (FGF) signaling, and low concentrations of BMP4 during in vitro culture. In experiment 1, bESCs were cultured for 48 h in the mesoderm induction medium (MIM) containing 3 μM CHIR99021 (GSK3 inhibitor/WNT activator) and 70 ng/mL activin A. Cells were then further cultured in a vehicle or RJW100 (10 μM) for an additional 48 and 96 hours. Similar to experiment 1, in experiment 2, bESCs were cultured in MIM and then further cultured in a vehicle or 10 ng/mL bFGF starting at 48, 72, or 96 h and harvested at 120 h. In experiment 3, after MIM culture, cells were cultured with 0, 1, 10, or 20 ng/mL BMP4 for an additional 72 h with a pulse of 10 ng/mL bFGF during the final 24 h of BMP4 exposure. Cells were subjected to RT-qPCR to examine expression of IM and eCE/bipotential gonad transcripts. We found that RJW100 did not promote expression of steroidogenic or IM/eCM genes. Furthermore, we found that 72 hours post-mesoderm induction led to upregulation of IM and eCE genes, even without exogenous bFGF and BMP4, and that increased BMP4 concentrations led to upregulation of lateral plate mesoderm markers. Moreover, paraxial mesoderm is not induced by these cell conditions. These data indicate the ability of bESCs to be differentiated towards the IM

and eCE lineages in vitro and show promising initial indicators that they could be further driven towards a somatic bipotential gonad-like state.

Introduction

Pluripotent stem cells (PSCs) can give rise to all primary germ layers and are a renewable cell source that can be used for generating any cell type of the body. Pluripotent stem cells can expand indefinitely; therefore, they can potentially produce an unlimited supply of a spectrum of cell types upon undergoing specific in vitro differentiation protocols. To produce mature cells of specific lineages, stepwise in vitro differentiation protocols are employed to drive PSCs into certain cell states that mimic the sequential events underlining in vivo embryonic development. During embryonic gastrulation, embryonic stem cells are classified into the three primary germ layers: mesoderm, endoderm, and ectoderm. In a similar fashion, most in vitro differentiation protocols initially induce PSCs to become one of these germ layer lineages. While there has been some progress in robustly and efficiently stimulating PSCs through the first cell fate decision of becoming a germ layer, much of this work has been achieved only in mouse models where embryonic gastrulation occurs differently compared to large mammal species. Moreover, approaches to recapitulate this process vary and may lead to alternate cell fates, thus failing to commit to a single lineage.

The mesoderm germ layer is the origin of muscle, cartilage, bone, and the urogenital system, which includes the kidneys, adrenal gland, and gonads. During gastrulation, the mesoderm layer is created when cells of the primitive streak ingress between the epiblast and hypoblast. Once established, the mesoderm layer is further refined into the paraxial, intermediate, and lateral plate mesoderm. The intermediate mesoderm, which contains the progenitor cells for the prospective gonad, is specified by temporal- and dose-dependent exposure to morphogens such as bone morphogenic

proteins (BMPs), transforming growth factor-beta (TGFβ), fibroblast growth factors (FGFs) and Wnt protein[1-3]. These morphogens transduce intricate, yet precise, intracellular signaling to achieve proper downstream gene expression and programmed cell differentiation. For example, while epiblast cells are induced into mesoderm via FGF and Wnt signaling[1,4] (forming the primitive streak), anterior-posterior patterning of the elongating embryo concomitantly occurs and is driven by the concerted balance of Wnt and Nodal signaling[5] . Moreover, mediolateral segmentation of the mesoderm occurs when a gradient of low, medium, and high BMP signaling drives mesoderm cells into the paraxial, intermediate, and lateral plate mesoderm domains, respectively[6].

Capitalizing on current understanding behind the molecular cell signaling mechanisms that constitutes early embryonic development has permitted researchers to attempt recapitulating these processes in vitro and derive tissue-lineage cells from PSCs. For instance, derivation of kidney progenitor-like cells from human PSCs has been demonstrated by several groups and protocols include a key transitional intermediate mesoderm-like state to prime cells for further differentiation[7-11]; a process which in vivo must precede renal formation. Indeed, exogenous inclusion of Wnt and Nodal activators such as CHIR and activin A, respectively, are needed to achieve appropriate gene expression related to the intermediate mesoderm (*OSR1*, *LHX1*). Others have reported capture and expansion of near explicit intermediate mesoderm-like cells from human PSCs[11] which presents opportunity to utilize these cells for other lineage differentiation such as adrenal or gonadal tissue. In the case of generating gonad-like cells, there has been much less research compared to renal-like cells and current work predominantly describes PSC differentiation into the male phenotype (testis- and Sertoli-like cells) for

potential applications in cell and hormone replacement therapy. Approaches to deriving testis-like cells include self-aggregation of PSCs into 3-dimensional organoids[12,13] and 2-dimensional monolayer culture[14]. Moreover, initial embryonic gonad specification is not sex dependent. In other words, as the gonad arises from the intermediate mesoderm, it is bipotential and can gain an ovary or testis identity upon further development. Indeed, by testing various concentrations and temporal exposure of PSCs to Wnt activators, FGFs, and BMPs, researchers have reported differentiation into a bipotential gonad-like cell as indicated by upregulation of genes such as *WT1* and *GATA4* which are known in vivo markers[15,16]. Steroidogenic-factor 1 (*SF1* or *NR5A1*) is an additional gene responsible for early embryonic gonad differentation[17] and overexpression of *NR5A1* increases the efficiency of bipotential gonad-like cell and testis-like cell induction[18,19]. More recently, gene screening studies uncovered the requirement of *NR5A1* for inducing human iPSCs into a granulosa cell-like phenotype which is major cell type constituting the ovary[20]. As the name implies, NR5A1 is essential for steroidogenic properties of cells, which is fundamental to the somatic cell compartments of both the testis and ovary. Collectively, data from these studies demonstrate the possibility of directing cell differentiation from PSCs and applications spanning many species from rodents to humans.

In this study, we aimed to determine the propensity of bovine embryonic stem cells (bESCs) to be induced into the intermediate mesoderm- and bipotential gonad-like cell state via in vitro culture. Based on current knowledge of in vivo developmental events, we tested the use of an SF1 agonist, RJW100, and several protocols, which included Wnt

activators, BMPs, and FGFs to determine the optimal drive of bESCs to express genes known to be important for mammalian intermediate mesoderm and gonadal cell lineages.

Material and methods

All materials were purchased from Thermo Fisher Scientific unless otherwise specified.

Culture of bovine embryonic stem cells (bESCs)

Bovine embryonic stem cells (n = 1 female line) were routinely cultured feeder-free in NBFR medium (N2B27 medium [1:1 DMEM/F12 and Neurobasal media, 0.5% v/v N-2 supplement, 1% v/v B-27 supplement, 2 mM MEM Non-Essential Amino Acid solution, 1% v/v GlutaMAX supplement, 0.1 mM 2-mercaptoethanol (M6250, Sigma), 100 U/mL Penicillin, and 100 µg/mL Streptomycin] supplemented with 1% bovine serum albumin (BSA) (0219989950, MP Biomedicals), 20 ng/mL bFGF (100-18B, PeproTech), 2.5 µM IWR-1 (I0161, Sigma), and 20 ng/mL Activin A (338-AC, R&D Systems)]. Cells were passaged onto vitronectin-coated plates every 2-4 days using TrypleExpress at 1:4-1:6 split ratio and cultured in humidified incubators at 37 ºC and 5% CO_2. When cells were passaged, media was supplemented with 10 µm ROCK inhibitor Y-27632 (ALX-270-333-M005, Enzo). Media was changed daily and bESCs used for mesoderm induction were between passage 18-26.

For mesoderm induction, bESCs were passaged onto 12-well vitronectin-coated plates at 40,000 cells per well (1 mL per well) in mesoderm-induction media (GMEM medium, 15% knockout serum replacement, 0.1 mM NEAA, 2mM GlutaMAX, 1mM Na Pyruvate, 0.1mM β-mercaptoethanol (M6250, Sigma Aldrich), 100 U/mL Penicillin, and

100 µg/mL streptomycin and supplemented with 3 µm CHIR99021 (Tocris Bioscience, 44-231-0) and 70 ng/mL Activin A. Cells were cultured in mesoderm-induction medium for 24, 48, or 72 hours with daily medium change and thereafter the cells were considered "mesoderm-like cells" (MeLCs) and used for subsequent experiments.

We first tested the effect of the SF1 agonist RJW100 on upregulating intermediate mesoderm and bipotential gonad marker genes. MeLCs were cultured in a mesoderm induction medium with vehicle (DMSO) or 10 µM RJW100 for 48 or 96 hours (Figure 3.1A). In a second experiment, MeLCs were cultured in mesoderm induction medium without activin A for an additional 72 hours and supplemented with 10 ng/mL bFGF beginning immediately after MeLC induction, 24 hours after MeLC induction, 48 hours after MeLC induction, or no supplementation (vehicle only) (Figure 3.1B). Based on the finding of which bFGF regimen best upregulated gene expression, in a third experiment, MeLCs were cultured in mesoderm induction media without activin A, with 10 ng/mL bFGF and with either 0, 1, 10, or 20 ng/mL of BMP4 for an additional 72 hours (Figure 3.1C). All experiments contained duplicate wells for each condition tested and had 3 biological replicates/independent differentiations. Cells were imaged every day during each differentiation on the Evos (Thermo Fisher) inverted microscope.

RNA isolation, cDNA synthesis, and RT-qPCR

Collected cells were pelleted and snap-frozen in liquid nitrogen with minimal PBS. RNA was isolated from cell pellets using the Qiagen RNeasy Micro Kit following manufacturer's instructions. Once the RNA was isolated, 1 µg of total RNA was used for

cDNA synthesis, following manufacturer's instructions (RevertAid cDNA Reverse Transcription Kit). For RT-qPCR, 1 µl of cDNA (50 ng total), 1x SsoAdvanced Universal SYBR Green Supermix (1725271, Bio-Rad), and 250 nM of forward and reverse primers (primer sequences listed in Table 2) were mixed for a 10 µl total volume reaction and pipetted into 96-well plates. The RT-qPCR reaction was carried out in the CFX96 Touch Deep Well Real-Time PCR Detection System (Bio-Rad). Cycling conditions were an initial denaturation step at 95 ºC for 30 sec followed by 40 cycles of denaturation at 95 ºC for 10 sec, annealing at 60 ºC for 30 sec, and extension at 60 ºC for 5 sec. To confirm specificity of PCR products for each gene, each assay included a melt curve analysis and non-template control. Relative expression was calculated by taking the inverse of the delta Ct values for each treatment group.

Immunocytochemistry

Fetal bovine (day 31 post-fertilization) mesonephros was fixed in 4% paraformaldehyde overnight in 4°C. Mesonephros tissue was soaked in sucrose with PBS solution (30% v/v) and embedded in OCT, placed in a -80°C freezer, and later cry sectioned. Sections were cut at 10 µm and placed on positively charged slides. Slides with tissue sections were subjected to antigen retrieval using citrate buffer (H-3300, Vector Laboratories) and were placed in a steamer set to 200°C for 10 mins. Slides were washed and incubated with blocking buffer (10% donkey serum, 1% BSA, 0.3 mM glycine) for 1 hour at room temperature (RT) in a humidified chamber. Sections were incubated with 2.25 µg/mL of anti-WT1 rabbit monoclonal antibody (ab89901, Abcam) or

with blocking solution only (no primary antibody) or a rabbit isotype IgG (negative controls) overnight in a humidified chamber at 4°C. After washing, 1 µg/mL of Hoechst 33342 and 1 µg/mL donkey-anti-rabbit FITC-conjugated secondary antibody was added for 1 hour at RT. Slides were washed and mounted with Prolong Gold mounting media and cover-slipped for imaging using the Revolve epifluorescent microscope.

For immunocytochemistry of monolayer cells in culture, cells were cultured on coverslips and fixed with 4% paraformaldehyde for 10 min at RT. After washing with PBS, cells were permeabilized for 10 min with 1% Triton X-100 in PBS, washed with PBS, and blocked with blocking buffer (0.3% Triton X-100 and 1% w/v BSA in PBS) for 45 min at RT. Cells were then incubated with blocking buffer containing anti-WT1 antibody (2.25 µg/mL) and anti-OCT4 antibody (2 µg/mL; AF1759, R&D Systems) or no-primary negative control overnight at 4°C. Cells were washed and incubated in blocking buffer containing 1 µg/mL of Hoechst 33342 and 2 µg/mL of FITC-conjugated donkey anti-rabbit and Texas Red-conjugated donkey anti-mouse secondary antibodies for 1 hour at RT. Cells were washed 3 times with PBS containing 0.3% Triton X-100 for 10 min. Immediately after staining, cells were mounted on slides with Prolong Gold anti-fade mounting media and imaged with a ImageXpress Micro Confocal Imaging System (Molecular Devices)

Statistical Analysis

Data from RT-qPCR experiments were analyzed for normality using Shapiro-Wilk test in Graph Prism. Normally- distributed data were subjected to one-way ANOVA and data that were not normally distributed were subjected to a Kruskal-Wallis test in Graph

Prism. Post-hoc tests (Tukey's and Dunn's for ANOVA and Kruskal-Wallis, respectively) were conducted when appropriate. Differences were considered significant if the comparisons were associated with $P < 0.05$.

Results

Prior to testing the efficacy of RJW100 to drive bESC differentiation, we first determined the human and bovine amino acid sequence homology of the ligand binding pocket of SF1 where RJW100 elicits its function. We found that the bovine and human ligand-binding domain share ~95% identity (Figure 3.2), thus providing initial evidence that the RJW100 agonist, designed for human compatibility, should be effective in bovine cells. Next, we wanted to ensure that *SF1* was present in MeLCs and determine length of mesodermal induction that led to highest *SF1* expression. As seen in Figure 3.3A, we detected highest expression of *SF1* after 24 and 48 hours of culture in mesoderm induction medium compared to undifferentiated bESCs ($P < 0.05$). Therefore, we chose to induce bESCs to MeLCs for 48 hours for proceeding experiments. When cells were cultured for 48 or 96 hours in vehicle or 10μM of RJW100, there was no difference in level of expression of *StAR* (Figure 3.3B). There was greater *WT1* expression at 48 hours in vehicle compared to bESCs ($P < 0.05$) and greater *GATA4* expression at 96 hours in both vehicle and RJW100 conditions compared to bESCs (Figure 3.3C and D). There was no difference between *GATA4* expression between vehicle and RJW100 at 96 hours ($P = 0.9$). Across all experimental groups, there was also no difference in *SF1* (Figure 3.3E) ($P = 0.14$). Finally, *CYP17A1* was upregulated in MeLCs compared to bESCs ($P = 0.05$). (Figure 3.3F). Collectively, these data indicate that the SF1 agonist RJW100 did not

promote steroidogenic or gonadal-like differentiation as indicated by mRNA expression of key markers.

Next, we tested the hypothesis that MeLCs exposed to a pulse of bFGF during bipotential gonad/intermediate mesoderm differentiation would upregulate gene expression of key markers at the end of induction. Compared to bESCs and 0, 24, 48, and 72 hours of 10 ng/mL bFGF exposure, MeLCs had higher expression of lateral plate/intermediate mesoderm marker *LHX1* (Figure 3.4A; $P < 0.001$). We also found the intermediate mesoderm marker *OSR1* to be significantly upregulated in all bFGF regimens compared to bESCs (Figure 3.4B; $P < 0.01$). When analyzing expression of bipotential gonad markers, there was no difference in *GATA4* ($P = 0.15$) across all experimental groups (Figure 3.4C). We also found *WT1* was highest expressed at 0, 24, 48, and 96 hours of bFGF compared to bESCs and MeLCs (Figure 3.4D; $P < 0.001$). There was no difference in expression of *WT1* between bESCs and MeLCs ($P = 0.15$). There was also no difference in expression of the paraxial mesoderm marker *PAX3* across all experimental groups (Figure 3.4E; $P = 0.06$), indicating induction conditions did not show strong propensity to drive cells to the paraxial mesoderm fate. However, the lateral plate mesoderm marker *FOXF1* was significantly upregulated compared to bESCs in 0, 24, and 48 hours of bFGF exposure (Figure 3.4F; $P < 0.05$).

Because all bFGF regimens tested caused elevation in *WT1* and *OSR1* expression, we chose to use a 24-hour pulse of bFGF in the next experiments when testing the synergistic effects of including various concentrations of BMP4 over the same culture period time. Similar to the bFGF experiment, we found the highest level of *LHX1* expression in MeLCs (Figure 3.5A; $P < 0.0001$). However, 10 and 20 ng/mL of BMP4 led

to significantly lower expression when compared to bESCs ($P < 0.01$). *OSR1* was significantly elevated in all experimental groups, including MeLCs, when compared to bESCs (Figure 3.5B; $P < 0.05$). Unlike in the bFGF experiment where there was no difference amongst exposure times to bFGF, we found an increase in *GATA4* when 10 or 20 ng/mL of BMP4 were present (Figure 3.5C; $P < 0.05$). *WT1* was significantly upregulated in 0, 1, 10, or 20 ng/mL BMP4, but not in MeLCs (Figure 3.5D; $P < 0.05$). There was similarly no difference in *PAX3* among all concentrations of BMP4 when compared to bESCs, however there was a difference in *PAX3* between 0 and 1 ng/mL BMP4 (Figure 3.5E; $P < 0.05$). As expected, increasing the concentration of BMP4 led to a significant increase in *FOXF1* (Figure 3.5F; $P < 0.05$), indicating a likely shift towards the lateral plate mesoderm lineage with rising levels of BMP4 which is similar to in vivo development.

To confirm specificity of the anti-WT1 antibody, we demonstrate positive signal in 31 day-fetal bovine mesonephros tissue; a transient organ that is a derivative of mesoderm and known to express WT1 (Figure 3.6). We further assessed WT1 expression in bESCs, MeLCs, and cells cultured with 0 and 1ng/mL BMP4 as these concentrations led to elevated *WT1* without upregulating *FOXF1.* In addition, we immunostained for pluripotency marker OCT4 (Figure 3.7). We found positive nuclear staining for OCT4 in bESCs and MeLCs and loss of signal in 0 and 1 ng/mL BMP4 cells, indicating likely loss of pluripotency after mesoderm induction. We found nuclear localization of WT1 in bESCs and nuclear and cytoplasmic staining in MeLCs and 0 ng/mL BMP4. We did not find WT1 in 1 ng/mL BMP4 cells.

Discussion

Pluripotent embryonic stems are an attractive source of renewable cells for regenerative medicine purposes and modeling diseases. Moreover, their capacity to give rise to all cell types of the body permits studying various facets of cell ontogeny, which are otherwise difficult to assess with in vivo studies. In this study, we employed bovine embryonic stem cells to attempt recapitulating mesoderm formation and early differentiation of the bipotential gonad with defined media conditions and in a monolayer culture system. We show that the inclusion of exogenous signaling factors, such as CHIR (Wnt activation), can drive bESCs into intermediate mesoderm-like cells that show early signs of coelomic epithelial-like phenotypes as indicated by appropriate gene and protein expression. However, we found that activin A, bFGF, and BMP4, and the SF1 agonist, RJW100, are not necessary to induce the intermediate mesoderm or early coelomic epithelium. We chose to use the aforementioned signaling factors because they seemingly mimic the molecular events that drive cell fate decisions of gonad development during early embryogenesis across several mammalian species[21]. Bipotential gonad formation requires ingression and proliferation of the ventromedial aspect of the coelomic epithelium[22]. Hence, we suggest that data from this study shows the early coelomic epithelium state and could commence toward bipotential gonad-like cells with further culture.

Elongation of the body axis occurs during gastrulation and results in the anterior-posterior polarity of a developing embryo. At the more posterior end of the primitive streak, cells expressing Brachyury (T) give rise to the mesoderm and are the ancestral cell population to the eventual ovary or testis. Timely divergence of mesoderm cells into

regionalized descendants, such as the intermediate mesoderm cells, is regulated by signaling molecules such as Wnt and migration of cells[3]. The more caudal and rostral aspect of the intermediate mesoderm is specified by gradients of FGF and retinoic acid, respectfully, with the caudal region becoming later specified into the coelomic epithelium (CE) and bipotential gonad[23-25]. Upon proliferation of the CE, cells begin to express *SF1* which turns on the somatic cell developmental program for early bipotential gonad formation[26]. We hypothesized that an SF1 agonist, such as RJW100, would ameliorate the activity of SF1 in T-expressing MeLCs, therefore causing greater upregulation of downstream genes such as *CYP17A1* and *STAR* and promote a bipotential gonad-like phenotype. RJW100 functions by binding to the lipophilic binding pocket of SF1 which enhances its ability to bind to promoter regions of DNA[27,28]. Despite finding *SF1* mRNA expression in MeLCs and predicted compatibility based on amino acid sequence homology, our results did not support the hypothesis as downstream genes were not upregulated. We postulate that 1) cells do not express SF1 at the protein-level thus RJW100 could not be effective, 2) cells may not exhibit the correct program/phenotype that is required to activate SF1 and drive downstream transcription, or 3) RJW100 is unable to properly bind and activate SF1 in bovine cells. Future studies should examine the bioactivity of RJW100 in steroidogenic bovine cells to confirm its efficacy.

Signaling by WNT and FGF during body axis extension, which occurs at peri-gastrulation and is regulated by T as well as other morphogens, drives fate decision of the cells towards more caudal body axis[29]. Concomitantly, BMPs specify the mediolateral cell fate during body patterning, especially in the mesoderm[30]. Based on the finding that RJW100 did not augment early gonadal gene expression and base media was sufficient

to increase some gene markers, we chose to study the continuous inclusion of CHIR and timed exposure of bFGF at fixed concentrations on IM and early bipotential gonad markers when differentiating bESCs. Our results show peak expression of *LHX1* in MeLCs, while an additional 3 days of culture in base media with 0, 24, 48, or 72 hours of bFGF led to decreased expression. This finding also held true when we tested concentrations of BMP4 during induction. These data corroborate work demonstrating the ability of activins to induce *Lim1* (i.e. *Lhx1*) and its important role in more anterior IM specification/kidney development[31] since our MeLC induction media includes activin A and subsequent removal during the additional 3-day culture period. *OSR1* was upregulated to a similar level across all FGF and BMP4 regimens, indicating equal propensity of cells to become intermediate mesoderm-like with zero to high exposure time to FGF or 0-20 ng of BMP4. Since *OSR1* is the earliest marker of IM and others have shown the necessity of *OSR1* for the urogenital phenotype[32-34] and generating somatic cells of the gonad from PSCs[36], we believe cells may be reaching the IM state with possible capability of becoming progenitor bipotential gonad-like. Nevertheless, *OSR1* is not exclusive of the IM or gonads: kidney progenitor and lateral plate mesoderm cells express *OSR1*[34,36] and it is used to demarcate kidney progenitor-like cells during in vitro differentiation of PSCs[10,37,38]. Therefore, our intermediate mesoderm/early coelomic epithelium-like cells should be further evaluated for markers of early nephrogenesis.

We additionally found a rise in *WT1,* which is also an early, and more restrictive, marker of gonadal progenitor cells[39], in induced cells across all FGF and BMP4 regimens compared to bESCs. This indicates that base media culture, which includes CHIR for Wnt activation, for 3 additional days after MeLC induction can provoke *WT1* expression. WT1

is found along the A-P axis of mice as early as E9.0, with overlapping expression of GATA4 and NR5A1 in the coelomic epithelium by E10.0 and onward[39]. Moreover, WT1 activates the NR5A1 promoter[17], thus driving early gonad development. Interestingly, *WT1* upregulation was accompanied by *GATA4* upregulation when 10 or 20 ng/mL of BMP4 was included in culture. This data further suggests that induced cells may be at the IM or early coelomic epithelial stage which could still be a correct developmental trajectory to become bipotential-gonad like and therefore possibly begin expression of NR5A1 with more time in culture. Nonetheless, others have reported the downstream expression *Gata4* by BMP4 specifically in the lateral plate mesoderm[40]. Therefore, it would be beneficial to include more genes in this panel to give clearer indications of which mesoderm lineage these cells are likely representing. We additionally highlight there was no difference in *PAX3* (paraxial mesoderm marker) with any timing of FGF exposure. Instead, increasing BMP4 concentrations led to increased expression of *FOXF1* (lateral plate mesoderm marker), which aligns with in vivo studies showing a higher gradient of BMPs specifies the lateral plate of developing embryos[30].

Our findings mostly corroborate other work looking at differentiation of ESCs from humans and mouse to gonad-like cells by using combinations of BMP4, various FGFs including bFGF, CHIR, and activin A[13,14,41]. Overexpression of key transcription factors such as *SF1*, *WT1*, *RUNX1*, and *GATA4* also can induce gonad-like cell formation [20,42], although our experiments did not use this approach and instead focused on small molecule media components. The efficiency of induction can be variable when using small molecules or genomic engineering for differentiating stem cells, therefore heterogeneity in cell identity may be present. Although not done in this study, cell-sorting

based on expression of key markers could aid in purifying cell populations of interest and used for downstream in vitro culture to achieve bipotential and even ovary or testis- like cells. Yet, in vivo early somatic progenitor cells of the bipotential gonad are not specified homogeneously, therefore some heterogeneity could be warranted, especially when forming organoids as self-organizing structures. Finally, future studies should examine early bovine embryonic development in vivo as findings from these studies could shed light on the species-specific molecular mechanisms that drive gonad formation and inform future in vitro culture conditions to recapitulate the process.

REFERENCES

1. Ciruna, B. & Rossant, J. FGF signaling regulates mesoderm cell fate specification and morphogenetic movement at the primitive streak. *Dev Cell* **1**, 37–49 (2001).

2. Aulehla, A. & Pourquié, O. Signaling gradients during paraxial mesoderm development. *Cold Spring Harb Perspect Biol* **2**, a000869 (2010).

3. Sweetman, D., Wagstaff, L., Cooper, O., Weijer, C. & Münsterberg, A. The migration of paraxial and lateral plate mesoderm cells emerging from the late primitive streak is controlled by different Wnt signals. *BMC Dev Biol* **8**, 1–15 (2008).

4. Yamaguchi, T. P., Takada, S., Yoshikawa, Y., Wu, N. & McMahon, A. P. T (Brachyury) is a direct target of Wnt3a during paraxial mesoderm specification. *Genes Dev* **13**, 3185–3190 (1999).

5. Brennan, J. *et al.* Nodal signalling in the epiblast patterns the early mouse embryo. *Nature* **411**, 965–969 (2001).

6. James, R. G. & Schultheiss, T. M. Bmp signaling promotes intermediate mesoderm gene expression in a dose-dependent, cell-autonomous and translation-dependent manner. *Dev Biol* **288**, 113–125 (2005).

7. Batchelder, C. A., Lee, C. C. I., Matsell, D. G., Yoder, M. C. & Tarantal, A. F. Renal ontogeny in the rhesus monkey (Macaca mulatta) and directed differentiation of human embryonic stem cells towards kidney precursors. *Differentiation* **78**, 45–56 (2009).

8. Takasato, M., Er, P. X., Chiu, H. S. & Little, M. H. Generation of kidney organoids from human pluripotent stem cells. *Nat Protoc* **11**, 1681–1692 (2016).

9. Xia, Y. *et al.* Directed differentiation of human pluripotent cells to ureteric bud kidney progenitor-like cells. *Nat Cell Biol* **15**, 1507–1515 (2013).

10. Takasato, M. *et al.* Directing human embryonic stem cell differentiation towards a renal lineage generates a self-organizing kidney. *Nat Cell Biol* **16**, 118–126 (2014).

11. Kumar, N. *et al.* Generation of an expandable intermediate mesoderm restricted progenitor cell line from human pluripotent stem cells. *Elife* **4**, 1–24 (2015).

12. Pryzhkova, M. V., Boers, R. & Jordan, P. W. Modeling Human Gonad Development in Organoids. *Tissue Eng Regen Med* **19**, 1185–1206 (2022).

13. Rore, H., Owen, N., Piña-Aguilar, R. E., Docherty, K. & Sekido, R. Testicular somatic cell-like cells derived from embryonic stem cells induce differentiation of epiblasts into germ cells. *Commun Biol* **4**, (2021).

14. Gonen, N. *et al.* In vitro cellular reprogramming to model gonad development and its disorders. *Sci Adv* **9**, (2023).

15. Knarston, I. M. *et al.* An In Vitro Differentiation Protocol for Human Embryonic Bipotential Gonad and Testis Cell Development. *Stem Cell Reports* **15**, 1377–1391 (2020).

16. Sepponen, K. *et al.* The role of sequential BMP signaling in directing human embryonic stem cells to bipotential gonadal cells. *Journal of Clinical Endocrinology and Metabolism* **102**, 4303–4314 (2017).

17. Wilhelm, D. & Englert, C. The Wilms tumor suppressor WT1 regulates early gonad development by activation of Sf1. *Genes Dev* **16**, 1839–1851 (2002).

18. Sepponen, K. *et al.* Steroidogenic factor 1 (NR5A1) induces multiple transcriptional changes during differentiation of human gonadal-like cells. *Differentiation* **128**, 83–100 (2022).

19. Ishida, T. *et al.* Differentiation of Human Induced Pluripotent Stem Cells Into Testosterone-Producing Leydig-like Cells. *Endocrinology* **162**, bqab202 (2021).

20. Smela, M. D. P. *et al.* Directed differentiation of human iPSCs to functional ovarian granulosa-like cells via transcription factor overexpression. *Elife* **12**, (2023).

21. Rotgers, E., Jørgensen, A. & Yao, H. H. C. At the crossroads of fate-Somatic cell lineage specification in the fetal gonad. *Endocr Rev* **39**, 739–759 (2018).

22. Karl, J. & Capel, B. Sertoli cells of the mouse testis originate from the coelomic epithelium. *Dev Biol* **203**, 323–333 (1998).

23. Yoshioka, H. *et al.* Mesonephric FGF signaling is associated with the development of sexually indifferent gonadal primordium in chick embryos. *Dev Biol* **280**, 150–161 (2005).

24. Diez, R. *et al.* Diez del Corral-2003 Opposing FGF and retinoid pathways control...pdf. *Cell Press* **40**, 65–79 (2003).

25. Abu-Abed, S. *et al.* The retinoic acid-metabolizing enzyme, CYP26A1, is essential for normal hindbrain patterning, vertebral identity, and development of posterior structures. *Genes Dev* **15**, 226–240 (2001).

26. Luo, X., Ikeda, Y. & Parker, K. L. A cell-specific nuclear receptor is essential for adrenal and gonadal development and sexual differentiation. *Cell* **77**, 481–490 (1994).

27. Mays, S. G. *et al.* Enantiomer-specific activities of an LRH-1 and SF-1 dual agonist. *Sci Rep* **10**, 22279 (2020).

28. Whitby, R. J. *et al.* Small molecule agonists of the orphan nuclear receptors steroidogenic factor-1 (SF-1, NR5A1) and liver receptor homologue-1 (LRH-1, NR5A2). *J Med Chem* **54**, 2266–2281 (2011).

29. Amin, S. *et al.* Cdx and T Brachyury Co-activate Growth Signaling in the Embryonic Axial Progenitor Niche. *Cell Rep* **17**, 3165–3177 (2016).

30. Niehrs, C., Dosch, R. & Onichtchouk, D. Embryonic patterning of Xenopus mesoderm by Bmp-4. *Of Fish, Fly, Worm, and Man: Lessons from Developmental Biology for Human Gene Function and Disease* 165–190 (2000).

31. Preger-Ben Noon, E., Barak, H., Guttmann-Raviv, N. & Reshef, R. Interplay between activin and Hox genes determines the formation of the kidney morphogenetic field. *Development* **136**, 1995–2004 (2009).

32. Wang, Q., Lan, Y., Cho, E. S., Maltby, K. M. & Jiang, R. Odd-skipped related 1 (Odd1) is an essential regulator of heart and urogenital development. *Dev Biol* **288**, 582–594 (2005).

33. Mae, S.-I. *et al.* Monitoring and robust induction of nephrogenic intermediate mesoderm from human pluripotent stem cells. *Nat Commun* **4**, 1367 (2013).

34. James, R. G., Kamei, C. N., Wang, Q., Jiang, R. & Schultheiss, T. M. Odd-skipped related 1 is required for development of the metanephric kidney and regulates formation and differentiation of kidney precursor cells. *Development* **133**, 2995–3004 (2006).

35. Yoshino, T. *et al.* Generation of ovarian follicles from mouse pluripotent stem cells. *Science (1979)* **373**, (2021).

36. Xu, J., Liu, H., Park, J.-S., Lan, Y. & Jiang, R. Osr1 acts downstream of and interacts synergistically with Six2 to maintain nephron progenitor cells during kidney organogenesis. *Development* **141**, 1442–1452 (2014).

37. Araoka, T. *et al.* Efficient and Rapid Induction of Human iPSCs/ESCs into Nephrogenic Intermediate Mesoderm Using Small Molecule-Based Differentiation Methods. *PLoS One* **9**, e84881 (2014).

38. Morizane, R. *et al.* Nephron organoids derived from human pluripotent stem cells model kidney development and injury. *Nat Biotechnol* **33**, 1193–1200 (2015).

39. Sasaki, K. *et al.* The embryonic ontogeny of the gonadal somatic cells in mice and monkeys. *Cell Rep* **35**, 109075 (2021).

40. Rojas, A. *et al.* Gata4 expression in lateral mesoderm is downstream of BMP4 and is activated directly by Forkhead and GATA transcription factors through a distal enhancer element. *Development* **132**, 3405–3417 (2005).

41. Shin, E.-Y., Park, S., Choi, W. Y. & Lee, D. R. Rapid Differentiation of Human Embryonic Stem Cells into Testosterone-Producing Leydig Cell-Like Cells In vitro. *Tissue Eng Regen Med* **18**, 651–662 (2021).

42. Xu, C. *et al.* Differentiation roadmap of embryonic Sertoli cells derived from mouse embryonic stem cells. *Stem Cell Res Ther* **10**, 1–12 (2019).

Figures and tables

Figure 3.1

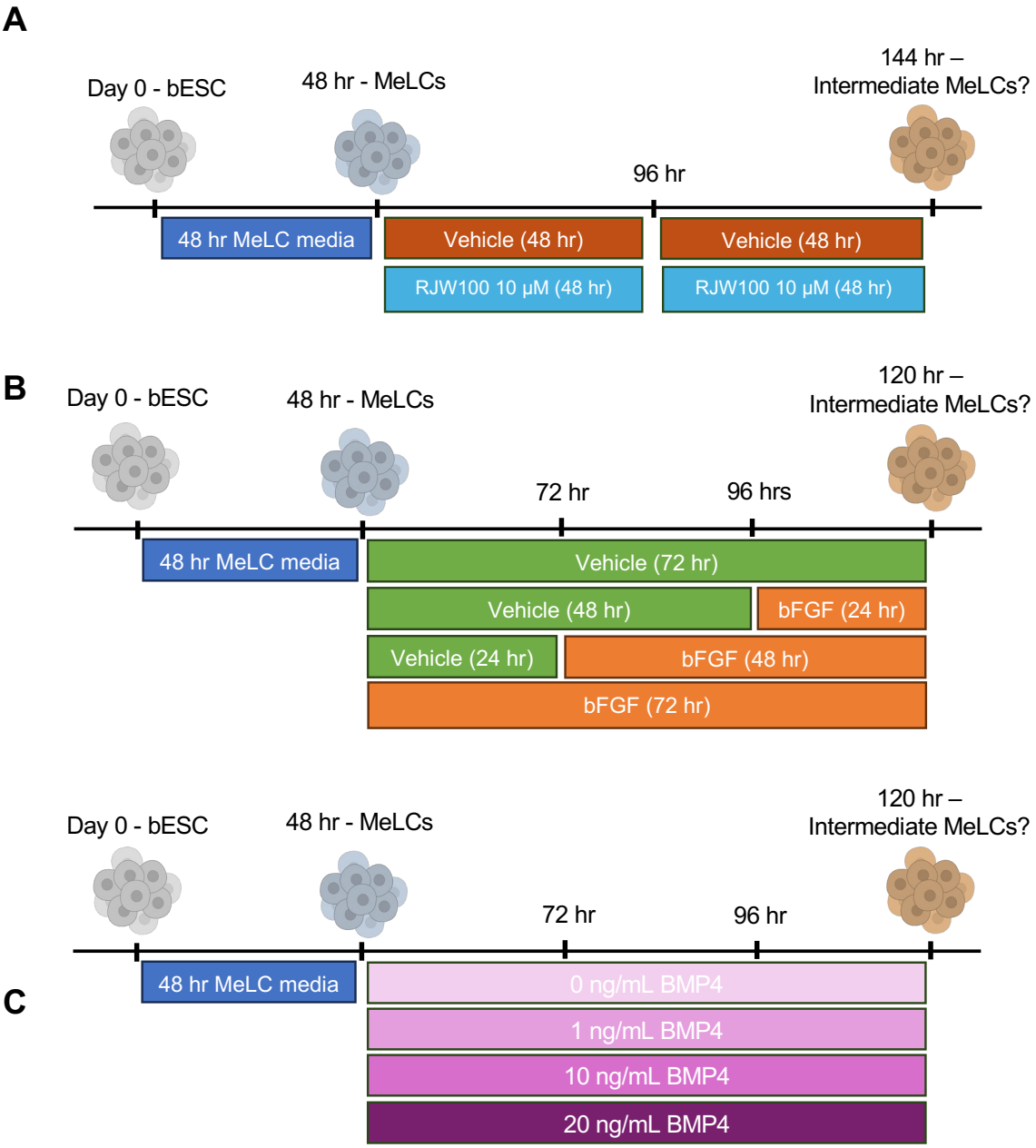

Figure 3.1. Experimental designs of bovine embryonic stem cell (bESC) in vitro mesoderm/bipotential gonad differentiation. (**A**) RJW100 experiment, (**B**) timed bFGF exposure experiment, (**C**) BMP4 concentrations experiments. MeLCs = mesoderm-like cells.

Figure 3.2

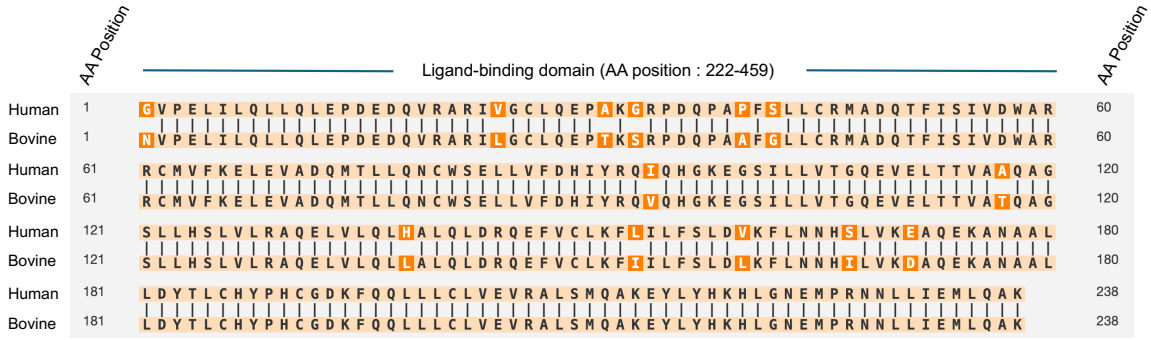

Bovine length: 238
Human length: 238
Alignment length: 238
Identity: 225/238 (94.54%)
Similarity: 230/238 (96.64%)
Gaps: 0/238 (0.00%)

Figure 3.2. Amino acid sequence homology between human and bovine SF1 ligand-binding domain.

Figure 3.3

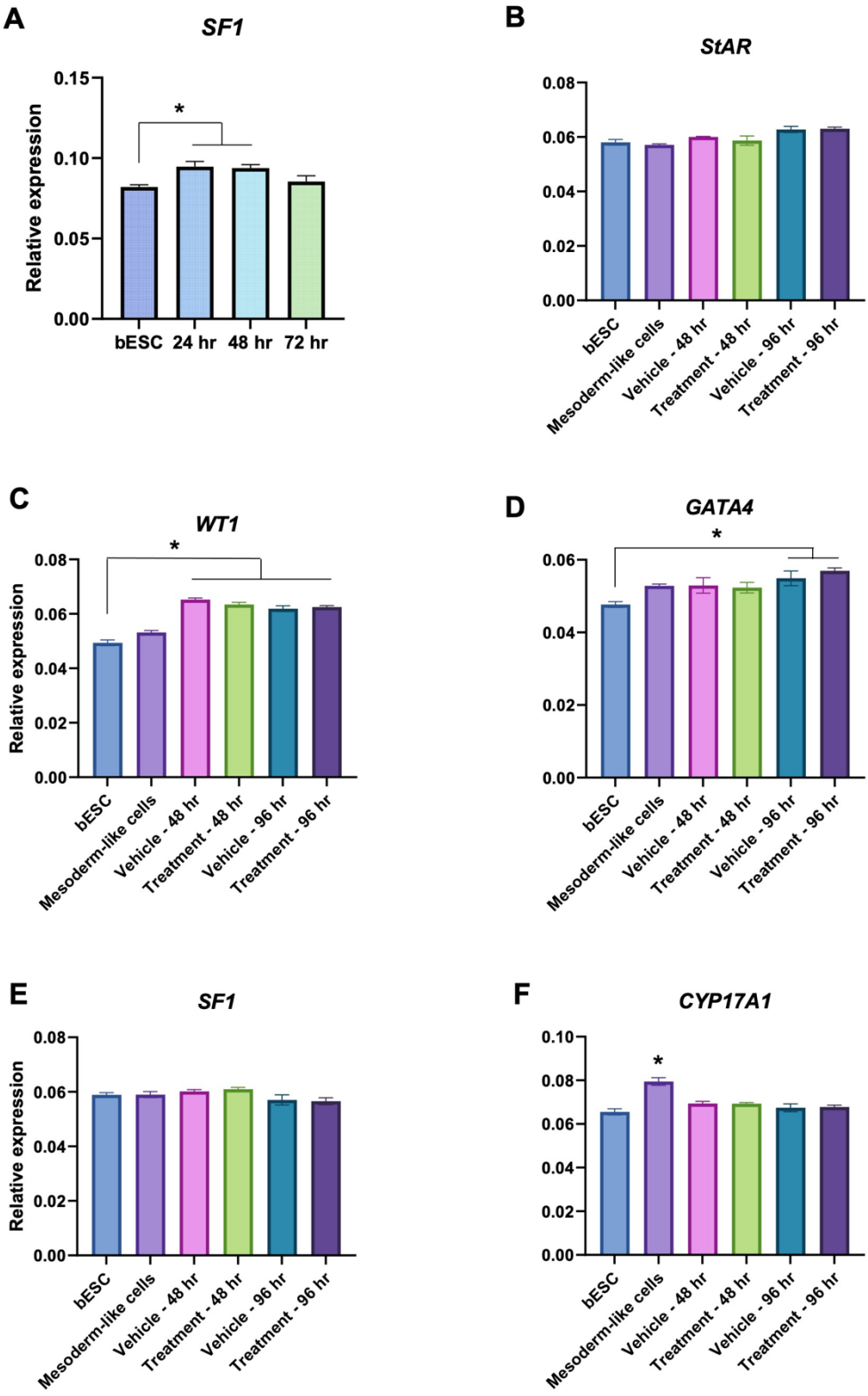
A
SF1
Relative expression
0.15
0.10
0.05
0.00
*
bESC
24 hr
48 hr
72 hr
B
StAR
0.08
0.06
0.04
0.02
0.00
bESC
Mesoderm-like cells
Vehicle - 48 hr
Treatment - 48 hr
Vehicle - 96 hr
Treatment - 96 hr
C
WT1
Relative expression
*
D
GATA4
*
E
SF1
Relative expression
F
CYP17A1
0.10
*

Figure 3.3. mRNA expression of steroidogenic and bipotential gonad genes before and after bovine embryonic stem cell (bESC) in vitro differentiation. (**A**) *SF1* expression over 24, 48, or 72 hours of mesoderm-induction. (**B-F**) expression of genes before and after bESCs are cultured with RJW100 or vehicle media. Data are presented as mean ± SEM. Significant differences compared to bESCs are noted by * = $P < 0.05$.

Figure 3.4

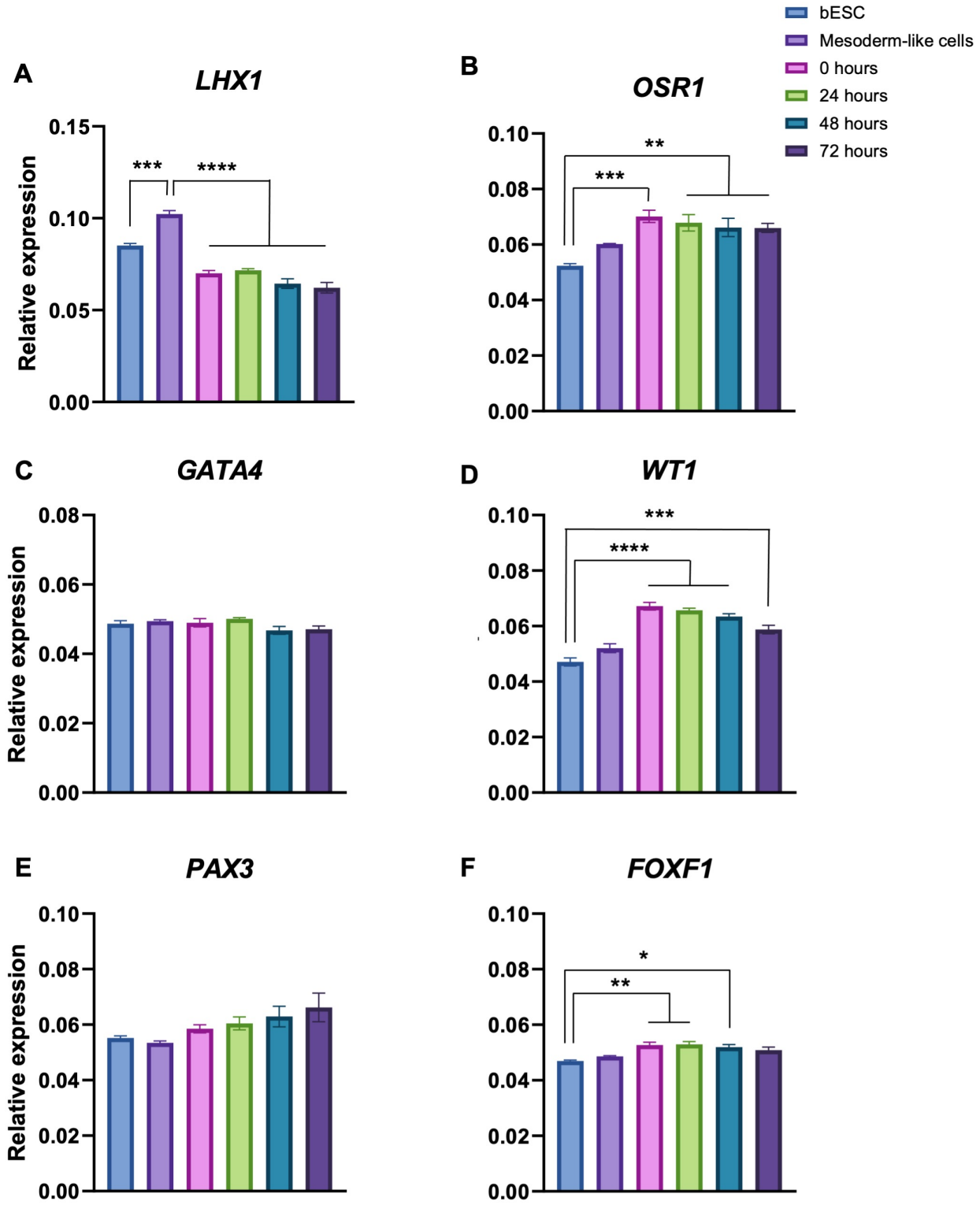
bESC
Mesoderm-like cells
0 hours
24 hours
48 hours
72 hours
A
LHX1
Relative expression
0.15
0.10
0.05
0.00
***
****
B
OSR1
0.10
0.08
0.06
0.04
0.02
0.00
**
***
C
GATA4
Relative expression
0.08
0.06
0.04
0.02
0.00
D
WT1
0.10
0.08
0.06
0.04
0.02
0.00
***
****
E
PAX3
Relative expression
0.10
0.08
0.06
0.04
0.02
0.00
F
FOXF1
0.10
0.08
0.06
0.04
0.02
0.00
*
**

Figure 3.4. mRNA expression of intermediate mesoderm (**A,B**), bipotential gonad (**C, D**) and paraxial (**E**) and lateral plate (**F**) mesoderm genes before and after bovine embryonic stem cell (bESC) in vitro differentiation using bFGF at various days of exposure. Data are presented as mean ± SEM. Significant differences are noted by * = P <0.05, ** = P <0.01, *** = P <0.001, **** = P <0.0001.

Figure 3.5

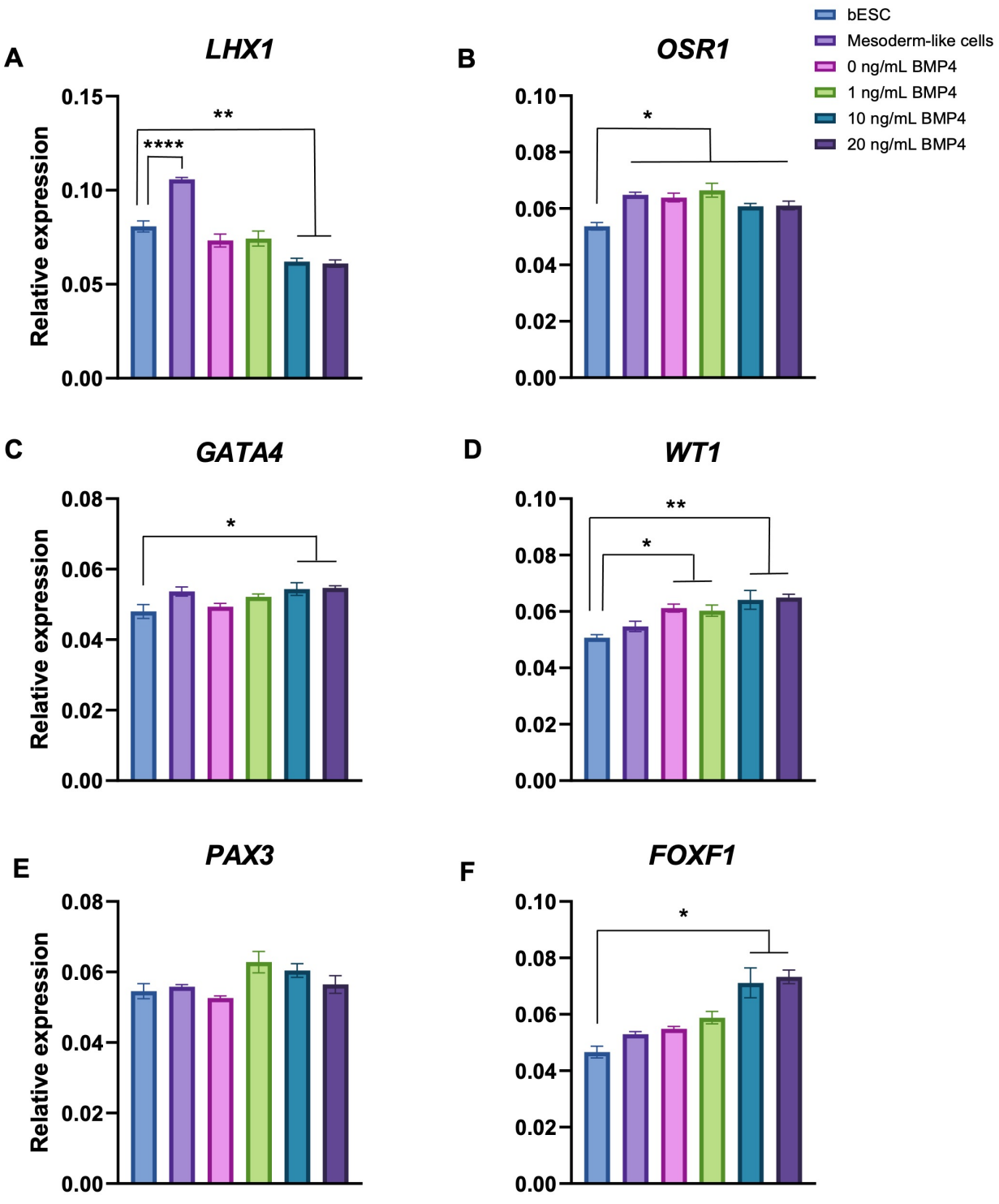
bESC
Mesoderm-like cells
0 ng/mL BMP4
1 ng/mL BMP4
10 ng/mL BMP4
20 ng/mL BMP4
A
LHX1
Relative expression
0.15
0.10
0.05
0.00
****
**
B
OSR1
0.10
0.08
0.06
0.04
0.02
0.00
*
C
GATA4
Relative expression
0.08
0.06
0.04
0.02
0.00
*
D
WT1
0.10
0.08
0.06
0.04
0.02
0.00
**
*
E
PAX3
Relative expression
0.08
0.06
0.04
0.02
0.00
F
FOXF1
0.10
0.08
0.06
0.04
0.02
0.00
*

Figure 3.5. mRNA expression of intermediate mesoderm (**A,B**), bipotential gonad (**C, D**) and paraxial (**E)** and lateral plate (**F**) mesoderm genes before and after bovine embryonic stem cell (bESC) in vitro differentiation using BMP4 at various concentrations. Data are presented as mean ± SEM. Significant differences are noted by * = P <0.05, ** = P <0.01, *** = P <0.001, **** = P <0.0001.

Figure 3.6

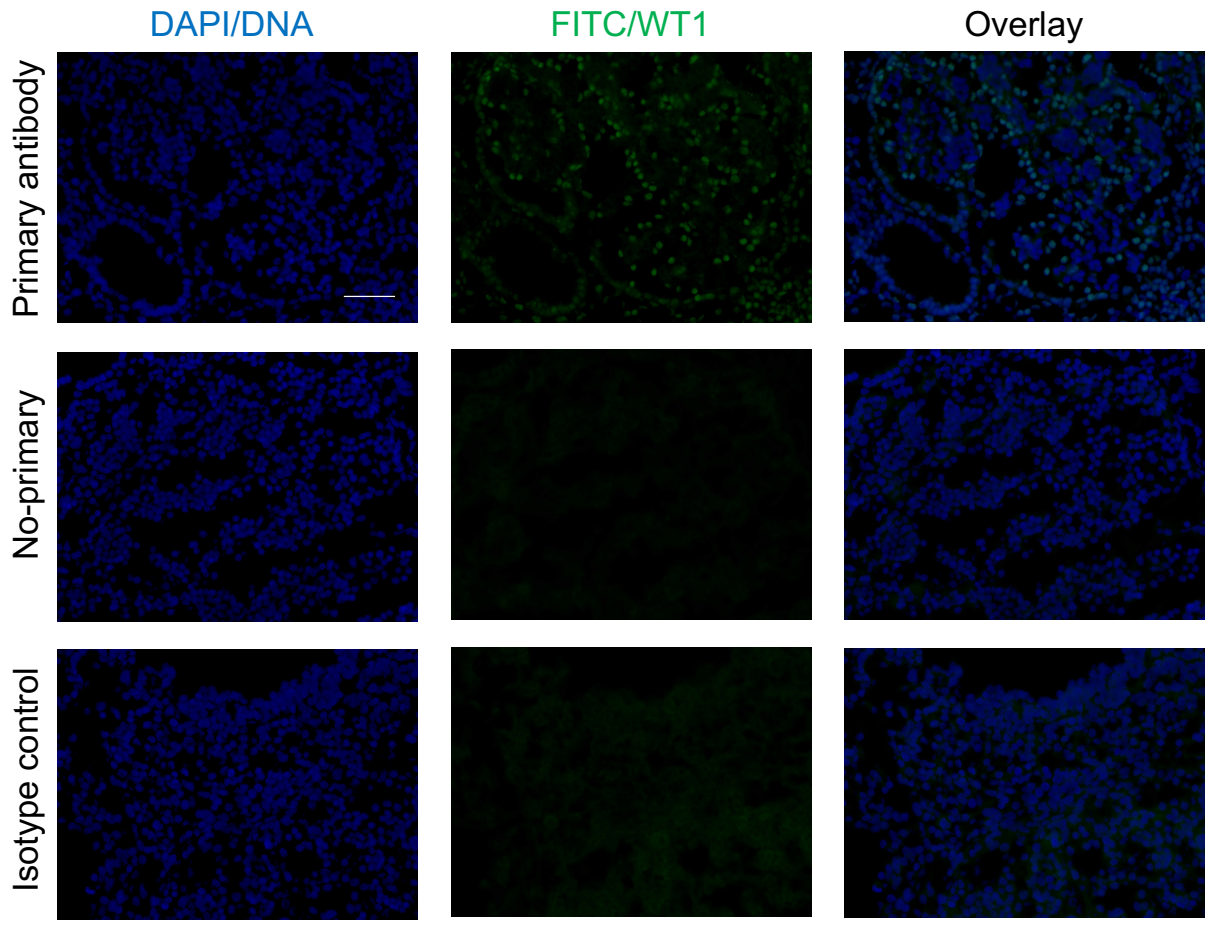

Figure 3.6. Fetal bovine (day 31 post-fertilization) mesonephros tissue immunostained for WT1. No-primary and rabbit isotype are negative controls. Scale bar = 100 μm.

Figure 3.7

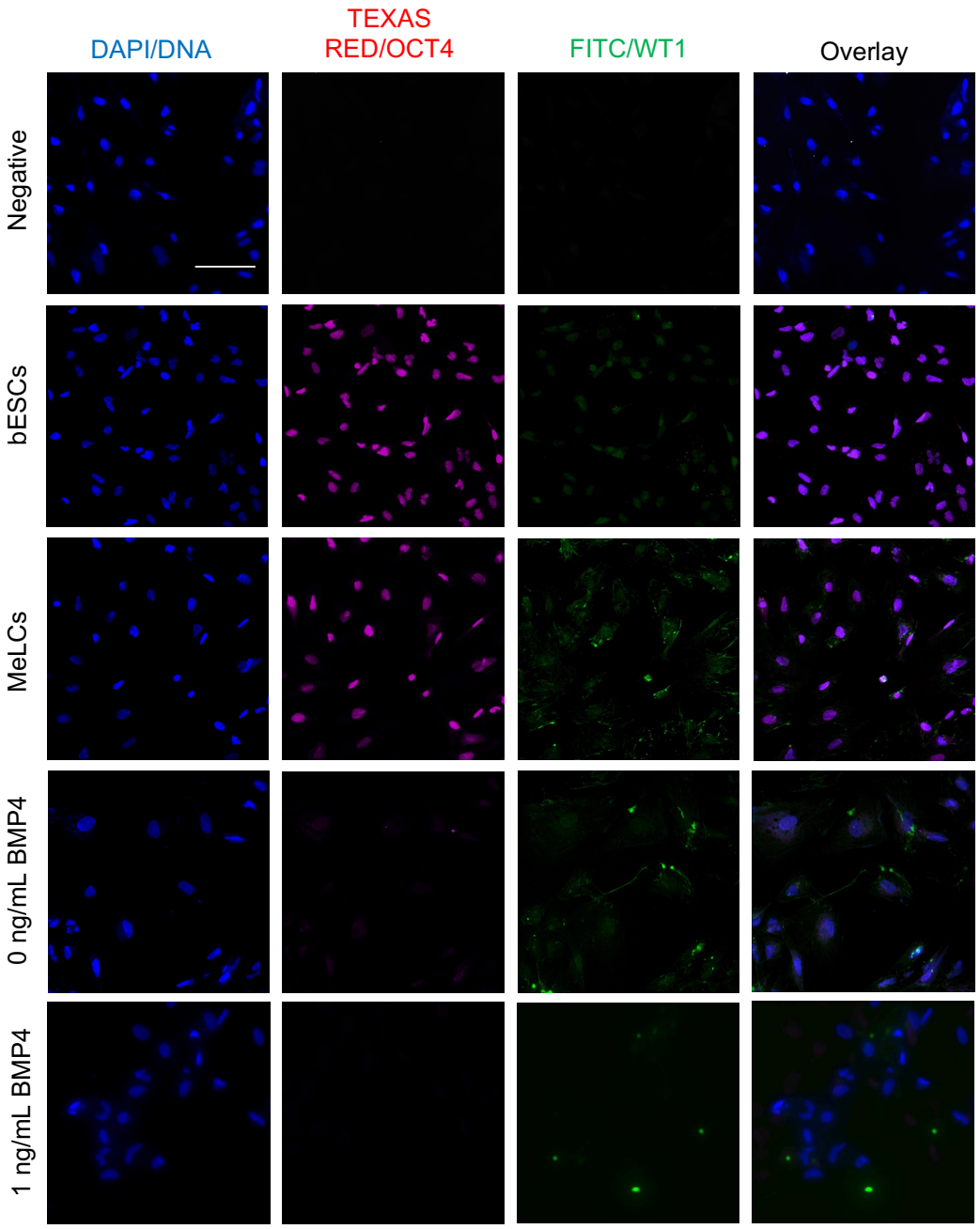

Figure 3.7. Immunocytochemistry staining in monolayer cultured cells for pluripotency (OCT4) and early coelomic epithelium marker (WT1). Bovine embryonic stem cells = bESCs, MeLCs = mesoderm-like cells. Scale bar = 100 μm.

Table 2. Primer list

Primer Name	Forward Sequence (5'-3')	Reverse Sequence (5'-3')	Product size (base pairs)
CYP17A1	GCG ACC ATC AGA GAA GTG CT	CAA GAA GCG CTC GGG CAT	192
FOXF1	GCC TCC TAC ATC AAG CAG CA	GTT CTG GTG CAG ATA CGG CT	108
GATA4	TGC GCC CCA TCA AAA CAG AG	GGG CCA TAC AGC TCC ACA AA	77
LHX1	TGG ACC GCT TCC TCT TGA AC	CTT GGT ACC GAA ACA CCG GA	152
NR5A1	CAA GGT GTC GGG CTA CCA CTA	CCA CCG TCA GGC ACT TCT GGA	176
OSR1	CCT GTG GAA ATC CAG CGC C	CAG TCT GTT CTG ACT TCC TGC TTA	111
PAX3	CCT TCA AAG CCC AGT ACA TGC	GTG CGT CTT CAG ATT TTC CAG	122
StAR	CAG AAG GGT GTC ATC AGA GCG	CAA AAT CCA CCT GGG TCT GC	169
WT1	CCT TCA CCG TCC ACT TCT CT	CCG TGC TGT ATC CCT GGT TG	183
H2A.2	GAG GAG CTG AAC AAG CTG TTG	TTG TGG TGG CTC TCA GTC TTC	104
ACTB	CTC TTC CAG CCT TCC TTC CT	GGG CAG TGA TCT CTT TCT GC	178

CHAPTER 5

Concluding remarks

Assisted reproductive technologies (ART) have greatly advanced the biomedical field and agriculture production over the last few decades. In this work, we describe several ways in which the bovine ovary, and particularly the follicles housed within, can be utilized for tissue cryopreservation and in vitro culture to promote preantral folliculogenesis with the end goal of ultimately producing viable oocytes. Moreover, we explored the potential of bovine embryonic stem cells to be differentiated towards somatic cells that constitute the bipotential gonad. Collectively, results from this work demonstrate important advancements towards developing novel technologies in fertility preservation and restoration as well as elucidating molecular and cellular events important for recapitulating early gonad development in a stem cell model.

Despite progress in safeguarding oocytes in situ via ovarian tissue cryopreservation by slow freezing or vitrification, there has been little investigation in downstream steps to revive the abundant preantral follicle post-thawing and stimulate folliculogenesis using in vitro culture. In Chapter 2, we showed that post-thawing and in vitro culture, bovine ovarian cortex tissue was more resilient to the effects of slow freezing compared to vitrification as indicated by better preantral follicle morphology, lower rates of apoptosis in the stromal cells, and less aberrant expression pattern of connexin 37 within the oocytes. This corroborates other research results showing success in slow freezing ovarian tissue of several species; however, as slow freezing has been the gold standard for tissue cryopreservation, vitrification has been utilized to a lesser extent and therefore its effects have not been as thoroughly studied. We emphasize the importance of user technique with the vitrification method, as slight differences in tissue handling during the vitrification process can significantly influence downstream results.

Furthermore, it is vital to acknowledge the variability in tissue structure and follicle counts between individuals, therefore affecting results. The highlighted benefit of in vitro culturing is the ability to circumvent surgical transplantation of thawed tissue; yet there remains a strong need to optimize culture conditions to promote folliculogenesis in vitro. Although this research did not examine follicles past the secondary stage, other research has demonstrated that in situ follicle culture in large mammals requires prolong culture time periods and remains greatly inefficient, hence further research is warranted.

As previously mentioned, culturing preantral follicles in vitro presents an alternative approach to capitalizing on immature oocytes found in the ovary. In Chapter 3, we explored the use of a dynamic bioengineered three-dimensional culture system (PEG hydrogels) to culture isolated bovine preantral follicles where the PEG hydrogels can be controllably degraded by the growing follicle, thus permitting volumetric follicle expansion in addition to structural support. We designed the hydrogel chemistry to include proteolytically-degradable peptide sequences that complement bovine preantral follicle enzyme profiles which were determined via PCR detection. We found that smaller follicles (primary stage) grew better in the PEG system compared to two-dimensional control, but the addition of ovarian support cells did not aid in follicle development and ovarian cells did not maintain expression of genes essential to theca cell differentiation. In a similar fashion to in situ follicle culture conducted in Chapter 2, we conclude that 1) follicle culture media conditions need to be better optimized and 2) the PEG hydrogel likely needs additional modifications such as including a basement membrane binding protein to promote cell/follicle adhesion. Nevertheless, our data indicate prospective promise in employing the PEG hydrogel system for in vitro follicle development with further

amendment of the media and hydrogel composition. Indeed, the uniqueness of PEG hydrogels is that they can be designed to be biomimetic, especially with the inclusion of support cells that can give rise to theca cells, and therefore should be further tested to create a complete and dynamic culture system for folliculogenesis.

In Chapter 4, we examined the propensity of bovine embryonic stem cells to be induced towards a cell state mimicking the early bipotential gonad of an embryo. Importantly, we show that mainly WNT activation in cells and culture time is sufficient to upregulate genes responsible for specification of intermediate mesoderm-like and early coelomic epithelium-like states in differentiated cells. This preliminary work provides a basis for understanding the importance of certain cell signaling pathways in generating targeted cell phenotypes. By creating somatic gonadal-like cells through pluripotent stem cells, approaches to in vitro gametogenesis can be refined to be exclusively stem-cell based (i.e. eliminate the requirement of fetal somatic cells for reconstitution of gonad-like structures during in vitro gametogenesis). Moreover, the development of stem cell-based models to study gonadogenesis in a large mammal species would authorize expansion in research aiming to elucidate mechanisms of early development, toxicology assays, and dissecting the origin of disease. In all, this dissertation underlines the applicational potential of better understanding ovarian biology in the bovine model, beginning from early embryonic development using stem cells through growth of follicles from adult females with hopes of yielding mature oocytes. The collective technologies explored in this dissertation demonstrate progress in female reproductive sciences. Use of novel ART will be fundamental to feeding a growing world with quality animal protein and to ensuring a healthy human population for generations to come.